

**Charles University
Faculty of Science**

Study programme: Biology
Branch of study: Experimental Plant Biology



Bc. Vojtěch Schmidt

The role of auxin in streptophyte algae

Role auxinu u streptofytních řas

Master's thesis

Supervisor: RNDr. Jan Petrášek, Ph.D.

Advisors: Mgr. Roman Skokan and Mgr. Stanislav Vosolsobě, Ph.D.

Prague, 2021

Declaration

I hereby declare that this thesis has been composed solely by myself, using only the cited literature and resources. This thesis or any major part thereof has not been submitted for any other or the same academic title.

Prohlášení

Prohlašuji, že jsem závěrečnou práci zpracoval samostatně a že jsem uvedl všechny použité informační zdroje a literaturu. Tato práce ani její podstatná část nebyla předložena k získání jiného nebo stejného akademického titulu.

V Praze dne 9.8. 2021

.....
Vojtěch Schmidt

Acknowledgments

I wish to express my sincere appreciation to my supervisor, RNDr. Jan Petrášek, Ph.D., for professional guidance regarding the formulation of experimental design, methodology, and valuable critical feedback. I am also grateful to him for the opportunity to become a member of the Laboratory of Hormonal Regulations in Plants, and for providing me, as a student, with superb working conditions therein.

I would like to pay my special gratitude to Mgr. Roman Skokan for patient explanations, valuable advice, and for teaching me most of the techniques I needed. Likewise, my big thanks belong to Mgr. Stanislav Vosolsobě, Ph.D. for great help with statistical evaluation of my data and countless valuable advice and ideas. I also thank Ing. Petre Dobrev, CSc., and his team for performing the LC-MS analysis. Altogether, I wish to thank all the members of our laboratory for creating a pleasant and stimulating environment for work.

I am grateful to my family, my partner Martina, and also her family for continuous support.

In addition, I would like to thank my bandmates from Ewenay for their forbearance during my limited time for rehearsals and to be productive for the band \m/.

Grant support

This work was supported by the Czech Science Foundation (project no. 20-13587S to Jan Petrášek)

Abstract

The phytohormone auxin is an important morphogen with an essential role in the development of land plants, where mechanisms of its action are well described. However, its role in green algae is poorly understood. Land plants are part of the phylum Streptophyta together with six closely related groups of predominantly freshwater green algae (charophytes). So far, the knowledge about the evolutionary origins of auxin action mechanism is mainly based on genomic information, and much less on experimental findings. In this work, the presence of auxin, its precursor, and catabolism products were shown in representative species of charophytes with varying levels measured compounds both produced endogenously and into the culture media. Thus, we gained a comprehensive insight into the possible strategies of auxin homeostasis across the non-land plant streptophytes. Also, an effect of exogenous auxin on the cell morphology and culture growth of the desmid *Closterium* was investigated. Image analysis of IAA-treated cells revealed a rather pleiotropic effect on cell morphology. The culture growth was inhibited by IAA. Additionally, IAA induced malformations in cell shape, and the extent of this phenomenon across individual cultures was dependent on the culture growth status. Lastly, we optimized the method of biolistic transformation for *Closterium*. The ultimate goal of this effort, i.e. the *in vivo* visualisation of a fluorescently-tagged translational fusion of the *Closterium* PIN auxin efflux carrier ortholog (*CpPIN*), was not yet achieved in this alga. However, heterologous expression in *Nicotiana tabacum* Bright Yellow-2 (BY-2) cells revealed *CpPIN* localization at the plasma membrane and endomembrane compartments.

Keywords: auxin, charophytes, auxin metabolism, *Closterium*, morphology, transformation

Abstrakt

Fytohormon auxin je významný morfogen s nezastupitelnou rolí ve vývoji suchozemských rostlin, u nichž jsou mechanismy jeho působení podrobně popsány. Avšak role auxinu u zelených řas je prozkoumána podstatně méně. Suchozemské rostliny jsou součástí skupiny streptofyta spolu s šesti příbuznými liniemi převážně sladkovodních řas (zvaných též charofyta). Současný pohled na evoluční počátky mechanismů působení auxinu se zakládá zejména na sekvenčních datech, méně potom na experimentálních poznatcích. V této práci byl prokázán výskyt auxinu, jeho prekurzoru a produktů katabolismu u reprezentativních zástupců charofyt. Hladiny těchto látek byly poměrně rozdílné, a to jak mezi druhy, tak mezi biomasou a okolním médiem, což přispělo k možnosti vyvodit různé strategie udržování auxinové homeostáze u charofyt. Dále byl studován efekt exogenního auxinu na buněčnou morfologii a na růst kultury krásivky *Closterium*. Obrazová analýza buněk ošetřených exogenním auxinem (IAA) ukázala jeho pleiotropní efekt na morfologii. Růst kultury byl auxinem inhibován. Rozsah morfologických malformací se také ukázal být závislým na růstu kultury. Nakonec byla optimalizována metoda biolistické transformace krásivky *Closterium* za účelem vnesení a *in vivo* vizualizace fluorescenčně značeného nativního ortologu proteínu PIN (*CpPIN*), což se přes tuto snahu zatím nepodařilo. Nicméně exprese v heterologním systému buněk *Nicotiana tabacum* Bright Yellow-2 (BY-2) vykazovala lokalizaci na plazmatické membráně a v endomembránových kompartmentech.

Klíčová slova: auxin, charofyta, metabolismus auxinu, *Closterium*, morfologie, transformace

List of frequent abbreviations

ABCB	-	ATP-BINDING CASSETTE subfamily B
AMI1	-	AMIDASE1
ARF	-	AUXIN RESPONSE FACTOR
Aux/IAA	-	Auxin/INDOLE ACETIC ACID
AUX1/LAX	-	AUXIN RESISTANT1/LIKE AUX1
BY-2	-	Bright Yellow-2
CAB1	-	CHLOROPHYLL A/B BINDING PROTEIN 1
cGFP	-	<i>Chlamydomonas</i> -adapted green fluorescent protein
DAO	-	DIOXYGENASE FOR AUXIN OXIDATION
ER	-	Endoplasmic reticulum
FW	-	Fresh weight
GH3	-	GRETCHEN HAGEN3
IAA	-	Indole-3-acetic acid
IAM	-	Indole-3-acetamide
ILR	-	INDOLE-LEUCINE RESISTANT 1
oxIAA	-	2-oxo-indole-3-acetic acid
PAA	-	Phenylacetic acid
PAT	-	Polar auxin transport
PID	-	PINOID
PILS	-	PIN-LIKES
PIN	-	PIN-FORMED
PM	-	Plasma membrane
TAA1	-	TRYPTOPHAN AMINOTRANSFERASE OF ARABIDOPSIS 1
TIR1/AFB	-	TRANSPORT INHIBITOR RESPONSE 1/AUXIN SIGNALING F-BOX
Trp	-	Tryptophan
YUC	-	YUCCA

Table of contents

1	Introduction.....	9
1.1	Introduction to algae and their early phylogenesis.....	9
1.2	Characteristics of streptophyte algal lineages	10
1.2.1	<i>Early diverging charophytes.....</i>	<i>10</i>
1.2.2	<i>Higher charophytes - the ZCC clade</i>	<i>11</i>
1.2.3	<i>Charophytes and terrestrialization.....</i>	<i>11</i>
1.3	Establishment of algae as model organisms.....	13
1.4	Auxin action mechanisms and their evolution	14
1.4.1	<i>Biosynthesis and metabolism</i>	<i>14</i>
1.4.2	<i>Signaling</i>	<i>17</i>
1.4.3	<i>Transport.....</i>	<i>19</i>
1.4.4	<i>What is known about auxin action in algae?</i>	<i>21</i>
2	Main objectives	25
3	Materials and methods	27
3.1	Chemicals.....	27
3.2	Plant material and culture conditions	28
3.2.1	<i>Algal strains and their cultivation</i>	<i>28</i>
3.2.2	<i>Nicotiana tabacum BY-2 cell line</i>	<i>29</i>
3.2.3	<i>Media composition.....</i>	<i>30</i>
3.3	Determination of <i>Closterium</i> culture density	33
3.4	Auxin metabolic profiling	33
3.4.1	<i>Preparation of algal cultures and sampling.....</i>	<i>33</i>
3.4.2	<i>Analysis of auxin profiles.....</i>	<i>34</i>
3.5	IAA treatment of <i>Closterium</i>	35
3.5.1	<i>Inoculation and culture conditions</i>	<i>35</i>
3.5.2	<i>Image analysis</i>	<i>35</i>
3.6	Biolytic transformation of <i>Closterium</i>	35
3.6.1	<i>DNA vectors used.....</i>	<i>35</i>
3.6.2	<i>Preparation of concentrated DNA</i>	<i>36</i>
3.6.3	<i>Preparation of the biological material</i>	<i>38</i>
3.6.4	<i>Preparation and coating of microcarriers.....</i>	<i>38</i>
3.7	Microscopy.....	39

3.8	Statistical analyses.....	39
4	Results	41
4.1	Cultivation of selected representatives of streptophyte algae and study of their native auxin profiles	41
4.1.1	<i>Selection of representative strains and their cultivation</i>	41
4.1.2	<i>Analysis of endogenous levels of auxins in algae</i>	44
4.2	The reaction of <i>Closterium</i> to exogenous auxin.....	49
4.2.1	<i>The effect of exogenously applied auxin on Closterium morphology</i>	49
4.2.2	<i>Inhibitory effect of IAA on Closterium culture growth</i>	51
4.3	Native and heterologous transformation of <i>Closterium</i> -derived gene constructs and optimization of biolistic transformation method for the alga <i>Closterium</i>	52
4.3.1	<i>Optimization - setup of the gene gun device</i>	53
4.3.2	<i>Optimization - the effect of the microcarrier amount</i>	53
4.3.3	<i>The effect of DNA concentration.....</i>	55
4.3.4	<i>The comparison of two fluorophores</i>	56
4.3.5	<i>Native expression of CpPIN was not successful</i>	58
4.3.6	<i>Heterologous expression of CpPIN in BY-2 cells</i>	58
5	Discussion.....	60
5.1	Endogenous levels of auxins in charophytes.....	60
5.1.1	<i>Endogenous auxin levels are variable among algae</i>	60
5.1.2	<i>Obstacles in data interpretation</i>	61
5.2	The reaction of <i>Closterium</i> to exogenous auxin is pleiotropic.....	62
5.3	Native and heterologous transformation of <i>Closterium</i> -derived gene constructs and optimization of biolistic transformation method for the alga <i>Closterium</i>	63
6	Conclusions.....	66
7	References.....	67

1 Introduction

1.1 Introduction to algae and their early phylogenesis

The term “algae” covers a relatively broad range of mutually polyphyletic photosynthetic organisms from several eukaryotic kingdoms. It includes the so-called red, green algae, and glaucophytes (Rhodophyta, Viridiplantae, and Glaucophyta, respectively) belonging to the kingdom of Archaeplastida. Another kingdom called SAR contains different algal phyla, such as diatoms, chrysophytes, phaeophytes (brown algae), and dinoflagellates. These groups individually have undergone a different endosymbiotic histories and vary in cell structure or metabolic and ecological strategies. All resulting from more than a billion years of separate evolution (Archibald, 2015; Morris *et al.*, 2018).

Green algae along with embryophytes form the green lineage (Viridiplantae). According to various applications of the molecular clock, the current estimate of the divergence of Viridiplantae ranges between 1000 to 1500 million years ago (Yoon *et al.*, 2004; Parfrey *et al.*, 2011; Morris *et al.*, 2018). Viridiplantae are usually being divided into two main lineages – Chlorophyta and Streptophyta, which mutually diverged around 1200 – 720 million years ago (Becker, 2013). Chlorophytes form the most species-rich group among green algae. Despite their origin and a lasting major presence in marine habitats, chlorophytes are now also abundant in freshwater and terrestrial ecosystems. The early diverging chlorophytes are typically represented by unicellular and planktonic flagellates and are united in the paraphyletic assemblage Prasinophyta. The more derived lineages (Ulvophyceae, Trebouxiophyceae, Chlorophyceae) comprise the core Chlorophyta, also known as the “UTC-clade” (Lewis and McCourt, 2004).

A recent study by Li *et al.* (2020) pointed out the existence of a third green lineage phylum – Prasinodermophyta, whose respective taxa were formerly assigned to Prasinophyta. Divergence of Prasinodermophyta predated the split of Chlorophyta and Streptophyta. Now this group represents the closest relatives of the algal common ancestor (AGF – Ancestral Green Flagellate; Leliaert *et al.*, 2012). Indeed, the nature of this hypothetical ancestor could resemble some current flagellate from prasinophytes, however, the level of its complexity is still nebulous (Leliaert *et al.*, 2011).

The presence in the freshwater or saltwater environment is a common trait for all groups of algae, but only green algae along with fungi became the first eukaryotes to colonize land

(Heckman *et al.*, 2001; Delaux *et al.*, 2015). This event was the starting point of a gradual alteration of climate and biogeochemical cycles resulting in massive speciation of species on land. Understanding the transition to land (terrestrialization) is one of the main driving forces of studying the green algae on all levels. For this work's purpose, this chapter will further discuss only the green algal phylogeny with an accent on streptophytes.

1.2 Characteristics of streptophyte algal lineages

To date, streptophyte algae (also called charophytes) are eclipsed by their sister chlorophyte lineage in species diversity, but not so much in morphological complexity. The streptophytes range from unicellular to three-dimensional multicellular thali, but unlike chlorophytes, they are mostly present in freshwater. The lineage Streptophyta comprises six algal lineages and land plants (Figure 1.1).

1.2.1 Early diverging charophytes

The Mesostigmatophyceae is a monotypic lineage containing only *Mesostigma viride*. It is a freshwater unicellular biflagellate, which morphologically resembles the simple prasinophytes, where *Mesostigma* had been classified formerly (Fawley & Lee, 1990). Not only it is the single representative among streptophytes with calcified scales on in place of a cell wall, it also possesses flagella in its vegetative state (Leliaert *et al.*, 2012).

The Chlorokybophyceae is also represented by a single member - *Chlorokybus atmophyticus*. This species is a rare terrestrial alga forming sarcinoid packets of two to four non-motile cells. It is reproduced asexually, mostly via biflagellate scaly zoospores (Rogers *et al.*, 1980). Sexual reproduction is unknown both in *Mesostigma* and *Chlorokybus* (Leliaert *et al.*, 2012).

The Klebsormidiophyceae diverged after the Mesostigmatophyceae and Chlorokybophyceae. But unlike the latter two, many members of the Klebsormidiophyceae are cosmopolitan and dwell in diverse freshwater and terrestrial habitats. This amphibious lineage contains five genera with distinct morphotypes such as sarcinoid unicells or cell packets in the genus *Interfilum*, or unbranched filaments in the genera *Hormidiella*, *Klebsormidium*, and *Entransia* (Mikhailyuk *et al.*, 2014). The recently included genus *Streptosarcina* has either packet-like or branched filamentous thalli (Mikhailyuk *et al.*, 2018). The Klebsormidiophyceae is sister to the clade including the remaining ('higher') charophytes diverging afterwards and land plants.

1.2.2 Higher charophytes - the ZCC clade

The ZCC clade is a monophyletic assembly of later-diverging charophyte groups – the Charophyceae, the Coleochaetophyceae, and the Zygnematophyceae in respective branching order (Figure 1.1; Turmel & Lemieux, 2018). Together with land plants, they share an important synapomorphy – the production of a phragmoplast during cytokinesis, thus, they are together classified as the Phragmoplastophyta (Figure 1.1). These feature likely contributed to the morphological complexity of charophytes with three-dimensional thalli (reviewed in Buschmann, 2020).

The most complex streptophyte algae are represented by the Charophyceae *sensu stricto* (also called stoneworts). Threedimensional macroscopic thalli of stoneworts comprise the central axis of large multinucleate internodal cells, which alternate with uninucleate nodal cells with branchlets. There are six genera within the Charophyceae, which all thrive in fresh or brackish waters attaching themselves to the substrate by rhizoids (Lewis & McCourt, 2004).

The Coleochaetophyceae is a group of two genera, which both grow in freshwater as epiphytes or attached to stones. *Chaetosphaeridium* is branched-filamentous, while some species of *Coleochaete* can additionally form planar multicellular discs. Oogamous sexual reproduction is common for the Charophyceae and the Coleochaetophyceae (Delwiche, 2016).

The Zygnematophyceae is characterized by its specific type of sexual reproduction called conjugation. Among charophytes, this group holds the first place in terms of taxonomic diversity. The thalli of Zygnematophyceae are filamentous or unicellular. Filaments are typical of the rather common genera *Spirogyra*, *Zygnema*, or *Mougeotia*. The so-called desmids are unicellular, yet of various complex shapes with apparent semicells divided by an isthmus, where the nucleus is located. The Zygnematophyceae has been identified as the sister group to land plants (Wodniok *et al.*, 2011; Timme *et al.*, 2012; Wickett *et al.*, 2014; Gitzendanner *et al.*, 2018; Cheng *et al.*, 2019).

1.2.3 Charophytes and terrestrialization

The transition to land leading to the divergence of land plants occurred in streptophyte algae more than 400 million years ago (Yoon *et al.*, 2004). Some features pertinent to terrestrial plant life are present within these organisms or have in fact evolved in them (Figure 1.1). For instance: hexameric cellulose synthase complex, synthesis of sporopollenin and lignin (Bowman, 2013), plasmodesmata (Sørensen *et al.*, 2011), and some phytohormone-related pathways (Rensing, 2018, 2020).

Interestingly, the land plant sister group Zygnematophyceae underwent a secondary reduction of body plan and lost some of the above-mentioned traits (Bowman, 2013). The common land plant ancestor most likely possessed a more complex body plan and a different set of adaptation to terrestrial existence than the present day Zygnematophyceae. But it does not necessarily mean that the algal transition to land occurred at that level. An alternative hypothesis places the terrestrialization within streptophytes at a much earlier point in the evolutionary timescale (Harholt *et al.*, 2016). The tree topology of the ZCC clade has a deep branching character highlighting the long independent evolution of respective lineages. This is most likely the reason why we observe a different combination of derived and ancestral traits within those three groups (Delwiche, 2016). In fact, the extant charophytes represent a remnant of a much greater ancient diversity (Delwiche, 2016).

Thus, inferring the ancestral characters within green plants requires an abundance of data from representative species across many lineages, both genomic information and experimental evidence (Rensing, 2020).

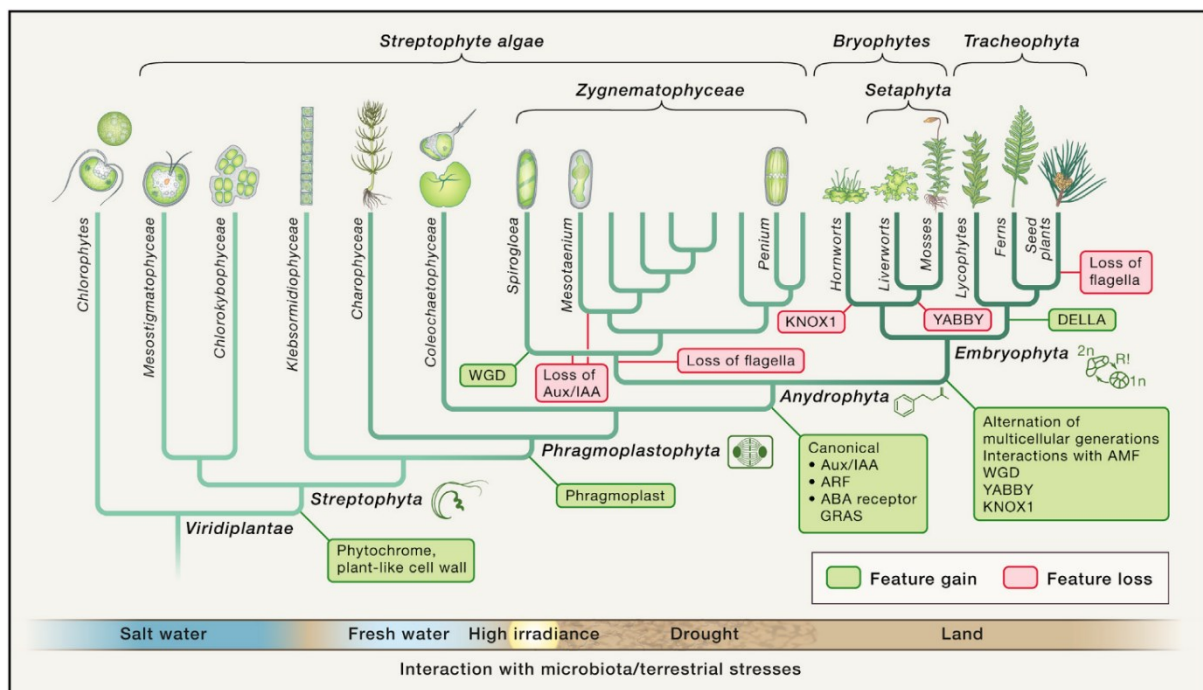


Figure 1.1 | Cladogram of streptophytes with the origin and losses of features related to the life on land. Adapted from Rensing (2020).

1.3 Establishment of algae as model organisms

Before the rise of molecular phylogenomics, phylogenetic relations were initially inferred from the homology of morphological character states. Nowadays, comparative genomics is a major method used to unravel the evolutionary patterns, as well as uniquely evolved traits between taxa. With the help of next-generation sequencing methods and advanced computing potential, the amount of annotated genomes starts to grow rapidly (Metzker, 2010).

Chlamydomonas reinhardtii was the first green algal genome to be sequenced (Merchant *et al.*, 2007). The full genome sequences of the moss *Physcomitrium patens* (formerly known as *Physcomitrella patens*) and the liverwort *Marchantia polymorpha* came to represent bryophytes (Rensing *et al.*, 2008; Bowman *et al.*, 2017). Comparative genomics has since shaped the following way of researching the early plant evolution, especially after bryophytes were shown to form a monophylum (Sousa *et al.*, 2018). Among charophytes, the first sequenced genome was that of *Klebsormidium nitens* (Hori *et al.*, 2014), soon followed by *Chara braunii* (Nishiyama *et al.*, 2018), the Zygnematophyceae *Spirogloea muscicola* and *Mesotaenium endlicherianum* (Cheng *et al.*, 2019), *Mesostigma viride* with *Chlorokybus atmophyticus* (Wang *et al.*, 2020), and another Zygnematophyceae *Penium margaritaceum* (Jiao *et al.*, 2020). Now only the Coleochaetophyceae lack published genomic information. In parallel to genome sequencing, there is also a massive project aiming to generate over a thousand plant and algal transcriptomes (Leebens-Mack *et al.*, 2019). Thus, sequenced representatives from various algal lineages are increasingly becoming available.

Sequential information is also a prerequisite for the subsequent establishment of model organisms. An essential part thereof is the possibility of transformation. This was already accomplished in several charophytes, especially in the Zygnematophyceae (reviewed by Zhou *et al.*, 2020). *Agrobacterium tumefaciens*-mediated stable transformation was reported in *Penium margaritaceum* (Sørensen *et al.*, 2014). Transient transformation was accomplished in *Mougeotia scalaris* (Regensdorff *et al.*, 2018), and both transient and stable transformation was published for *Closterium peracerosum-strigosum-littorale* complex (Abe *et al.*, 2008, 2011). Successful management of these methods should allow for functional testing of various molecular and physiological traits, though this appears so far to only have been realized in *Closterium* (Abe *et al.*, 2011; Kanda *et al.*, 2017). Naturally, the investigation of the evolutionary origin of auxin action and its possible role in green algae will also necessitate reliable and reproducible use of genetic modification methods in algae.

1.4 Auxin action mechanisms and their evolution

Phytohormone auxin acts as a major modulator of almost every aspect of the land plant development. The modulating cue is carried by specific auxin concentration, which is regulated by metabolism and transport. Among plant hormones, auxin is the longest-studied from the time of Darwin, who observed the first plant growth responses to this substance (for review see Enders & Strader, 2015). In this chapter, mechanisms of auxin action are presented based on the research performed in angiosperms, most of the available knowledge was gained using the model *Arabidopsis thaliana*. This is followed by reviewing the up-to-date knowledge about the possible conservation of these mechanisms in green algae.

1.4.1 Biosynthesis and metabolism

Auxin biosynthesis, conjugation, and degradation are metabolic processes contributing to its local homeostasis. The most studied and the most abundant active auxin form is the indole-3-acetic acid (IAA) - a weak acid derived from the amino acid L-tryptophan (Trp).

Biosynthesis of Trp occurs in plastids and starts from chorismate (a product of the shikimate pathway), which is also the precursor for other aromatic amino acids. The important intermediate in Trp biosynthesis is the indole-3-glycerol phosphate (IGP), as the substrate for the TRYPTOPHAN SYNTHASE (TS) complex converting IGP to indole and then to Trp (Ouyang *et al.*, 2000). In the cytoplasm, Trp is the precursor in four so-called Trp-dependent pathways of IAA biosynthesis, namely via indole-3-acetaldoxime (IAOx), indole-3-acetamide (IAM), tryptamine (TRA), and indole-3-pyruvic acid (IPyA) pathway (Ljung, 2013). The latter has been shown as the predominant pathway of producing IAA (Figure 1.2). Firstly, Trp is deaminated to IPyA by the TRYPTOPHAN AMINOTRANSFERASE OF ARABIDOPSIS1 (TAA1), or by homologous TAA RELATED1 (TAR1) and TAR2. IPyA is then converted to IAA by oxidative decarboxylation catalyzed by the YUCCA (YUC) family of flavin monooxygenases (Zhao, 2014). The role of other Trp-dependent pathways in IAA homeostasis is still unclear since some enzymes involved in potential reactions remain unknown (reviewed by Casanova-Sáez & Voß, 2019). The production of IAA in Trp-auxotrophic *Arabidopsis* plants pointed to the existence of a Trp-independent pathway (Normanly *et al.*, 1993). It was shown that the aforementioned IGP is the branching point of this pathway, and is converted to indole by INDOLE SYNTHASE (INS) in the cytoplasm (Ouyang *et al.*, 2000). Also, INS and possibly the Trp-independent source of IAA generally play an important role in apical-basal pattern formation in early embryogenesis (Wang *et al.*, 2015). Still, there might be a possibility

of converting the cytosolic indole to Trp, thus the relevance of the Trp-independent pathway is not yet resolved (Nonhebel, 2015).

However, free IAA amounts to only a fraction of the total auxin pool. The vast majority of total IAA content is present in biologically inactive forms, conjugated to other molecules to form temporal (reversible) storage forms or irreversibly directed toward degradation. Conjugation, deconjugation, and degradation thus comprise a complex regulatory network of IAA homeostasis. Based on the molecular character of IAA, there are two types of its conjugates: ester-linked (with sugars and sugar alcohols) and amide-linked (with amino acids, peptides, and proteins; reviewed by Ludwig-Müller, 2011; Korasick *et al.*, 2013). The rate of IAA conjugation is greater by orders of magnitude than the rate of biosynthesis (Kramer & Ackelsberg, 2015). There are several gene families identified in *Arabidopsis* to be involved in conjugation (Figure 1.2). Amino acids are conjugated to IAA by the members of the GRETCHEN HAGEN 3 (GH3) family (Ludwig-Müller, 2011). Deconjugation is promoted by IAA-LEUCINE RESISTANT1 (ILR) amidohydrolase (Bartel & Fink, 1995). IAA-Asp and IAA-Glu are irreversible catabolic precursors (Porco *et al.*, 2016). The major catabolic pathway occurs via oxidizing IAA to 2-oxindole-3-acetic acid (oxIAA) by DIOXYGENASE FOR AUXIN OXIDATION (DAO) proteins (Porco *et al.*, 2016; Stepanova & Alonso, 2016). IAA itself contributes to the tight regulation of its own levels, for instance by promoting the expression of *GH3* and *DAO* genes (Stepanova & Alonso, 2016). It should be noted that the absolute values of IAA levels and composition of auxin conjugates are both tissue and species-specific (Ljung, 2013).

Within the plant body, IAA is mainly produced in apical meristems and young growing leaves (Ljung *et al.*, 2001). Thence, IAA is transported in the root-ward direction to sinks (Marchant *et al.*, 2002). However, almost every plant tissue is capable of IAA synthesis leading to the generation of local auxin maxima, which were also shown to be developmentally important (Brumos *et al.*, 2018).

Apart from IAA, plants also produce other substances that had been identified as auxins, namely: indole-3-butyric acid (IBA), 4-chloroindole-3-acetic acid (4-Cl-IAA), and phenylacetic acid (PAA). IBA was eventually revealed to be an inactive and reverse-convertible metabolite of IAA, produced by β -oxidation of IAA in peroxisomes and significant in maintaining IAA homeostasis (Damodaran & Strader, 2019). Much less is known about the physiological roles of other native auxins (discussed by Cook, 2019). PAA and 4-Cl-IAA were shown to be perceived by several auxin receptors (Shimizu-Mitao & Kakimoto, 2014). 4-Cl-IAA, however, only appears to be produced in legumes (Fabaceae; Lam *et al.*, 2015). PAA is

a widespread product of cellular metabolism and was proposed to play a role in plant interaction with microorganisms (Cook, 2019). There are also synthetic auxin analogs, such as 2,4-dichlorophenoxyacetic acid (2,4-D) and 1-naphthaleneacetic acid (1-NAA), which in certain aspects behave as auxins (Simon & Petrášek, 2011). These synthetic forms are often useful in experiments such as transport assays, because of their predominant specificity to influx or efflux, and low interference with cellular auxin metabolism (Ljung, 2013; Petrášek *et al.*, 2014). Synthetic auxins are also utilized in culture media because of their long-term stability compared to IAA (Dunlap *et al.*, 1986).

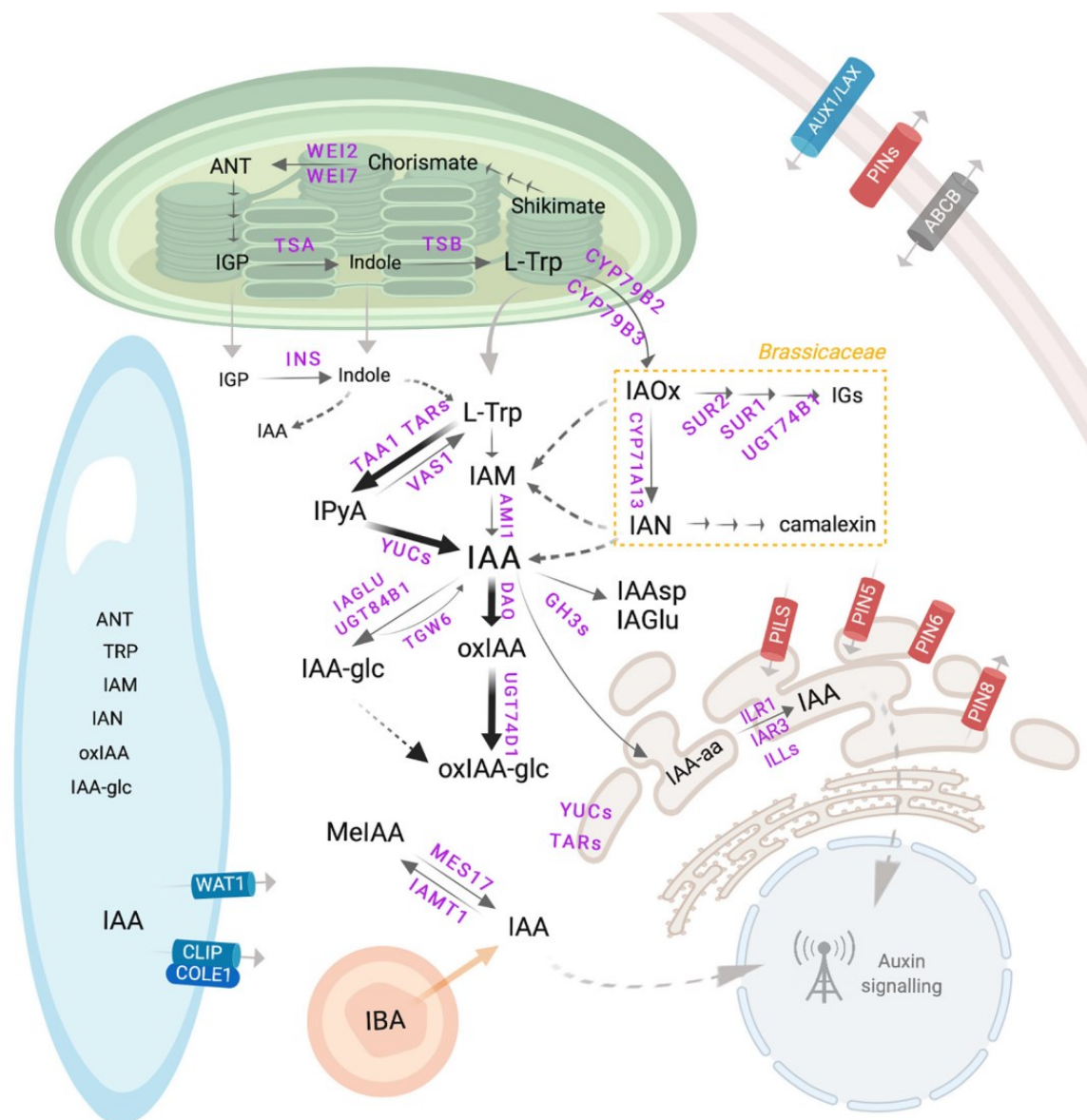


Figure 1.2 | Model of cellular auxin homeostasis in plants. The scheme depicts the production of Trp in plastids and subsequent IAA biosynthesis, conjugation and catabolism pathways. Blue and orange organelle mark a vacuole and a peroxisome, respectively. Adapted from Casanova-Sáez & Voß (2019).

1.4.2 Signaling

Auxin has several receptors, but its main perception occurs via the canonical signaling pathway in the nucleus, which induces transcriptional response (Figure 1.3). The fulcrum of the canonical nuclear signaling pathway consists of (1) auxin receptor TRANSPORT INHIBITOR RESISTANT1/AUXIN SIGNALING F-BOX (TIR1/AFB) from the family of F-box proteins, (2) the co-receptor Auxin/INDOLE-3-ACETIC ACID (Aux/IAA), and (3) AUXIN RESPONSE FACTORS (ARFs; reviewed by Leyser, 2018).

TIR1/AFB is a part of the S-PHASE KINASE-ASSOCIATED PROTEIN1-CULLIN F-BOX (SCF) complex of E3 ubiquitin-ligase (SCF^{TIR1/AFB}; Tan *et al.*, 2007). Aux/IAA proteins form a family of indirect transcriptional repressors, which inhibit transcription by heterodimerizing with ARFs. ARFs are a family of transcription factors recognizing Auxin Response Elements (AREs), specific TGTCTC sequence motifs in promoters of auxin-induced genes (Ulmasov *et al.*, 1995; Ulmasov *et al.*, 1999). Moreover, Aux/IAAs bind the corepressor TOPLESS (TPL), which interacts with histone deacetylases (HDACs) and therefore stabilizes heterochromatinization of relevant sequences (Figure 1.3; Weijers & Wagner, 2016).

When auxin becomes more abundant in the cell, it acts as a “molecular glue” facilitating the interaction of Aux/IAA and SCF^{TIR1/AFB} (Gray *et al.*, 2001; Tan *et al.*, 2007). Subsequently, Aux/IAA is polyubiquitinated by the activated SCF^{TIR1/AFB} complex and thus marked for degradation in the 26S proteasome (Gray *et al.*, 2001). Released from Aux/IAA repressors, ARFs are subsequently able to form homodimers, which allows their binding to AREs and induces a particular transcriptional response (Boer *et al.*, 2014). In *Arabidopsis*, the three principal gene families active in this transcriptional auxin response are significantly expanded and redundant: 6 TIR1/AFBs (TIR1, AFB1-5), 29 Aux/IAAs, and 23 ARFs (Hagen & Guilfoyle, 2002; Liscum & Reed, 2002; Dharmasiri *et al.*, 2005). Although not every single paralog was functionally tested, the importance of these three families in plant development were demonstrated. For instance, some well-known mutant phenotypes from forward genetic screens were shown to be related to auxin signaling: ARF5 = MONOPTEROS, Aux/IAA12 = BODENLOS (Hamann *et al.*, 2002). TIR1/AFBs were more recently proven to be essential in early embryogenesis (Prigge *et al.*, 2020). These amounts of paralogs involved in the canonical signaling pathway imply a significant complexity of the transcriptional auxin response network. The canonical pathway is also involved in root growth inhibition as an example of rapid and partially non-transcriptional response on given auxin concentration (Fendrych *et al.*, 2018). An alternative auxin receptor TRANSMEMBRANE KINASE1 (TMK1) from the family of receptor-like kinases was proposed as an upstream element of ROP-GTPases, this

may broaden the potential spectrum of non-transcriptional auxin responses (reviewed by Dubey *et al.*, 2021).

AUXIN BINDING PROTEIN1 (ABP1) had long been presumed to be an auxin receptor. Since the biochemical proof of its auxin binding ability (Löbner & Klämbt, 1985), many studies have suggested that ABP1 mediates some auxin-regulated cellular processes (reviewed by Tromas *et al.*, 2010). However, these theories were eventually challenged, when the original embryo lethal *abp1* phenotypes were shown result from an off-target mutation (Gao *et al.*, 2015). The recent revision of the proposed developmental roles of ABP1 showed only mild phenotypic defects in *abp1* knock-out mutants (Gelová *et al.*, 2021). While the involvement of ABP1 in auxin perception certainly does not appear as significant as in earlier years, its extent remains to be specified.

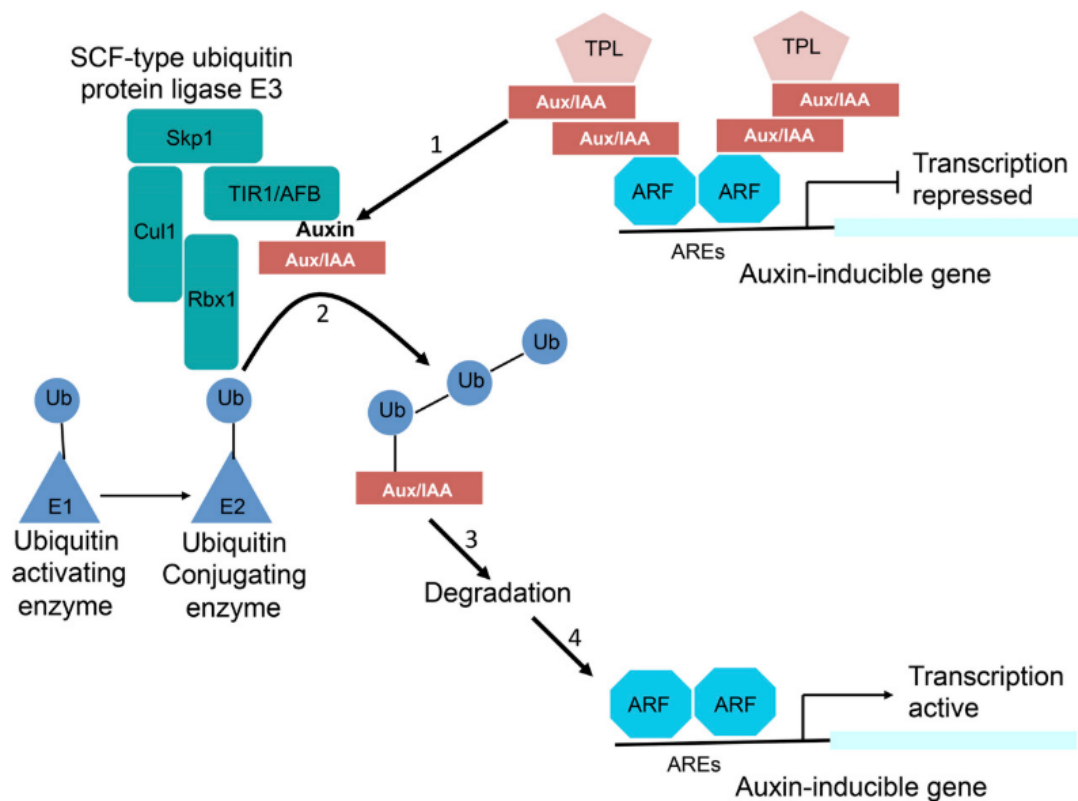


Figure 1.3 | Scheme of nuclear auxin signaling pathway. As a molecular glue, auxin promotes the interaction between TIR1/AFB receptor and co-receptor Aux/IAA, repressor of ARF transcription factors. The interaction leads to polyubiquitination of the latter by TIR1/AFB, which is part of the SCF complex of E3 ubiquitin ligase. Aux/IAA are marked for proteasomal degradation and ARFs then activate or reprime transcription of relevant genes. Adapted from Leyser (2018).

1.4.3 Transport

Besides local cellular metabolism, the spatiotemporal distribution of auxin is additionally determined by its transport across plant tissues. Plants employ two types of auxin transport: long distance and short distance (Zažímalová *et al.*, 2010). Most of the auxin produced in young shoot tissues is transported on longer distances by passive phloem flow to root sinks. The slower, short-distance type is the directional cell-to-cell movement, also known as “polar auxin transport” (PAT), which is mediated by a regulated asymmetric distribution of auxin transport proteins at the plasma membrane (PM; Figure 1.4; Adamowski & Friml, 2015). PAT defines the local morphogenic gradients of auxin, which control growth responses or cell differentiation. For instance, PAT is crucial for gravitropism of both shoot and root, for phototropism of the shoot, for the function of apical meristems, or in the development of vascular tissues (Vanneste & Friml, 2009).

The principle of auxin cell-to-cell movement is based on the chemiosmotic hypothesis of polar ion diffusion (Rubery & Sheldrake, 1974). Because IAA is a weak acid (pK_a 4.7), a part

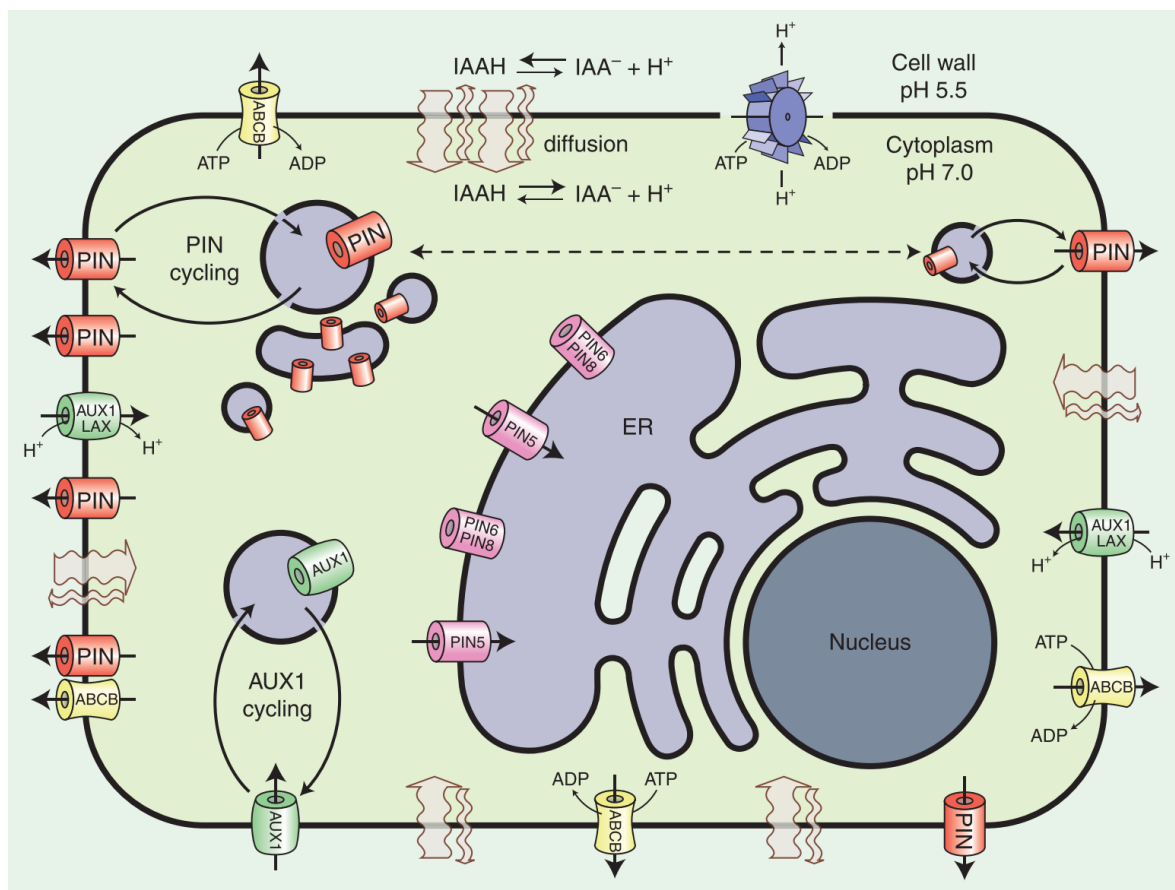


Figure 1.4 | IAA transport on a cellular level. Scheme depicts the principle of IAA diffusion through PM and localizations of IAA membrane transporters. PM-targeted PIN proteins are depicted in red and ER-targeted in pink. The scheme does not include PILS proteins, which localize to ER membrane. Adapted from Zažímalová *et al.* (2010).

of its pool is protonated (IAAH) in the apoplast (pH 5.5) and can enter the cell by passive diffusion. Once IAA is in the cytosol (pH 7), it dissociates to anion form (IAA⁻), which is unable to passively pass through the membrane, requiring the action of transport proteins (Figure 1.4; Vanneste & Friml, 2009).

The cellular uptake of the IAA⁻ is mediated by the AUXIN RESISTANT 1/LIKE-AUXIN RESISTANT 1 (AUX1/LAX) influx carriers from the family of permeases, which act as proton co-transporters (reviewed by Swarup & Bhosale, 2019). AUX1/LAX proteins also connect PAT to the long-distance transport by their activity in phloem and unloading of auxin (Swarup *et al.*, 2001; Marchant *et al.*, 2002). Within PAT, prominent actors determining the direction of auxin transport are represented by the PIN-FORMED (PIN) family of efflux carriers (Petrášek & Friml, 2009). Eight PIN protein paralogs have been identified in *Arabidopsis* (PIN1-8). In general, these proteins consist of two hydrophobic regions, each with five transmembrane domains, which are separated by a hydrophilic loop (HL) protruding to the cytoplasm. PIN1, 2, 3, 4, and 7 possess a larger HL and they are typically targeted to the PM (Adamowski & Friml, 2015). PM PIN proteins then act as the actual efflux carriers, determining the direction of auxin flow via their polar localization at the plasma membrane (Petrášek *et al.*, 2006; Wisniewska *et al.*, 2006). PIN-dependent transport is regulated on multiple levels (reviewed by Zwiewka *et al.*, 2019). The abundance of PIN proteins was shown to be under the transcriptional control of auxin itself (Vieten *et al.*, 2005). The activity of PINs is regulated by an array of posttranslational modifications. For instance, ubiquitination promotes PIN degradation (Leitner *et al.*, 2012). Phosphorylation and dephosphorylation in specific sites of HL of PIN proteins by PINOID kinase (PID), D6 PROTEIN KINASE (D6PK), and PROTEIN PHOSPHATASE 2A (PP2A) modulate their polar localization and efflux activity (Michniewicz *et al.*, 2007; Zourelidou *et al.*, 2014; Zwiewka *et al.*, 2019).

Some other members of the PIN family, namely PIN5 and PIN8, possess a highly reduced HL and reside in the membrane of the endoplasmic reticulum (ER; Mravec *et al.*, 2009; Ding *et al.*, 2012). Finally, there is PIN6 with middle-sized HL, which exhibits both ER and PM localization (Figure 1.4; Simon *et al.*, 2016). The ER-localized PIN proteins are presumed to regulate intracellular auxin homeostasis, together with another family of ER membrane-resident proteins called PIN-LIKES (PILS) (Mravec *et al.*, 2009; Barbez *et al.*, 2012).

Auxin efflux and influx is additionally mediated by the members of ATP-BINDING CASSETTE subfamily B/MULTIDRUG RESISTANCE/P-GLYCOPROTEIN family (ABCB/MDR/PGP; further ABCB), but these typically localize to the PM in a non-polar manner (reviewed by Xu *et al.*, 2014 and Geisler *et al.*, 2017).

1.4.4 What is known about auxin action in algae?

There are several indications for the widespread presence of auxin in green algae (Sztein, *et al.*, 2000; Žižková *et al.*, 2017), but also in other eukaryotes (Basu *et al.*, 2002; Reineke *et al.*, 2008), and prokaryotes (Žižková *et al.*, 2017). It is now a matter of discussion, which biosynthetic pathway(s) may occur in green algae. The IPyA pathway is conserved in land plants, but some works detected orthologs of both key players (TAA and YUCCA) also in charophytes and suggested, that this pathway might have originated therein (Romani, 2017). However, the more recent development argues that this pathway is in fact restricted to land plants (reviewed by Bowman *et al.*, 2021). Moreover, the IPyA pathway was proposed to emerge in land plants partly via horizontal gene transfer (for YUCCA; Yue *et al.*, 2014) and partly by neofunctionalization from another gene (for TAA; Bowman *et al.*, 2017). Orthologs of AMIDASE 1 (AMI1) were, however, identified across whole green lineage suggesting the presence of auxin biosynthesis from IAM in green algae (Bowman *et al.*, 2021). The presence of other potential pathways of auxin biosynthesis in charophytes, both Trp-dependent and Trp-independent are also possible, but still speculative (Nishiyama *et al.*, 2018). For controlling the auxin homeostasis, land plants utilize a variety of enzymes for auxin (de)conjugation and degradation. GH3 orthologs of conjugating enzymes were identified in *Klebsormidium nitens* and *Chara braunii* (Nishiyama *et al.*, 2018), whereas ILR amidohydrolase orthologs are found broadly among streptophytes (Figure 1.5; Bowman *et al.*, 2021). Some products of the reactions catalysed by these enzymes were detected both in several chlorophytes and charophytes, but in very low abundance compared to IAA levels (Žižková *et al.*, 2017). This finding supports the hypothesis of biosynthesis/degradation strategy of auxin homeostasis, but the current evidence does not provide a clear picture.

Some orthologs of the auxin transcriptional signaling pathway genes or their domains were identified within green algae, especially in charophytes (Figure 1.5; Mutte *et al.*, 2018). The prototypic ARF (type C, proto-C-ARF) was shown to be present in the genome of early-diverging *Chlorokybus atmophyticus*, which suggests its ancient origin in the common ancestor of streptophytes (Wang *et al.*, 2020). This ortholog was recently shown to mutually oligomerize and interact with AuxREs promoter elements and with TPL corepressor of *Arabidopsis* (Martin-Arevalillo *et al.*, 2019). Proto-C-ARFs were identified in all charophyte lineages diverging after the Chlorokybophyceae, while proto-A/B-ARFs emerged in higher charophytes (Figure 1.5; Flores-Sandoval *et al.*, 2018; Nishiyama *et al.*, 2018; Cheng *et al.*, 2019; Martin-Arevalillo *et al.*, 2019). Aux/IAA orthologs were identified in the stonewort *Chara braunii* and the desmid *Penium margaritaceum*, but lack conserved domains for interaction with TIR1/AFB

(Mutte *et al.*, 2018; Nishiyama *et al.*, 2018; Jiao *et al.*, 2020). Mutte *et al.* (2018) proposed the existence of a TIR1/AFB precursor in charophytes by detecting the presence of several domains, which exhibited similarities with TIR1/AFB and CORONATINE INSENSITIVE 1 (COI1) receptor and therefore implied the common origin of auxin and jasmonate signaling. Based on these findings it was suggested, that the canonical pathway of auxin signaling, as it is known in land plants, is not present in green algae (Mutte *et al.*, 2018; Bowman *et al.*, 2019; Bowman *et al.*, 2021). Algal proto-ARFs then may be a part of some pre-existing auxin-independent network, which would have been integrated into an auxin-responsive regulatory system when TIR1/AFB gained the capacity to bind Aux/IAA in an auxin-dependent manner around the time of plant terrestrialization (Bowman *et al.*, 2021).

Ohtaka *et al.* (2017) experimentally investigated the possibility of a physiological auxin response in the early-diverging charophyte *Klebsormidium nitens*, reporting an auxin-induced inhibition of cell division and elongation. In the chlorophyte alga *Chlorella vulgaris*, certain concentrations of auxin were shown to both simulate and suppress culture growth, and even induce the accumulation of photosynthetic pigments and other metabolites (Piotrowska-Niczyporuk & Bajguz, 2014). Considering the absence of the canonical signaling pathway, non-transcriptional or other unknown transcriptional responses provide a potential explanation for these observations, however, this issue remains largely unexplored.

Orthologs of all auxin transporters described in the previous subchapter were shown to be present in charophytes (reviewed by Vosolsobě *et al.*, 2020). Polar localization of PIN proteins determines the direction of auxin flow and thereby spatially defines auxin gradients, which play an indispensable role in the morphogenesis of complex structures in land plants. PIN gene orthologs were identified in both early and later diverging charophytes (Figure 1.5; Vosolsobě *et al.*, 2020). Moreover, a unique PIN radiation was uncovered in the genome of the stonewort *Chara braunii* (Nishiyama *et al.*, 2018). A PIN ortholog from *Klebsormidium nitens* (*KfPIN*) was shown to be PM-localized and functional as auxin carrier when heterologously expressed in land plant models *Physcomitrium patens*, *Arabidopsis thaliana*, and *Nicotiana tabacum* BY-2 cell line (Skokan *et al.*, 2019). This work also showed the activation of *KfPIN* auxin transport activity by the PID protein kinase from *Arabidopsis* in frog oocytes. However, *KfPIN* was later shown as unable to complement neither the *pin1* mutant phenotype nor the phenotype of the quadruple mutant of PM-localized PIN proteins of *Arabidopsis* (Zhang *et al.*, 2020). PIN-mediated auxin transport thus possibly occurs in extant charophytes, but its native role is unclear. Also, PAT was detected in the stonewort *Chara corallina* by Boot *et al.* (2012), who showed one-directional, basipetal transport of auxin in internodal cells. Yet, the molecular

background responsible for this transport type in *Chara* is unknown. In antheridia of a different stonewort, *Chara vulgaris*, the antibody against *AtPIN2* revealed the presence of a PIN2-like protein, which suggests a potential role of those carriers in *Chara* morphogenesis (Žabka *et al.*, 2016). In charophytes, the ortholog of AUX1/LAX influx carriers was identified only in *Klebsormidium nitens* (Nishiyama *et al.*, 2018). PIN and AUX1/LAX orthologs are also present in clades of the derived UTC group of chlorophytes, but there the evolutionary acquisition of these orthologs might be explained by HGT rather than common origin with streptophytes, as the latter scenario would be less parsimonious (Vosolsobě *et al.*, 2020). PILS proteins were shown to be evolutionary distinct from and older than PIN proteins and were found in many lineages across the Viridiplantae (Feraru *et al.*, 2012; Vosolsobě *et al.*, 2020). ABCB transporters are ancient and omnipresent proteins with a broader substrate specificity (Cho & Cho, 2013; Xiong *et al.*, 2015), thus their orthologs were unsurprisingly identified in the entire green lineage (Figure 1.5; de Smet *et al.*, 2011; Nishiyama *et al.*, 2018). Auxin transport seems to be the most conserved mechanism of auxin action among streptophytes.

All important components of auxin action mechanisms are present in the genomes of both bryophyte model organisms, *Physcomitrium patens* and *Marchantia polymorpha* (Figure 1.5; Rensing *et al.*, 2008; Bowman *et al.*, 2017; Nishiyama *et al.*, 2018). The canonical pathways of auxin biosynthesis and signaling were shown to be functional and necessary for the development of bryophytes, but unlike in angiosperms, with very limited redundancy (Eklund *et al.*, 2015; Kato *et al.*, 2015; Lavy *et al.*, 2016). PIN-mediated transport is involved in tropisms and phylloid patterning of *Physcomitrium* gametophyte (Bennett *et al.*, 2014), and in gametophore emergence from protonema (Viaene *et al.*, 2014). Interestingly, sporophytes of *Physcomitrium pinb* mutants occasionally exhibited a branched phenotype uncommon in mosses and bearing the resemblance of cooksonoid plant fossils (Bennett *et al.*, 2014; Libertín *et al.*, 2018).

The basic toolkit of auxin action mechanisms has a stepwise origin in charophytes, but is only complete and fully conserved throughout land plants. The role of auxin as a morphogen might have developed after the transition to land. However, the monophyly of bryophytes indicates, that this group might have utilized the toolkit in a model partially or entirely nonhomologous to tracheophytes (Sousa *et al.*, 2018). This implicates the need to study auxin biology also in algae in order to find out, how a possible by-product gradually became a signal coordinating the development and stress responses of plants, in other words, studying green algae might help us to track the path from “just IAA” to auxin.

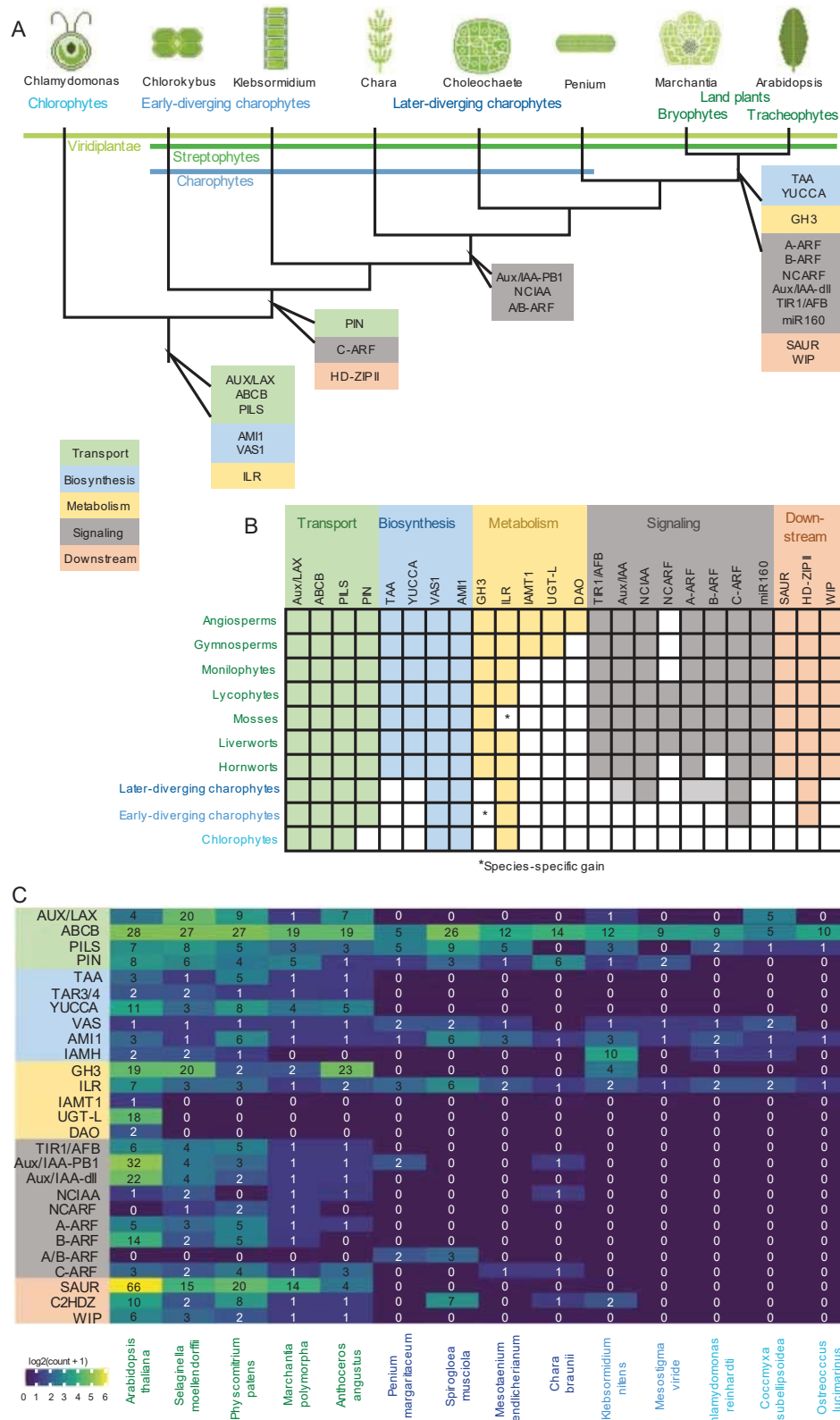


Figure 1.5 | Origin of the important orthologs of auxin mechanism genes in streptophytes. A) Phylogenetic relation of the representative genera with corresponding origin of genes involved in auxin action mechanisms. **B)** Presence of the gene families across major groups of land plants and green algae. **C)** Heat map of the paralog number of studied genes for selected sequenced species of land plants and green algae. Adapted from Bowman (2021).

2 Main objectives

This work is part of a broader project, which investigates the evolutionary origin and significance of auxin transport in streptophyte algae, and to which I contribute with following objectives:

Cultivation of selected representatives of streptophyte algae and study of their native auxin profiles

To date, there is evidence for the presence of auxin and its metabolites in several algal species, although, mostly in chlorophytes (Sztein *et al.*, 2000; Stirk *et al.*, 2013; Žižková *et al.*, 2017). To my knowledge, the data for the comparison of auxin profiles across streptophytes are still missing. In the spirit of de Vries *et al.* (2018), the first part of this objective aims to select and cultivate at least one representative species from five of the six lineages of streptophyte algae (charophytes), with an additional effort to cover more morphotypes among diverse lineages. The availability of published sequential information is an important criterion for selecting strains. The Charophyceae are not included in this work as *Chara braunii* (strain NIES-1604) is the study material of my colleagues Katarina Kurtović, M.Sc. and Mgr. Stanislav Vosolsobě, Ph.D. The second part comprises the analysis of the native auxin profile for each representative. The data will help clarify the extent of IAA biosynthesis and metabolism among charophytes, which could be correlated with the presence or absence of relevant ortholog genes.

In the next objectives, this work will further focus on the desmid *Closterium peracerosum-strigosum-littorale* complex (strain NIES-68, further *Closterium*).

The reaction of the alga *Closterium* to exogenous auxin

In charophytes, auxin response was reported only on *Klebsormidium nitens* (Ohtaka *et al.*, 2017). Mgr. Roman Skokan, the advisor of this project, discovered interesting malformed phenotypes of IAA-treated *Closterium* cells suggesting an unknown form of auxin response. This part aims to test the effect of four different concentrations of exogenously supplied IAA on culture growth, and to apply image analysis to determine which morphological parameters of *Closterium* cells are affected by these specific doses of externally applied IAA.

Native and heterologous transformation of *Closterium*-derived gene constructs and optimization of biolistic transformation method for the alga *Closterium*

So far, experimentally, the heterothallic desmid *Closterium* has been the subject of studying conjugation, the type of sexual reproduction of the Zygnematophyceae (Sekimoto & Fujii, 1992; Tsuchikane & Sekimoto, 2019). The effort to understand the conjugation processes in *Closterium* also resulted in its successful transient and stable nuclear transformation by particle bombardment (Abe *et al.*, 2008, 2011), as well as in the production of CRISPR/Cas9 knock-out lines (Kanda *et al.*, 2017). These achievements coupled with the simple cultivation of *Closterium* convinced us to introduce this alga as a model organism in our laboratory for studying auxin transport in charophytes.

Plasmids developed for *Closterium* transformation via particle bombardment and the sequence of *Closterium* PIN ortholog (*CpPIN*) were provided by prof. Sekimoto. To study *CpPIN* localization, Mgr. Roman Skokan and Ing. Karel Müller, Ph.D. prepared the fluorescence-tagged gene constructs of *CpPIN*. To that end, this objective will involve the optimization of the particle bombardment method for *Closterium* with the BioRad PDS 1000/He system available at our institute, using fluorophore-harboring gene constructs as reporters of successful transformation (Abe *et al.*, 2008). The transformation of *CpPIN* gene construct into *Closterium* is a subsequent aim. As a complementary approach, *CpPIN* will be introduced via particle bombardment into model cell culture line *Nicotiana tabacum* Bright Yellow-2 (BY-2; Barbez *et al.*, 2013).

3 Materials and methods

3.1 Chemicals

Chemicals used in this work were provided by Sigma-Aldrich (Merck, Darmstadt, Germany), Lach-Ner, s.r.o. (Neratovice, Czech Republic), Lachema, a.s. (Brno, Czech Republic), Carl Roth GmbH (Karlsruhe, Germany), Serva Electrophoresis GmbH (Heidelberg, Germany), Duchefa Biochemie B. V (Haarlem, Netherlands), Penta, s.r.o. (Prague, Czech Republic), and MP Biomedicals (Santa Ana, California, USA). Chemicals are listed in Table 3.1 with their corresponding suppliers.

Inorganics	Supplier	Organics	Supplier
Ca(NO ₃) ₂ · 4H ₂ O	Sigma-Aldrich	Agar	Duchefa Biochemie
CaCl ₂	Lachema	Ampicillin	MP Biomedicals
CaCl ₂ · 2H ₂ O	Sigma-Aldrich	Cobalamine (B12)	Sigma-Aldrich
CoCl ₂ · 6H ₂ O	Lach-ner	Biotin (B7)	Sigma-Aldrich
CuSO ₄ · 5H ₂ O	Lachema	DMSO	Sigma-Aldrich
FeCl ₃ · 6H ₂ O	Sigma-Aldrich	EDTA	Serva
FeSO ₄ · 7H ₂ O	Penta	Ethanol (96%,100%)	Lach-ner, Merck
H ₂ SO ₄	Lachema	Glycerol	Lach-ner
H ₃ BO ₃	SigmaAldrich	HEPES	Sigma-Aldrich
K ₂ HPO ₄	Penta	IAA	Sigma-Aldrich
KH ₂ PO ₄	Lach-ner	Isopropyl alcohol	Lach-ner
KNO ₃	Roth	Kanamycin	MP Biomedicals
MgSO ₄ · 7H ₂ O	Sigma-Aldrich	Peptone	Duchefa Biochemie
MnCl ₂ · 4H ₂ O	Sigma-Aldrich	Spermidine	Sigma-Aldrich
Na ₂ EDTA · 2H ₂ O	Sigma-Aldrich	Sucrose	Lach-ner
Na ₂ MoO ₄ · 2H ₂ O	Sigma-Aldrich	Thiamine (B1)	Sigma-Aldrich
NaCl	Lach-ner	TRIS	MP Biomedicals
NaNO ₃	Lachema	Yeast extract	Duchefa Biochemie
ZnSO ₄ · 7H ₂ O	Penta	Media premixes	Supplier
β-Na ₂ glycerophosphate · 5H ₂ O	Sigma-Aldrich	Murashige & Skoog basal salt mixture (#SLCB4697)	Sigma-Aldrich
		Bold's Basal Medium premix (#B5282)	Sigma-Aldrich

Table x | Suppliers of organic and inorganic compounds, and media premixes used in this work. This table does not include chemicals used for the analysis of auxin profiles.

3.2 Plant material and culture conditions

3.2.1 Algal strains and their cultivation

Selected algal strains were obtained from The Culture Collection of Algae at the University of Texas, Austin, USA (UTEX), The Culture Collection of Algae at the University of Göttingen, Germany (SAG), and The Microbial Culture Collection at the National Institute for Environmental Studies, Tsukuba, Japan (NIES). Unless stated otherwise, strains were correspondingly cultured either on 50 ml of solid medium (1,5% agar, w/v) in 100ml Erlenmeyer flasks or in 100ml liquid medium in 250ml Erlenmeyer flasks. The flasks were sealed with a double-folded aluminium foil for better aeration.

The medium pH was adjusted with 1M HCl and KOH using Orion Dual Star pH meter (Thermo Fisher Scientific, Waltham, Massachusetts, USA), pH values for each strain are listed in Table 3.2. Individual strains were cultivated as follows:

Spirogyra pratensis (strain SAG 170.80) and *Mougeotia scalaris* (strain SAG 164.80) were cultivated in 150 ml and 100 ml of liquid Bold's Basal Medium (BBM; Bischoff & Bold, 1963; Table 3.3), respectively, and supplied with soil extract (10 ml/l, preparation described in chapter 3.2.3). *Interfilum paradoxum* was kept on solid Modified Bristol medium (MBM; Ichimura & Itoh, 1977; Table 3.4) supplemented with peptone (1g/l). *Mesostigma viride* (strain NIES-995), and *Closterium peracerosum-strigosum-littorale* complex (strain NIES-68) were cultivated in liquid C medium, *Klebsormidium nitens* (strain NIES-2285) on solid C medium, and *Coleochaete scutata* (strain NIES-4262) both on solid and in liquid C medium (Ichimura, 1971; Table 3.5). *Chlorella sorokiniana* (strain UTEX 1602) and *Mesotaenium endlicherianum* (strain SAG 12.97) were cultivated on solid Bold's Basal Medium with a tripled nitrate dose (3NBBM; Table 3.3) and in the case of *Chlorella* supplemented with soil extract (30 ml/l). *Chlorokybus atmophyticus* (strain SAG 34.98) was firstly cultivated on solid "Erddekot + Salze" Basal medium (ES; SAG Culture Collection, 2007; Table 3.6) with soil extract (30 ml/l). Approximately 60 days from the first inoculation, *Chlorokybus* and *Chlorella* were transferred on C medium with and without soil extract (30 ml/l), respectively.

After the delivery of the strains, the original cultures were left in shade for one day, then they were transferred into the cultivation room and within one week inoculated to relevant media. Although the recommended temperature and lighting conditions for individual strains differed slightly, all were cultivated together under the same conditions in the common cultivation room, as follows: 23°C, 16 h light:8 h dark regime 30-40 $\mu\text{mol photons/m}^2/\text{s}$ illumination (Osram LED ST8E-EM 16W/4000 K).

Inoculation was performed under aseptic conditions in the flow-hood. Cultures of *Closterium* and *Mesostigma* have been subcultured every 3 weeks and other strains once per 30-40 days. Strains kept in liquid media were inoculated by pipetting (with cut-off tips), in the case of *Mougeotia* and *Spirogyra* by transferring 1000 µl of the filamentous biomass into a fresh medium. *Closterium* and *Mesostigma* cultures were inoculated by transferring 650 µl of cells sitting at the bottom of the original flask into a fresh medium. Strains kept on agar were inoculated by scraping roughly 1 cm² of biomass with a spatula and spreading it over the surface of a new medium.

	Strain	Media parameters			Sequential information
		medium	pH	soil extract	
<i>Chlorella sorokiniana</i>	UTEX 1602	3NBBM, <u>C</u> (agar)	7.0	✓ (3NBBM only, 30 ml/l)	G
<i>Mesostigma viride</i>	NIES-995	<u>C</u>	7.5		(G)
<i>Chlorokybus atmophyticus</i>	SAG 34.98	ES, <u>C</u> (agar)	7.5	✓ (30 ml/l)	(G)
<i>Interfilum paradoxum</i>	NIES-2180	<u>MBM+Peptone</u> (agar)	6.0		
<i>Klebsormidium nitens</i>	NIES-2285	<u>C</u> (agar)	7.5		G
<i>Coleochaete scutata</i>	NIES-4262	<u>C</u>	7.5		
<i>Mesotaenium endlicherianum</i>	SAG 12.97	<u>3NBBM</u> (agar)	7.0		G
<i>Spirogyra</i> sp.	SAG 170.80	<u>BBM</u>	7.0	✓ (10 ml/l)	(T)
<i>Mougeotia scalaris</i>	SAG 164.80	<u>BBM</u>	7.0	✓ (10 ml/l)	
<i>Closterium p-s-l complex</i>	NIES-68	<u>C</u>	7.5		

Table 3.2 | Summarization of media parameters and published sequential information for selected strains. Types of media used for the analysis are marked with underlining. **G**, **(G)**, and **(T)** stand for published genome, the genome of a different strain, and transcriptome of a different strain, respectively.

3.2.2 *Nicotiana tabacum* BY-2 cell line

Our laboratory obtained the *Nicotiana tabacum* Bright Yellow-2 (BY-2) cell line from prof. Nagata (Nagata *et al.*, 1992). BY-2 cultures were cultivated in darkness at 27°C in an orbital incubator (150 rpm; New BrunswickTM Innova[®]44, Eppendorf, Hamburg, Germany) in 30 ml of liquid BY-2 medium (pH 5.8, Table 3.7) and subcultured weekly by 1 ml. Stock BY-2 calli were maintained on solid BY-2 medium (0.6% agar, w/v) and subcultured monthly (Petrášek *et al.*, 2003).

3.2.3 Media composition

Composition of media used in this work is listed in Tables 3.3 – 3.8. All media for algae were supplied with vitamins as per (Ichimura, 1971) as follows: B12 (cobalamin; total concentration in medium 7.4 pM), B7 (biotin; 8.2 nM), B1 (thiamine; 38 nM). The vitamin stocks were prepared in 50 mM HEPES buffer in dH₂O (pH 7.8; B12 (1×10⁻⁵ g/ml), B7 (2×10⁻⁴ g/ml), B1 (1×10⁻⁵ g/ml)). These stocks were sterilized by filtering (0.22µm millipore filter, Millex, Merck Millipore), stored at -20°C, and added into the culture medium (1 ml stock per 1 l medium) after autoclaving and cooling. Soil extract supplied to media for several strains (Table 3.2) was prepared as follows: Clean, non-fertilized soil was collected in the botanical garden of The Faculty of Science (Charles University; GPS: 50.0713442N, 14.4227844E). The soil was mixed with dH₂O in a 1:3 ratio and sterilized by autoclaving. After leaving to stand overnight at a room temperature, the mixture was autoclaved again to eliminate the germinating fungal spores activated after the first autoclave step. The decanted extract was separated from the soil by overnight filtering and autoclaved again. The soil extract was stored at -20°C. A corresponding volume was added to the media before autoclaving.

Table 3.3	
Bold's Basal medium	amount per 1 l (dH ₂ O)
NaNO ₃ ¹⁾	250 mg
K ₂ HPO ₄	175 mg
KH ₂ PO ₄	75 mg
MgSO ₄ · 7H ₂ O	75 mg
EDTA	50 mg
KOH	31 mg
CaCl ₂ · 2H ₂ O	25 mg
NaCl	25 mg
H ₃ BO ₃	11.42 mg
ZnSO ₄ · 7H ₂ O	8.82 mg
FeSO ₄ · 7H ₂ O	4.98 mg
CuSO ₄ · 5H ₂ O	1.57 mg
MnCl ₂ · 4H ₂ O	1.44 mg
MoO ₃	0.71 mg
CoNO ₃ · 6H ₂ O	0.49 mg
NiCl ₂	0.003 mg
KI	0.003 mg
VOSO ₄ · 3H ₂ O	0.0022 mg
Na ₂ SeO ₃	0.002 mg
SnCl ₄	0.001 mg

Table 3.4	
Modified Bristol medium	amount per 1 l (dH ₂ O)
KNO ₃	250 mg
KH ₂ PO ₄	175 mg
MgSO ₄ · 7H ₂ O	75 mg
K ₂ HPO ₄	75 mg
NaCl	25 mg
CaCl ₂ · 2H ₂ O	10 mg
A5 solution *	0.1 ml
Fe solution **	0.1 ml
*A5 solution	stock solution (per 100 ml)
H ₃ BO ₃	286 mg
MnSO ₄ · H ₂ O	153 mg
ZnSO ₄ · 7H ₂ O	22 mg
CuSO ₄ · 5H ₂ O	8 mg
Na ₂ MoO ₄ · 2H ₂ O	3 mg
**Fe solution	stock solution (per 100 ml)
FeSO ₄ · 7H ₂ O	200 mg
conc. H ₂ SO ₄	26 µl

Table 3.3 | Chemical composition of Bold's Basal medium (BBM). Listed components were obtained in 50x concentrated BBM premix (B5282, Sigma-Aldrich), thus used as 20ml per 1 l of the medium. ¹⁾ For BBM with triple nitrate (3NBBM) the diluted premix was supplied with additional 500 mg of NaNO₃ per 1 l of the medium (Bischoff & Bold, 1963).

Table 3.4 | Chemical composition of Modified Bristol medium (MBM). 1 l of the medium was supplied with 1 g of peptone (Ichimura, 1977).

Table 3.5			
C medium	stock solution (per 100 ml)	applied volume from stock (per 1 l)	Total amount per 1 l (dH ₂ O)
TRIS	5.0 g	10 ml	500 mg
Ca(NO ₃) ₂ · 4H ₂ O	1.5 g	10 ml	150 mg
KNO ₃	1.0 g	10 ml	100 mg
β-Na ₂ glycerophosphate · 5H ₂ O	0.5 g	10 ml	50 mg
MgSO ₄ · 7H ₂ O	0.4 g	10 ml	40 mg
PIV metals *	-	3 ml	-
*PIV metals	stock solution (per 10 ml)	applied volume from stock (per 100 ml)	Total amount (per 100 ml PIV)
Na ₂ EDTA · 2H ₂ O	-	-	100 mg
FeCl ₃ · 6H ₂ O	118 mg	100 µl	19.6 mg
MnCl ₂ · 4H ₂ O	360 mg	100 µl	3.6 mg
ZnSO ₄ · 7H ₂ O	220 mg	100 µl	2.2 mg
CoCl ₂ · 6H ₂ O	40 mg	100 µl	0.4 mg
Na ₂ MoO ₄ · 2H ₂ O	25 mg	100 µl	0.25 mg

Table 3.5 | Chemical composition of C medium. All listed components were dissolved to individual stock solutions, except Na₂EDTA · 2H₂O, which was dissolved directly before applying other stock solutions within the preparation of PIV metals solution. TRIS was excluded from the media for IAA treatments (Ichimura, 1971).

Table 3.6			
“Erddekokt + Salze” Basal medium	Amount per 1 l (dH ₂ O)		
KNO ₃	200 mg		
MgSO ₄ · 7H ₂ O	10 mg		
K ₂ HPO ₄	10 mg		
Soil extract	30 ml		
Micronutrient solution*	5 ml		
*Micronutrient solution (MS)	stock solution (per 10 ml)	applied volume from stock (per 100 ml)	Total amount (per 100 ml of MS)
MnSO ₄ · H ₂ O	8 mg	100 ul	0.08 mg
ZnSO ₄ · 7H ₂ O	10 mg	200 ul	0.2 mg
Na ₂ MoO ₄ · 2H ₂ O	10 mg	500 ul	0.5 mg
H ₃ BO ₃	20 mg	50 ul	0.1 mg
CuSO ₄ · 5H ₂ O	4 mg	100 ul	0.04 mg
CoCl ₂ · 6H ₂ O	9 mg	12.5 ul	0.01125 mg
FeSO ₄ · 7H ₂ O	-	-	70 mg
EDTA	-	-	80 mg

Table 3.6 | Chemical composition of “Erddekokt + Salze” Basal medium (ES). Components for the Micronutrient solution (MS) were dissolved to individual stock solutions, except for $\text{FeSO}_4 \cdot 7\text{H}_2\text{O}$ and EDTA, which were dissolved directly within MS preparation.

Table 3.7	
BY-2 medium	amount per 1 l (dH ₂ O)
Murashige & Skoog mix (#SLCB4697)	4.33 g
Sucrose	30 g
KH ₂ PO ₄	0.2 g
Inositol	0.1 g
2,4-D solution (20 mg in 200 ml of H ₂ O)	2 ml
Thiamine (from stock: 1 mg in 1 ml of H ₂ O)	1 ml

Table 3.7 | Chemical composition of BY-2 medium. For better solubility, 2,4D-solution was dissolved with one solid piece of KOH. Thiamine stock was added to the media after autoclaving and cooling (Nagata *et al.*, 1992).

Table 3.8	
Lysogeny Broth medium	amount per 1 l (dH ₂ O)
Yeast extract	5 g
Peptone	10 g
NaCl	10 g
Antibiotic (from stock) *	1 ml
*Antibiotic stock solutions	Amount per 1 ml(dH ₂ O)
Ampicillin	100 mg
Kanamycin	100 mg

Table 3.8 | Chemical composition of Lysogeny Broth (LB) medium for *E. coli*. pH was adjusted to 7.0. Required antibiotics were added to the medium after autoclaving and cooling (Luria & Burrous, 1957).

3.3 Determination of *Closterium* culture density

Culture cell density was determined using the Fuchs-Rosenthal counting chamber (hemocytometer) with 0.200mm depth and with (2x) 16 square groups of 1 mm² each, consisting of 16 mini-squares of 0.0625 mm² each. The counting chamber was mounted on Zeiss Axiovert 40C Inverted Phase Contrast Microscope (Carl Zeiss AG, Oberkochen, Germany). To determine the cell density for inoculating a set amount of cells for biolistic transformation (Chapter 4.3), biomass drawn from the bottom several flasks (culture age 10-14 days) was pooled into a reduced volume of medium and the samples were taken for cell counting diluted 30x in C medium before counting. During the construction of growth curves of IAA-treated cultures (Chapter 4.2) dilution was not necessary. Cells were counted by using the principle of two inclusion and two exclusion lines within the 1mm² square borders. Cell density was calculated using the following formula:

$$[\text{cells per ml}] = \frac{\emptyset \text{ number of cells in grid} \times \text{dilution} \times 1000}{3.2 (\text{volume of counting grid in mm}^3)}$$

3.4 Auxin metabolic profiling

3.4.1 Preparation of algal cultures and sampling

Native auxin profiles were analysed in two stages of culture growth: 10-day and 31-day; for simplification: “young” and “old”, respectively. Young and old variants (4 replicates per each) were inoculated on/in 60 ml (in 250ml flasks) and 30 ml (in 100ml flasks) of corresponding media, respectively. Twice as much biomass was inoculated per 60 ml of medium, compared to the 30 ml variants. Due to the number of analysed strains, the cultivation for sampling was performed in three batches.

Sampled biomass was harvested after 10 days (young) and 31 days (old) as follows: Algae on a solid medium were harvested with a spatula, algae in liquid media were harvested by pipetting with cut-off tips. Biomass was transferred on the nylon net filter (20 µm, Merck Millipore), where the excess moisture was filtered away using underpressure. The total fresh weight of biomass per flask was measured and noted. *Mesostigma*, being a flagellate, was harvested by pipetting with follow-up centrifugation (1000 x g) and removal of the supernatant. The biomass was transferred to 2ml thick-walled microcentrifuge tubes, weighed, frozen in liquid nitrogen, and stored at -80°C.

Liquid blank media were sampled by pipetting (500 µl), solid blank media samples were taken by 5ml cut-off pipette tips. Media corresponding to the algal cultures were sampled as

blank media, but with an additional step of centrifugation (1000 x g; in case of liquid media) to remove any residual biomass, or by sampling from the bottom side (in case of solid media) with lacking biomass cover. All media samples were transferred to 2ml thick-walled microcentrifuge tubes, weighed (in case of solid media), frozen in liquid nitrogen, and stored at -80°C.

3.4.2 Analysis of auxin profiles

The following procedures were performed by Ing. Petre Ivanov Dobrev, CSc. and his team. Auxin and its metabolites listed in Table 3.9 were extracted from the homogenized samples by the methanol/water/formic acid mixture method (using corresponding labelled standards), as described in Dobrev & Kamínek (2002) and Přerostová *et al.* (2021). Extractions were analysed according to Přerostová *et al.* (2021) as follows: IAA and its derivatives were separated on Kinetex EVO C18 column (2.6 µm, 150 x 2.1 mm, Phenomenex, Torrance, CA, USA). Mobile phases consisted of A) 5 mM ammonium acetate in water, and B) 95/5 acetonitrile/water (v/v). The following gradient programme was applied: 5% B in 0 min, 7% B in 0.1 to 5 min, 10 to 35 % in 5.1 to 12 min, 100 % B at 13 to 14 min, and 5% B at 14.1 min. Hormone analysis was done on LCMS system consisting of UHPLC 1290 Infinity II (Agilent, Santa Clara, California, USA) coupled to 6495 Triple Quadrupole mass spectrometer (Agilent). MS analysis was done in MRM mode, using the isotope dilution method. Data acquisition and processing were performed with Mass Hunter software B.08 (Agilent).

Analysed compounds	Description
Indole-3-acetic acid (IAA)	Bioactive auxin
2-oxoindole-IAA (oxIAA)	IAA metabolite
Indole-3-acetamide (IAM)	IAA precursor
oxIAA-aspartate (OxIAA-Asp)	IAA metabolite
Phenylacetic acid (PAA)	Phenolic acid with a weak auxin activity

Table 3.9 | Spectrum of analysed compounds in the analysis of auxin profiles. Each compound is supplemented with the description of its role in plants (reviewed by (Ljung, 2013; Zhang and Peer, 2017; Cook, 2019).

3.5 IAA treatment of *Closterium*

3.5.1 Inoculation and culture conditions

Inocula of 175 000 cells from 30-day culture were inserted into 100ml Erlenmeyer flasks with 50 ml of C medium with vitamins (pH 5.5 set with 1M HCl and TRIS component was omitted). Cultures had been treated with IAA (1 μ M, 2.5 μ M, 5 μ M, and 10 μ M; added from 100mM stock solution in DMSO) and with DMSO as a control. The amount of solvent (DMSO) was equalized in all variants according to the 10 μ M variant (5 μ l). IAA and DMSO were added upon inoculation. All variants had three technical replicates. The experiment was performed in a cardboard box (to eliminate background illumination) kept in the cultivation room with the following conditions inside: 24°C, 16 h light/8 h dark regime, 15 μ mol photons/m²/s illumination (Philips MASTER TL-D 36W/840). Cultures were sampled after 11 days for image analysis.

3.5.2 Image analysis

DIC images of IAA-treated *Closterium* cells were analysed with NIS-Elements software (version 5.21) as segmented binary objects generated by the thresholding module. Occasional imprecise segmentation was corrected manually, as well as the separation of touching objects. Mutually overlapping cells were excluded from the analysis. The software scale for measurement was calibrated by the calibration slide.

To determine, how exogenous IAA affects cell size, parameters such as length, width, area, and perimeter were measured. IAA effects on cell shape were determined by calculating the circularity and the ratio of maximal and minimal Feret's diameters (Fmax/Fmin ratio). Circularity shows, how a shape of a certain perimeter is different from a circle of the same area (formula: $Circularity = 4\pi Area/Perimeter^2$), whereas maximal and minimal Feret's diameters are the maximal and minimal distances between parallel tangents of an object. Fmax/Fmin ratio shows the curvature of an object.

3.6 Biolistic transformation of *Closterium*

3.6.1 DNA vectors used

For the optimization part of *Closterium* transformation, cGFP and mScarlet-H, both under chlorophyll a/b binding protein 1 native promoter and terminator (*CpCAB1*) were introduced as reporters of transformation (Figure 3.1). *CpPIN* coding sequence with an inserted sequence of mScarlet-H tag was under the *CpCAB1* promoter for *Closterium* transformation (Abe *et al.*, 2008), or G10-90 constitutive promoter and nopaline synthase terminator (Tnos) for BY-2

transformation (Figure 3.1; Ishige *et al.*, 1999). Constructs for *Closterium* transformation were cloned into the pSA106 vector (conferring bacterial resistance to ampicillin; Abe *et al.*, 2008), G10-90::CpPIN:mScarlet-H construct was cloned into pDGB1 α 1 vector (conferring bacterial resistance to kanamycin; Sarrion-Perdigones *et al.*, 2013). The preparation of gene constructs and cloning was performed by Mgr. Roman Skokan and Ing. Karel Müller, Ph.D. (for details see the Ph.D. thesis of Mgr. Roman Skokan; Skokan, 2021). pSA106 vector and CpPIN coding sequence were obtained from prof. Sekimoto.

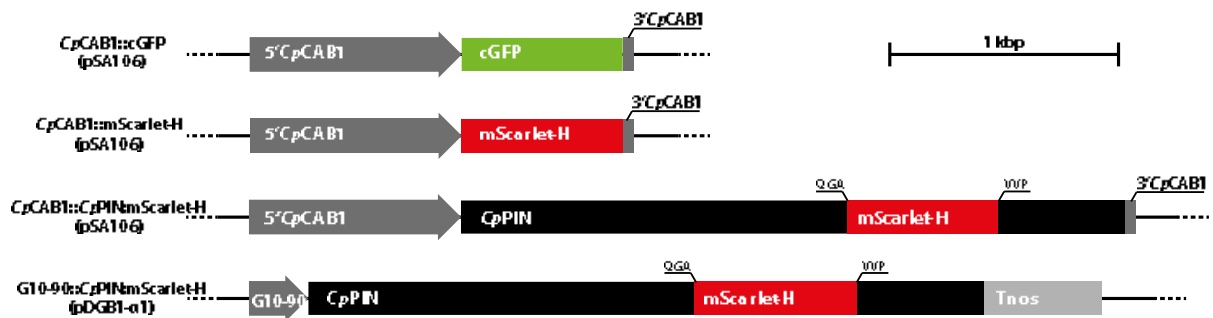


Figure 3.1 | Schemes of gene constructs used in this work. Promoters are represented by grey boxes with arrowheads. mScarlet-H fluorophore was inserted between the sequences for QGA*VVP amino acids of the CpPIN coding sequence.

3.6.2 Preparation of concentrated DNA

Plasmid vectors were introduced to competent bacteria cells (*Escherichia coli*, strain XL1-Blue, Agilent) by a heat shock transformation method as follows: 1 μ l of 100x diluted plasmid DNA (100 pg) was mixed with 50 μ l of bacterial suspension in a 1.5ml Eppendorf tube. After the 30-minute incubation in ice, the mixture was inserted into the thermo-block for a heat shock at 42°C for 45 s. After the 3-minute incubation in ice, 500 μ l of LB medium (Luria & Burrous, 1957; Table 3.8) was added, then the mixture was incubated at 37°C in an incubator for 1 hour. Then the mixture was centrifuged at 1700 x g for 3 min and the majority of supernatant was discarded afterwards. In aseptic conditions, the pellet was re-suspended in the residual medium, and spread onto solid (1.5% agar, w/v) LB selection medium in 9cm Petri dishes. Dishes were incubated overnight at 37°C. Samples from emerged colonies were picked with a sterilized toothpick and inoculated on a fresh solid LB selection medium. The toothpick with remaining cells was inserted into the 12ml test tubes containing 2 ml of liquid LB selection medium. Both solid and liquid media were incubated overnight at 37°C in an incubator or in a water bath with a shaking, respectively. Plasmids were isolated from the liquid cultures by QIAprep Spin Miniprep Kit (Lot no. 163046402; Qiagen, Hilden, Germany) according to the manufacturers

instructions. The insert presence was verified by digestion with restriction enzymes (Table 3.10). The 20µl reaction consisted of the DNA solution (5 µl), FastDigest (FD) buffer (2 µl; Thermo Fisher Scientific), FD enzyme (1 µl per each; Table 3.10), and ddH₂O (remaining volume to 20 µl). Fragmented DNA was visualised on agarose gel electrophoresis (1% , w/v, Serva) with 0.01% (v/v) SYBR[®] Safe DNA Gel Stain (Thermo Fisher Scientific). Gels were scanned in Syngene Gbox documentation system (Synoptics Ltd, Cambridge, England).

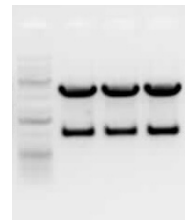
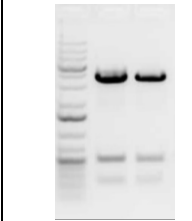
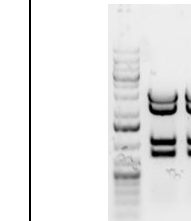
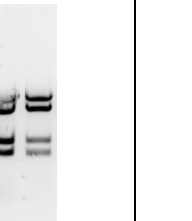
Construct	<i>CpCAB1::cGFP</i>	<i>CpCAB1::mScarlet-H</i>	<i>CpCAB1::CpPIN:mScarlet-H</i>	G10:90:: <i>CpPIN:mScarlet-H</i>
Vector	pSA106	pSA106	pSA106	pDGB1α1
Restriction enzyme(s)	KpnI + NcoI	NotII+ NcoI	KpnI + NotI	PstI
Resulting fragments' length (kbp)	3.6 + 1.0	3.8 + 0.5 + 0.24	3.0 + 2.2 + 1.0 + 0.8	4.3 + 1.9 + 0.91 + 0.63
Gel electrophoresis (scan)				

Table 3.10 | Verification of the insert presence by digestion with restriction enzymes. The table shows the types of restriction endonucleases used for the digestion, resulting length of fragments and scan images of electrophoresis gels (with generuler 1 kb plus ladder on the left; Thermo Fisher Scientific).

For a high-volume amplification, corresponding verified colonies on the solid media were inoculated by a toothpick to 100ml Erlenmeyer flasks with 20 ml of LB selection medium and incubated overnight at 37°C in a water bath with shaking. Plasmids were isolated by QIAprep Spin Miniprep Kit (bacterial biomass equivalent of 5 ml of the grown liquid suspension per one Prep column).

In order to achieve higher plasmid concentration in a set volume of water, the plasmid DNA was precipitated using the sodium acetate (NaAc) & ethanol DNA precipitation method, as follows: The DNA sample was mixed with the 1/10 volume of NaAc (3M, pH 5.2) and 2.5 volume of 96% ethanol. After 45-minute incubation on ice, the mixture was centrifuged at 10000 x g/4°C for 10 min. In two consecutive steps, the pellet was twice resuspended in 900 µl of 70% ethanol and centrifuged at 10000 x g/4°C for 5 min. Then, the pellet was air-dried in an open tube and re-suspended in ddH₂O to 1µg/µl concentration.

3.6.3 Preparation of the biological material

Closterium cells for transformation were prepared according to Abe *et al.* (2008) with slight modifications as follows: *Closterium* cells from several 11 to 13-day cultures were harvested by pipetting to a small volume of C medium. The total cell number was calculated as described in Chapter 3.3. Harvested cells were centrifuged at 995 x g for 2 min with slow acceleration and deceleration and then resuspended in C medium to the cell density of approximately 10 million cells per ml. From this cell suspension, 2 million cells (200 μ l) were inoculated per one Petri dish ($d = 6$ cm) containing solid C medium (1.5% agar, w/v) and spread evenly with a spatula. After the evaporation and/or soaking of the excess liquid medium, the dishes were sealed by surgical tape and placed in a cultivation box (Sanyo, MLR-315H; Sanyo Electric Co. Ltd., Osaka, Japan) at 23°C under continuous light with 10 μ mol photons/m²/s light intensity (Osram FL40SS-W/37) for 48 h. Then the transformation procedure was performed (Chapter 3.6.4 and 4.3). Afterwards, dishes were placed back in the cultivation box for 48 h under the same conditions (to induce the activity of the *CpCAB1* promoter) before observation.

BY-2 cells for transformation were prepared according to (Barbez *et al.*, 2013) as follows: 5 ml of BY-2 cell suspension from 2-day old culture was transferred on a stack of 2 filter papers and filtered with underpressure. Then, the top filter paper with cells was placed into a Petri dish ($d = 6$ cm) with solid BY-2 medium (0.6% agar, w/v). The BY-2 cells were transformed soon afterwards and observed after 20 h after the transformation.

3.6.4 Preparation and coating of microcarriers

This procedure was performed according to the BioRad manual for the PDS-1000/He system (BioRad, 2013) as follows: 3 mg of gold microcarriers (BioRad; 0.6 μ m diameter for *Closterium*, 1.6 μ m diameter for BY-2) were mixed with 100 μ l of 70% ethanol in a 1.5ml tube and vortexed for 3 min. After a 1min incubation on ice, the suspension was centrifuged (1 min at 3500 x g). Then, the supernatant was removed, and the pellet was resuspended in 50 μ l of ddH₂O and vortexed. After 1 min, the suspension was centrifuged (1 min at 400 x g). After the removal of the supernatant, the pellet was resuspended in 50 μ l of 50% glycerol. The suspension was homogenized in ultrasonic bath for 10 s.

The following microcarrier coating procedure corresponds to 1 bombardment for BY-2 (1x 500 μ g of microcarriers), or 10 bombardments for *Closterium* (10x 50 μ g of microcarriers, or in the case of microcarrier amount optimization, the volume of suspension was adjusted accordingly): In a 1.5ml Eppendorf tube, 8 μ l of golden microcarrier suspension was mixed with 2.4 μ l of plasmid DNA by pipetting and vortexing in short pulses. The mixture was

incubated on ice for 15 minutes. Then, 8 μl of 2.5M CaCl_2 and 3.2 μl of cold 0.1M spermidine were added respectively and mixed again by pipetting and vortexing in short pulses. The mixture was incubated on ice for 10 minutes. In three consecutive steps, the suspension was carefully centrifuged (15 s at 50 x g) and resuspended in 100 μl of 70% ethanol, then in 50 μl of 100% ethanol and finally in 10 μl (for BY-2) or 100 μl (for *Closterium*) of 100% ethanol. While mixing continuously, 10 μl aliquots of the mixture were transferred to the centre of macrocarrier disks by pipetting. The final volumes of prepared mixtures were adjusted accordingly to the planned number of bombardments.

The bombardment was performed with BioRad PDS-1000/He System (Bio-Rad Laboratories Inc., Hercules, California, USA). The plate with BY-2 cells was placed to position 2 (6cm gun-to-target distance), microcarriers were accelerated by the helium pressure of 1100 psi. The vacuum in the chamber was set to 27 inches of Hg. In the case of *Closterium*, the parameters of the method varied transformation, as the method was subjected to optimization (Chapter 4.3).

3.7 Microscopy

DIC microscopy was performed with Nikon Eclipse E600 (Nikon Corporation, Tokyo, Japan) equipped with DVC 1310C digital camera (National Instruments, Austin, USA) connected to Lucia software (version 4.7, Laboratory Imaging, Prague, Czech Republic). Confocal microscopy was carried out with Nikon Eclipse Ti (Nikon Corporation) with a spinning disk unit (Yokogawa CSU-X1, Andor Technology, Belfast, N. Ireland) connected to Prime BSI sCMOS camera (Teledyne Photometrics, Tucson, USA). The confocal setup was controlled by NIS-Elements software (version 5.20.02, Laboratory Imaging).

3.8 Statistical analyses

Statistical analyses were performed in RStudio (Version 1.4.1103; RStudio Team, 2020). This software was also utilized for the construction of charts using the **ggplot2** package (Version 3.3.3; Wickham, 2016). The significance between control media and samples of biomass and culture media measured by LC-MS analysis was determined by t-test. The dynamics of auxins in biomass, culture media, and control (blank) media were modelled by linear regression and confidence intervals were determined by bootstrap sampling of measured data with 1000 variances according to Schönbrodt (2012). Data from the IAA treatment of *Closterium* were

statistically analysed using Tukey multiple comparisons test applied on linear mixed-effects model with the **lme4** package (Version 1.1-26; Bates *et al.*, 2015). Figures were composed in Adobe Illustrator (version 24.0; Adobe Systems).

4 Results

4.1 Cultivation of selected representatives of streptophyte algae and study of their native auxin profiles

4.1.1 Selection of representative strains and their cultivation

For studying the endogenous levels of auxin and its metabolites in algae, at least one representative strain was selected from five of the six lineages of streptophyte algae, with an effort to cover various morphotypes in more diverse groups. The following strains were selected and introduced into our cultivation setup (Figure 4.1 and 4.2): *Chlorella sorokiniana* (strain UTEX 1602) was selected as an outgroup representative of chlorophyte algae (Trebouxiophyceae) with the published genome (Arriola *et al.*, 2017). *Mesostigma viride* (strain NIES-995; Mesostigmatophyceae) and *Chlorokybus atmophyticus* (strain SAG 34.98; Chlorokybophyceae) were selected as the sole representatives of their respective lineages. *Interfilum paradoxum* (strain NIES-2180) and the full genome-sequenced *Klebsormidium nitens* (strain NIES-2285; Hori *et al.*, 2014) was selected as a unicellular and a filamentous representative of the Klebsormidiophyceae, respectively. Planar disc-forming *Coleochaete scutata* (strain NIES-4262) was chosen as the representative of the Coleochaetophyceae. *Mougeotia scalaris* (strain SAG 164.80) and *Spirogyra sp.* (strain SAG 170.80) represented the filamentous Zygnematophyceae. From unicellular Zygnematophyceae, early diverging and sequenced *Mesotaenium endlicherianum* (strain SAG 12.97; Cheng *et al.*, 2019), and the desmid *Closterium peracerosum-strigosum-littorale* complex (strain NIES-68) were selected. Media types used in cultivation of the strains described above are depicted in Figures 4.1 and 4.2.

A small yet detectable presence of bacteria was observed in the cultures of *Spirogyra* and *Mougeotia*. By contrast, *Chlorokybus*, *Coleochaete*, and *Mesostigma* cultures showed a much higher bacterial contamination, which was already the case upon their purchase from their respective culture collections. Decontamination efforts were not performed, as these would be very time-consuming and perhaps impossible.

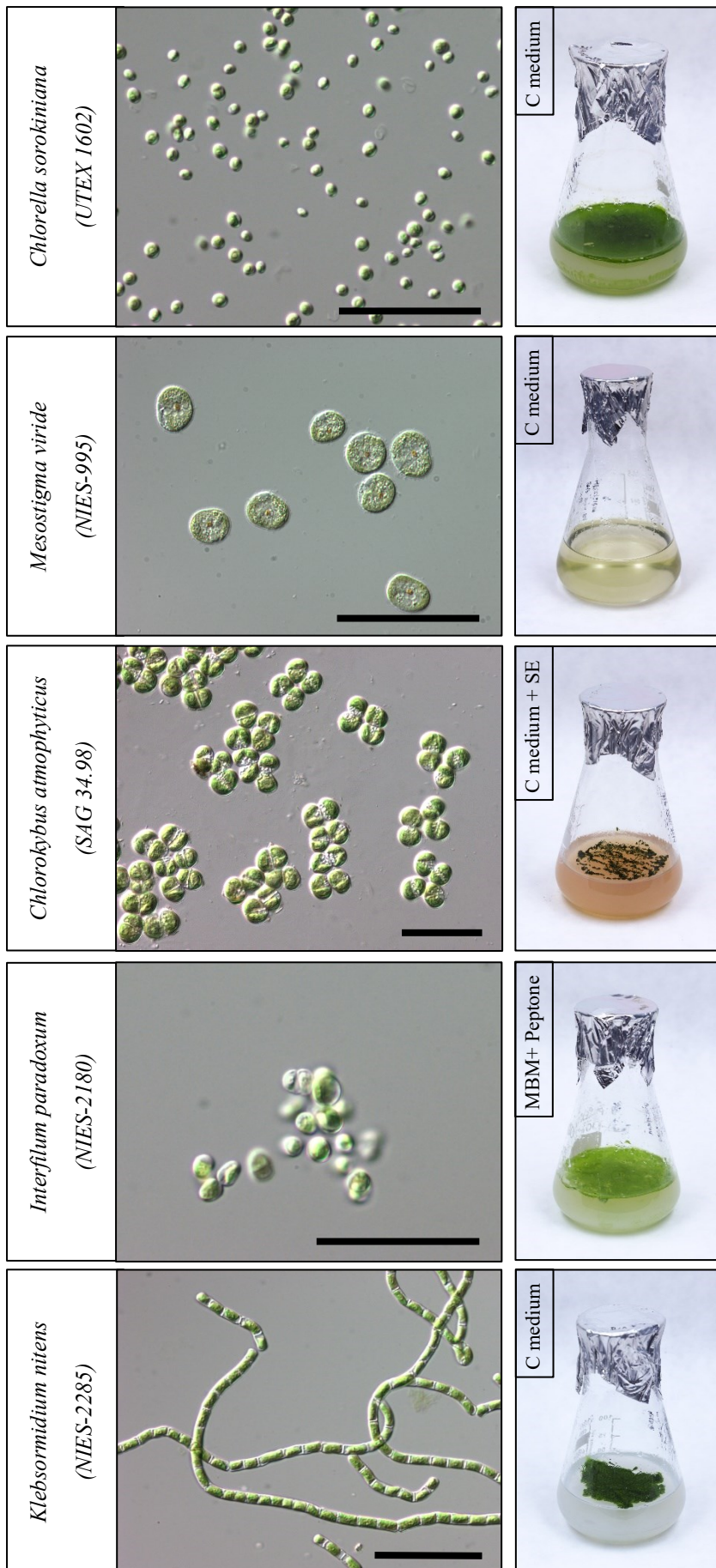


Figure 4.1 | DIC microscopy images of cultivated representatives of extant streptophyte algae (KCM grade), *Chlorella sorokiniana* represents chlorophyte algae as an outgroup strain; scale = 50 μ m. On the right side of each microphotograph the corresponding medium with culture is depicted, SE stands for soil extract.

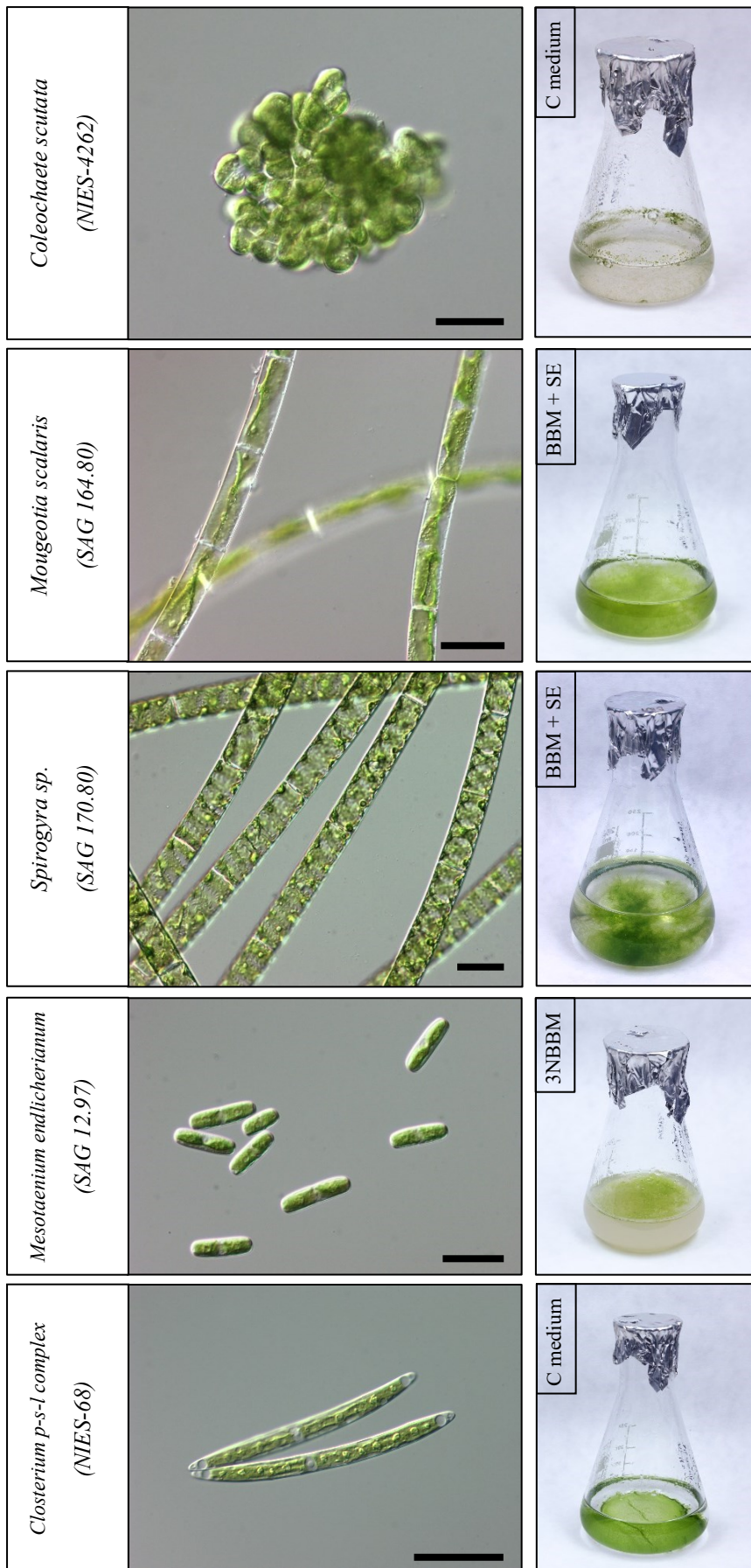


Figure 4.2 | DIC microscopy images of cultivated representatives of higher streptophyte algae (ZCC clade); scale = 50 μ m. On the right side of each microphotograph the corresponding medium with culture is depicted, SE stands for soil extract.

4.1.2 Analysis of endogenous levels of auxins in algae

Levels of auxins, namely: IAA, oxIAA, IAM, oxIAA-Asp, and PAA were measured in algal biomass, in the corresponding culture media and in blank media (control without biomass), all sampled at two stages of culture growth: young (10-day) and old (31-day). The only exception was for *Mesostigma*, which was sampled only in the young stage, as the old cultures were heavily contaminated and contained a significant portion of dead cells. Measured values are listed in Table 4.1. A heatmap was constructed to visualize the differences between biomass, culture media, and blank media (Figure 4.3). Also, models of IAA dynamics were estimated by the linear regression with bootstrap sampling of measured data to correctly visualize the relation between two culture stages.

IAA was detected in biomass of all studied species and its levels varied from units of pmol/g of fresh weight (FW) to dozens of pmol/g FW. *Chlorella*, *Mesostigma*, *Chlorokybus*, and *Interfilum* exhibited similar levels of IAA (Table 4.1). However, in the case of *Mesostigma*, the IAA detected in the biomass could have been taken up from the medium, judging by similar levels detected also in the blank medium. *Chlorella*, *Chlorokybus*, and *Interfilum* released IAA into the media, but the latter to a lesser extent than the former two (Table 4.1, Figure 4.3 and 4.4). IAA levels were rather low in *Klebsormidium* biomass, with a similar concentration in media. *Coleochaete* produced between 20 to 30 pmol/g FW of IAA both in young and old stages, but the release to medium was negligible (Table 4.1). In *Mesotaenium*, *Closterium* and especially in *Mougeotia*, endogenous IAA concentrations increased with culture age, the young vs. old difference in *Mougeotia* was the largest among all sampled algae. This alga also exhibited a massive release of IAA into the medium reaching over a thousand pmol/g ml (Table 4.1). By contrast, endogenous levels of IAA are lower in closely related *Spirogyra*, even when compared with blank media (Table 4.1, Figure 4.4).

Some products of IAA catabolism (oxIAA, oxIAA-Asp) and an IAA biosynthetic precursor (IAM), as known from auxin metabolism and biosynthesis pathways in land plants, were also detected in the sampled algae. *Interfilum* exhibited exceptional levels of some catabolites, but these could have been taken up from the medium (Table 4.1). When filtering out the effect of blank media, the production of these compounds (putative catabolism) is apparent in representatives of all lineages, mostly in *Coleochate* (Figure 4.3). Still, IAA catabolites were mostly present in much lower concentrations compared to free IAA (Table 4.1).

Table 4.1			Analysed compounds [pmol/g FW (biomass), or pmol/ml (media)]														
species (+medium)	type	age	IAA	SD	p	oxIAA	SD	p	oxIAA-Asp	SD	p	IAM	SD	p	PAA	SD	p
<i>Chlorella</i> (C, agar)	biomass	Y	15.87	2.00	**	3.33	0.30	***	0.47	0.05		0.05	0.01	***	83.86	30.51	
		O	28.94	5.31	***	2.87	0.11		0.37	0.03	**	0.10	0.01	***	77.59	24.66	
	medium	Y	8.92	5.44		2.64	0.46	**	0.20	0.05	**	0.03	0.01	**	73.62	31.67	
		O	14.52	2.40	**	2.98	0.25		0.22	0.03	***	0.05	0.01	**	103.64	10.23	
	blank	Y	1.00	0.62		1.89	0.01		0.40	0.05		0.02	0.00		68.68	5.96	
		O	0.55	0.38		2.32	0.38		0.46	0.21		0.02	0.47		80.56	0.02	
<i>Mesostigma</i> (C)	biomass	Y	15.92	4.40		0.33	0.08	***	0.16	0.03	***	0.04	0.00	***	171.32	44.22	**
		O															
	medium	Y	11.55	1.60		0.06	0.02		0.03	0.00	*	0.01	0.00	*	2.96	1.68	
		O															
	blank	Y	12.89	2.83		0.04	0.01		0.02	0.00		0.00	0.00		2.01	1.91	
		O															
<i>Chlorokybus</i> (C+SE, agar)	biomass	Y	11.98	1.30	**	2.22	0.14	*	0.19	0.05		0.27	0.07	***	71.78	11.43	***
		O	18.83	2.48	***	0.27	0.02	***	0.07	0.01	***	0.15	0.01	***	100.01	10.31	***
	medium	Y	17.74	1.40	**	3.74	0.36		0.08	0.01	***	0.13	0.01		77.47	15.34	***
		O	29.20	3.44	***	0.73	0.07	***	0.35	0.46		0.09	0.00	**	173.56	17.27	**
	blank	Y	1.07	0.40		3.62	0.56		0.18	0.02		0.10	0.02		168.09	15.61	
		O	0.54	0.20		2.98	0.30		0.17	0.01		0.07	0.00		218.48	15.07	
<i>Interfilum</i> (MBM+peptone, agar)	biomass	Y	13.71	4.74	**	35.75	3.81		1.82	0.31	**	1.63	0.09	*	122.47	20.65	
		O	15.63	8.99	***	23.53	3.17	***	0.59	0.16		0.93	0.14	**	106.24	44.14	
	medium	Y	3.14	1.74		33.91	1.41		1.02	0.11		1.29	0.03	*	113.74	11.17	
		O	6.58	1.04	*	46.18	4.23	***	0.39	0.07	***	0.89	0.04	***	166.76	29.29	**
	blank	Y	2.28	1.14		35.23	2.78		1.01	0.14		1.46	0.08		126.98	10.06	
		O	1.44	0.48		61.16	3.60		0.62	0.04		1.36	0.10		118.71	11.26	
<i>Klebsormidium</i> (C, agar)	biomass	Y	2.71	1.11	.	3.14	0.37	***	0.54	0.05	*	0.06	0.01	***	98.93	10.12	**
		O	2.47	0.79	**	2.67	0.07		0.46	0.05		0.03	0.00	*	106.60	18.92	
	medium	Y	2.70	1.69		2.26	0.33	*	0.29	0.01	*	0.02	0.00	*	74.32	16.74	
		O	2.82	1.24	**	2.77	0.17		0.36	0.08	*	0.02	0.00		72.89	10.53	
	blank	Y	1.00	0.62		1.89	0.01		0.40	0.05		0.02	0.00		68.68	5.96	
		O	0.55	0.38		2.32	0.47		0.46	0.02		0.02	0.00		80.56	22.52	
<i>Coleochaete</i> (C)	biomass	Y	26.97	5.56	***	2.35	0.16	***	0.69	0.11	***	0.15	0.02	***	17.84	16.88	
		O	26.26	4.82	***	2.79	0.09	***	0.66	0.04	***	0.35	0.04	***	13.43	13.01	
	medium	Y	0.39	0.18		0.10	0.02	***	0.13	0.03	**	0.00	0.00		2.03	1.84	
		O	0.32	0.26	.	0.25	0.05	***	0.06	0.01		0.01	0.00	***	1.45	1.24	.
	blank	Y	0.38	0.12		0.01	0.00		0.24	0.04		0.00	0.00		3.14	2.26	
		O	0.09	0.03		0.01	0.00		0.06	0.01		0.00	0.00		3.03	1.91	
<i>Mesotaenium</i> (3NBBM, agar)	biomass	Y	4.03	3.19	*	2.02	0.51		0.70	0.43	*	0.03	0.01	***	200.12	25.38	
		O	14.31	9.76	*	1.19	0.20	***	0.46	0.15	***	0.07	0.06	***	38.50	19.50	*
	medium	Y	0.82	0.43		2.99	0.12		0.27	0.20		0.01	0.00	*	212.96	20.33	***
		O	19.27	14.88	***	1.54	0.45	*	0.21	0.10		0.03	0.01	***	344.20	99.77	***
	blank	Y	0.95	0.68		2.68	0.61		0.25	0.13		0.01	0.00		199.87	60.43	
		O	0.47	0.27		2.31	0.34		0.14	0.01		0.01	0.00		201.42	53.61	
<i>Closterium</i> (C)	biomass	Y	1.28	0.36	***	0.30	0.10	***				0.03	0.00	***	11.31	2.72	***
		O	6.01	2.30	***	0.58	0.12	***				0.10	0.03	***	24.97	8.00	***
	medium	Y	0.13	0.07		0.03	0.01					0.00	0.00	**	0.76	0.09	**
		O	0.13	0.10		0.81	0.03	***				0.01	0.00	***	7.73	0.81	***
	blank	Y	0.19	0.06		0.03	0.01					0.00	0.00		0.49	0.06	
		O	0.14	0.05		0.04	0.01					0.00	0.00		0.71	0.22	
<i>Mougeotia</i> (BBM+SE)	biomass	Y	5.61	1.47	**	1.64	1.28	**	0.42	0.19	***	0.05	0.00	.	10.05	2.09	**
		O	44.20	9.86		0.55	0.09	***	0.27	0.06	***	0.05	0.00	**	22.58	7.62	*
	medium	Y	79.35	47.59	*	0.71	0.10	***	0.04	0.01		0.03	0.00	*	2.29	1.11	
		O	1223.42	484.74	***	1.00	0.11	***	0.07	0.01	***	0.04	0.00		5.34	3.06	
	blank	Y	26.56	9.66		0.41	0.04		0.03	0.01		0.04	0.00		2.96	1.14	
		O	22.83	12.72		0.33	0.01		0.03	0.00		0.03	0.00		2.75	1.88	
<i>Spirgyra</i> (BBM+SE)	biomass	Y	2.33	0.83	***	0.12	0.02	***	0.25	0.05	***	0.01	0.01	**	12.19	3.77	**
		O	2.16	0.34	**	0.12	0.02	***	0.38	0.32	***	0.01	0.00	***	5.95	3.07	
	medium	Y	12.73	4.53	.	0.02	0.01	***	0.03	0.00		0.00	0.00	***	2.19	1.02	
		O	27.27	10.31		0.05	0.01	***	0.05	0.01	***	0.00	0.00	***	2.83	2.77	
	blank	Y	26.56	9.66		0.41	0.04		0.03	0.01		0.04	0.00		2.96	1.14	
		O	22.83	12.72		0.33	0.01		0.03	0.00		0.03	0.00		2.75	1.88	

Table 4.1 | Levels of auxins in algal biomass and culture media. Levels are presented as concentrations in pmol/g FW or ml of media and expressed as means with their standard deviations (for biomass and media: $n = 4$, for blank media: $n = 2$, each sample measured in technical duplicates). Levels of significance between biomass/media and blank (control) and are indicated as follows: ‘‘ $p < 0.1$, * $p < 0.05$, ** $p < 0.01$, *** $p < 0.001$ (t-test). Yellow bars visualize the levels within one column. Hatching indicates the absence of data; abbreviations: Y: young, O: old, SD: standard deviation, p: p-value.

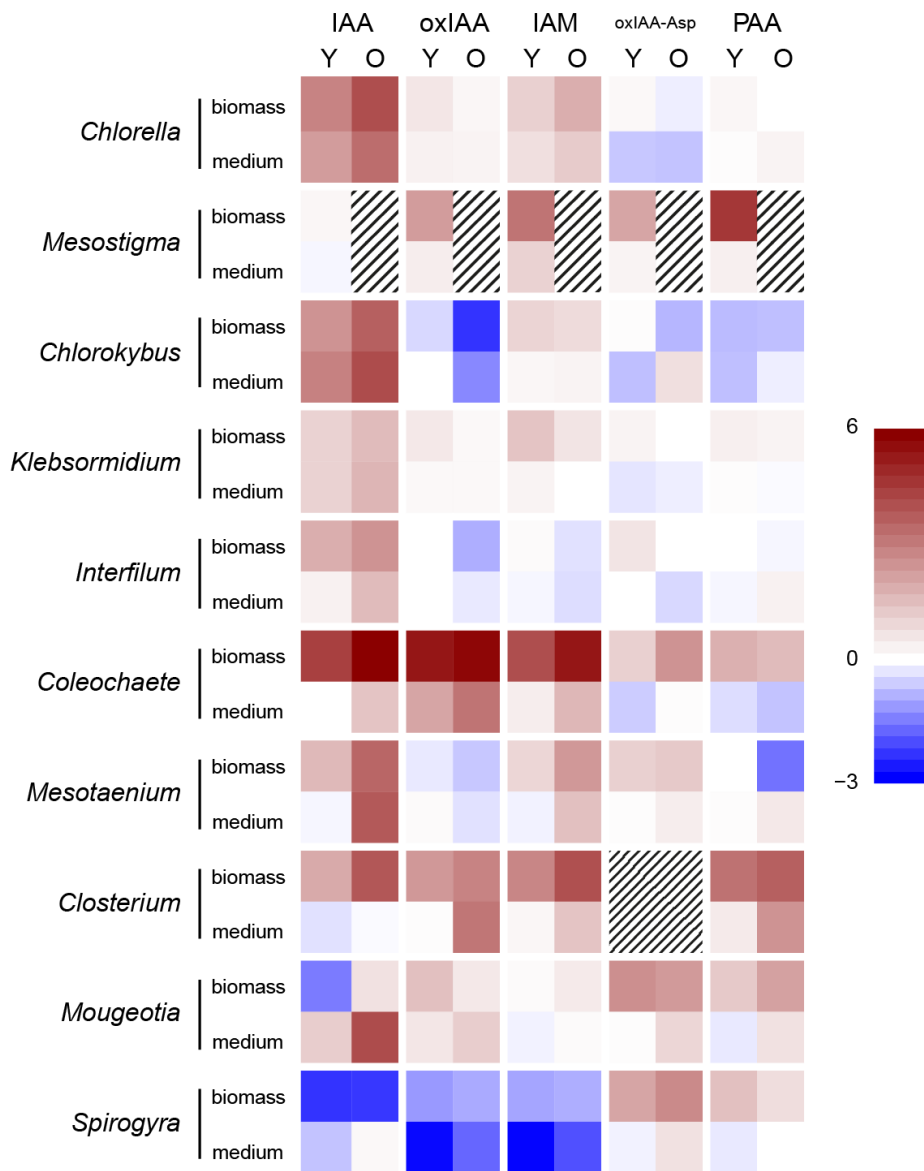
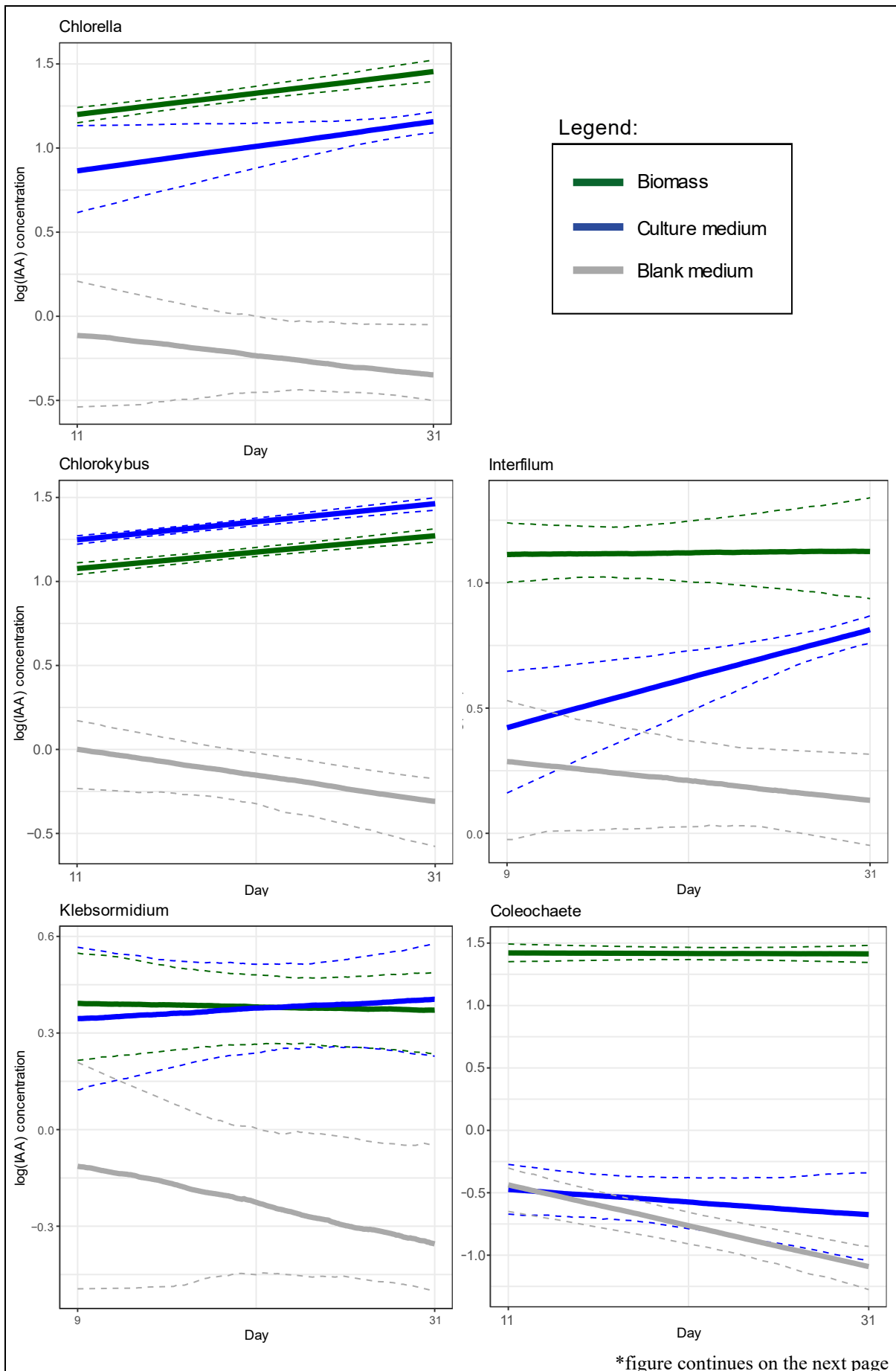


Figure 4.3 | Heatmap of detected auxins related to their levels in blank media. Means of measured values in biomass and culture media were divided by the mean value measured in the corresponding blank medium. Logarithms of resulting values were rendered as a heatmap with the color scale indicating multiples of the corresponding blank medium (red = increase, blue = decrease); abbreviations: Y: young, O: old.



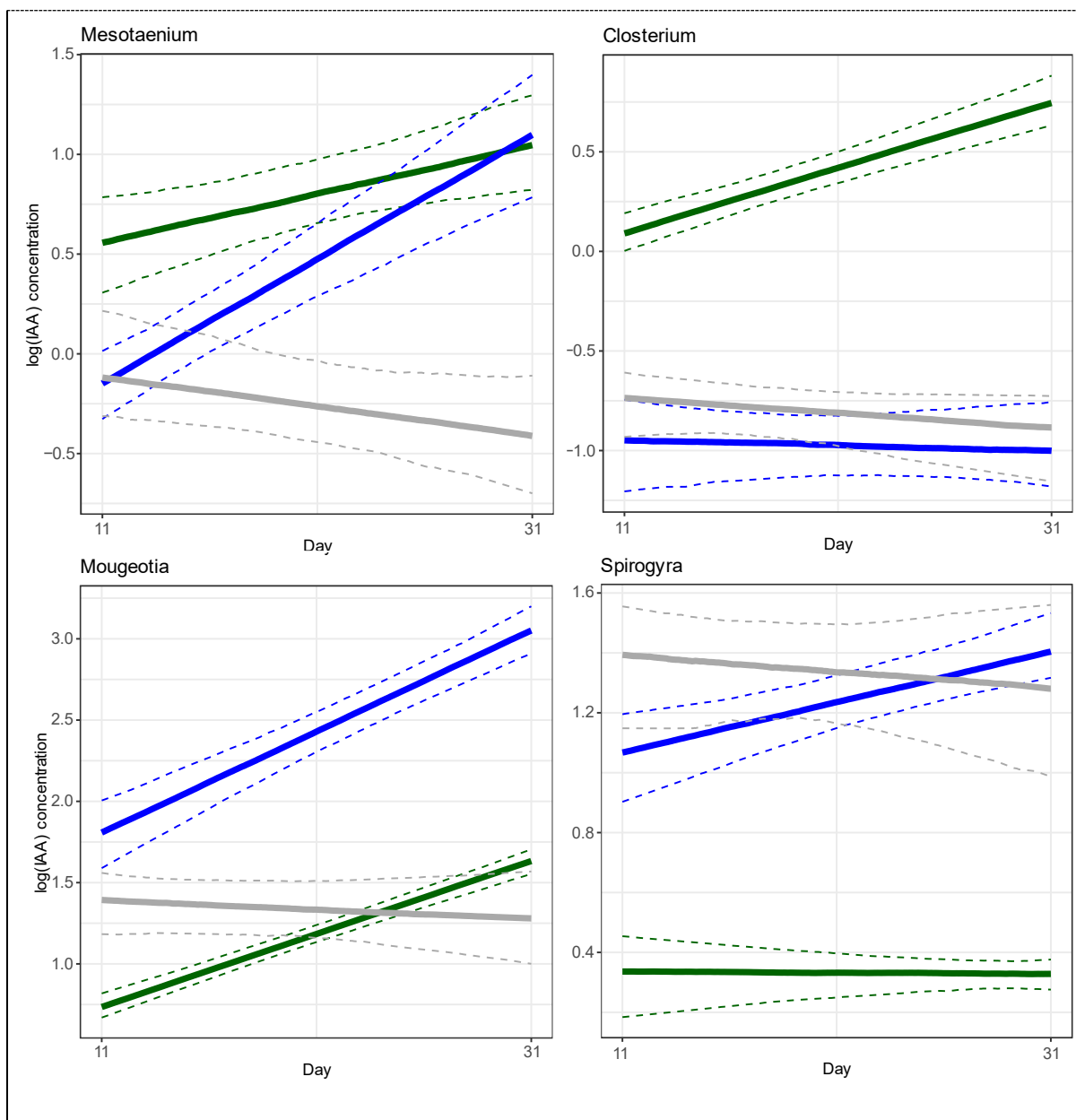


Figure 4.4 | Model of IAA content dynamics in algal biomass, culture media, and blank media between two sampling points (young vs. old culture). The model was constructed by linear regression and 95% confidence intervals (dashed line) were determined by bootstrap sampling of the data measured at two sampling points (day 11 - young, day 31 - old). Values are expressed as decadic logarithms of estimated IAA concentrations in pmol/g or ml. Due to the partial absence of data for *Mesostigma*, the model was not constructed for this alga.

PAA was detected in hundreds of pmol/g or ml and PAM in dozens of pmol/g or ml in several samples, but these values were restricted only to variants cultivated on media solidified with agar (Table 4.1). However, *Mesostigma*, *Coleochaete*, *Closterium*, *Mougeotia*, and *Spirogyra* (all in liquid media) exhibited the presence of PAA in biomass and only a fraction levels in blank media (Table 4.1).

4.2 The reaction of *Closterium* to exogenous auxin

4.2.1 The effect of exogenously applied auxin on *Closterium* morphology

Inocula of *Closterium* cells were cultivated in media with four different concentrations of IAA (1 μM , 2.5 μM , 5 μM , 10 μM). After 11 days of cultivation, cells were sampled and their morphological parameters, i.e. length, width, area, perimeter, circularity, and the ratio of maximal to minimal Feret's diameters were measured by image analysis.

Closterium cells (strain NIES-68) typically have a narrow, elongated, and slightly curved shape, with over 100 μm in length (Figure 4.2A). IAA treatment induced substantially diverse phenotypes. For instance, cells were crooked, asymmetrical, bulged at the isthmus, or elongated with multiple isthmi suggesting incomplete cytokinesis, or even exhibited the combination of all (Figure 4.5B).

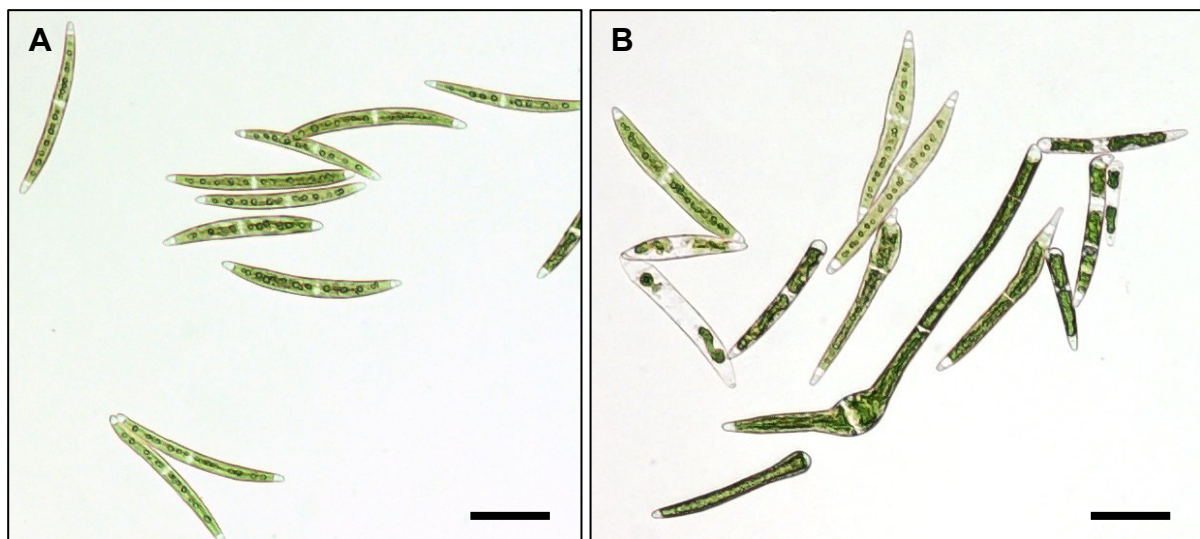
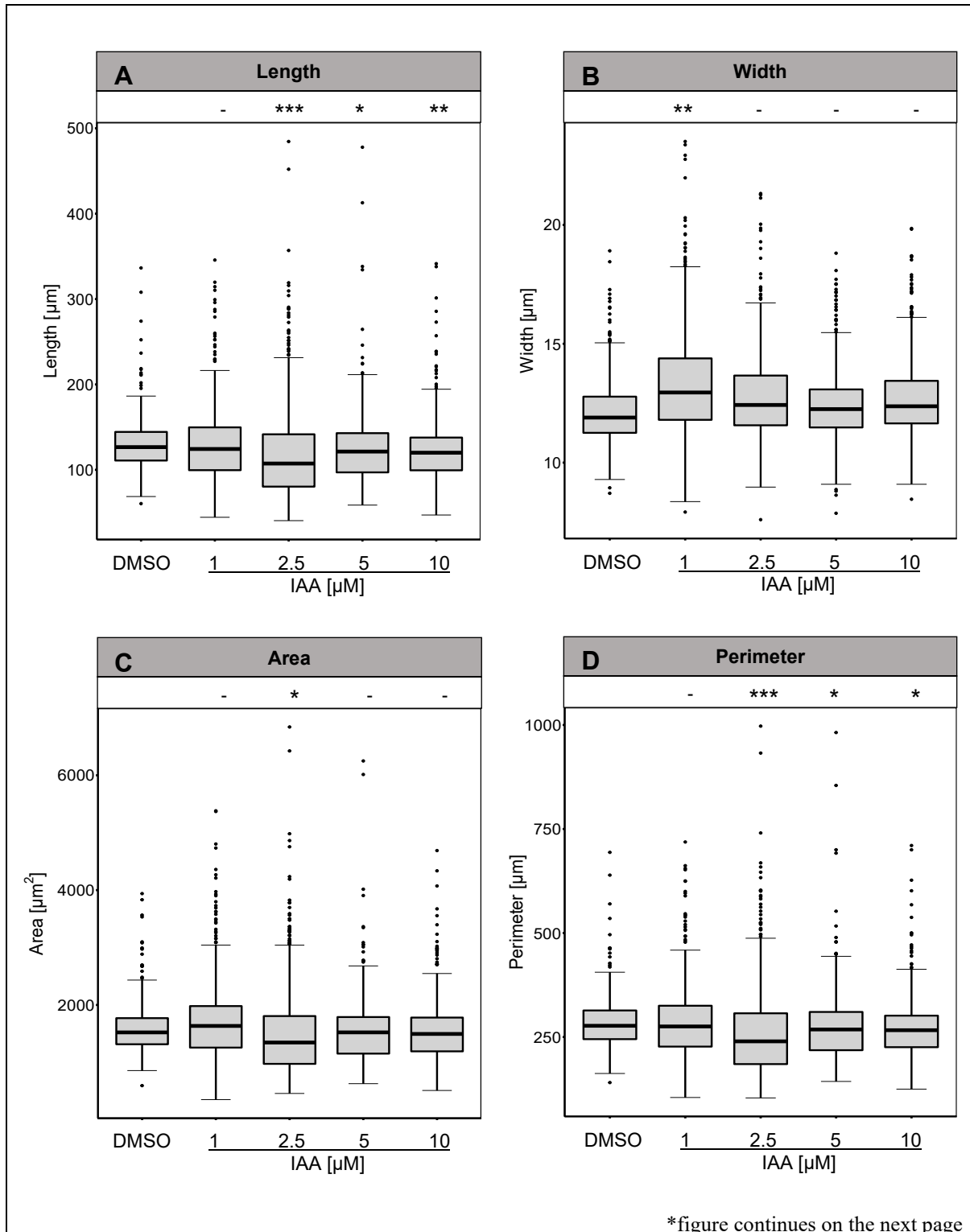


Figure 4.5 | Phenotypes of control and IAA-treated cells. A) control (DMSO), B) 2.5 μM IAA, scale = 50 μm

Cells with various malformations were present in all tested variants, but among individual concentrations of the treatment, the 2.5 μM variant was shown to have the most significant effect on the majority of parameters (Figure 4.5B and 4.6). In terms of cell length, area, and perimeter the average values are slightly lower in the 2.5 μM variants, when compared to the control. Higher average values were shown for the width (only 1 μM significant) and circularity (1 μM , 2.5 μM , and 10 μM significant; Figure 4.6B and E). The ratio of max/min Feret's diameters was significantly lower after 2.5 μM IAA treatment indicating that more cells are either more curved or wider with relation to cell length. All tested concentrations (especially 1 μM and 2.5 μM) resulted in a higher variability of the measured parameters, with more outlying values, both higher and lower (Figure 4.6). These data suggest

that after auxin treatment a majority of cells were slightly smaller, less elongated, and more circular, but on the other hand, there was also a higher number of cells with oppositely deviated values. The effect of IAA on *Closterium* morphology manifested more extensively in the lower range of the concentrations used.



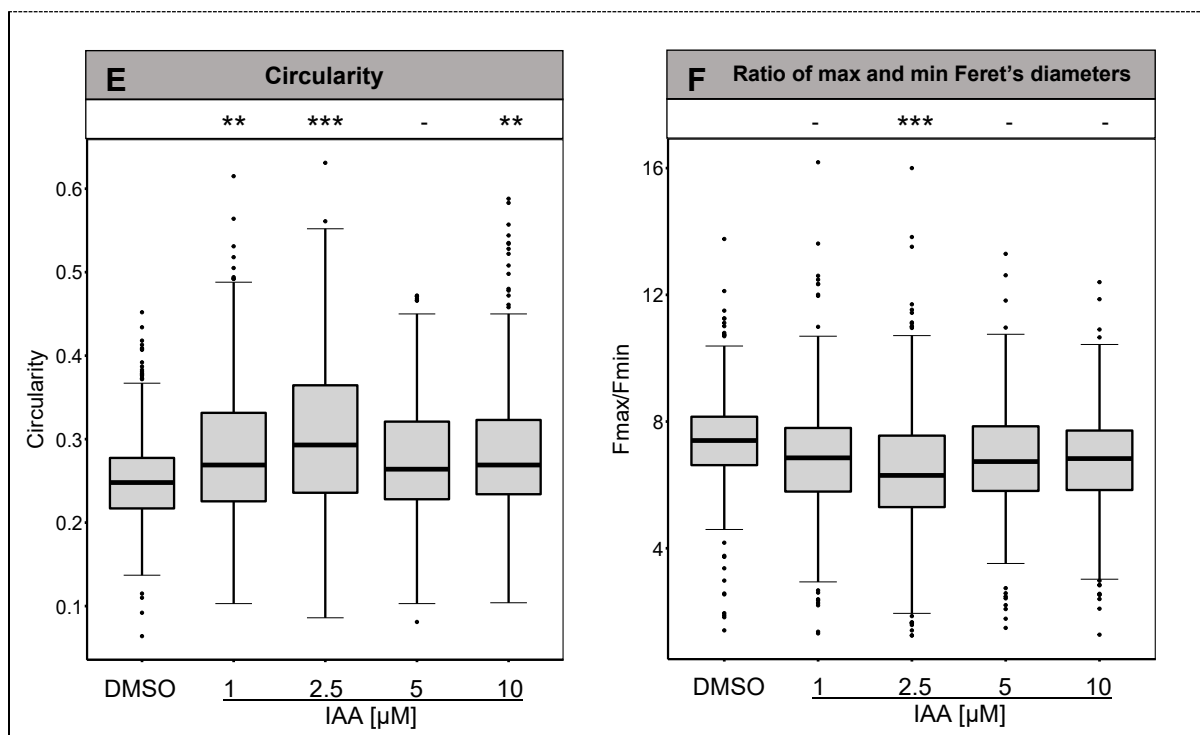


Figure 4.6 | Analysis of *Closterium* morphological parameters affected by various IAA concentrations. Length (A), width (B), area (C), perimeter (D), circularity (E), and the ratio of maximal and minimal Feret's diameters (F) are presented as boxplots. Level of significance is related to the control (DMSO) and indicated by asterisks and a dash ('-' $p > 0.05$, * $p < 0.05$, ** $p < 0.01$, *** $p < 0.001$; Tukey multiple comparisons test for linear mixed effects model; variants were tested as 3 biological replicates, each with $n > 150$).

4.2.2 Inhibitory effect of IAA on *Closterium* culture growth

During *Closterium* IAA treatment, all cultures were sampled to determine the cell count for the construction of growth curves.

The exposure of *Closterium* cultures to IAA showed a concentration-dependent effect on growth, i.e. the higher amount of IAA was applied, the slower the culture grew (Figure 4.7). Because only live cells were included in the cell count determination, a lethal effect on the culture growth was revealed for the 10 μM IAA concentration, which manifests after six days from inoculation (Figure 4.7A).

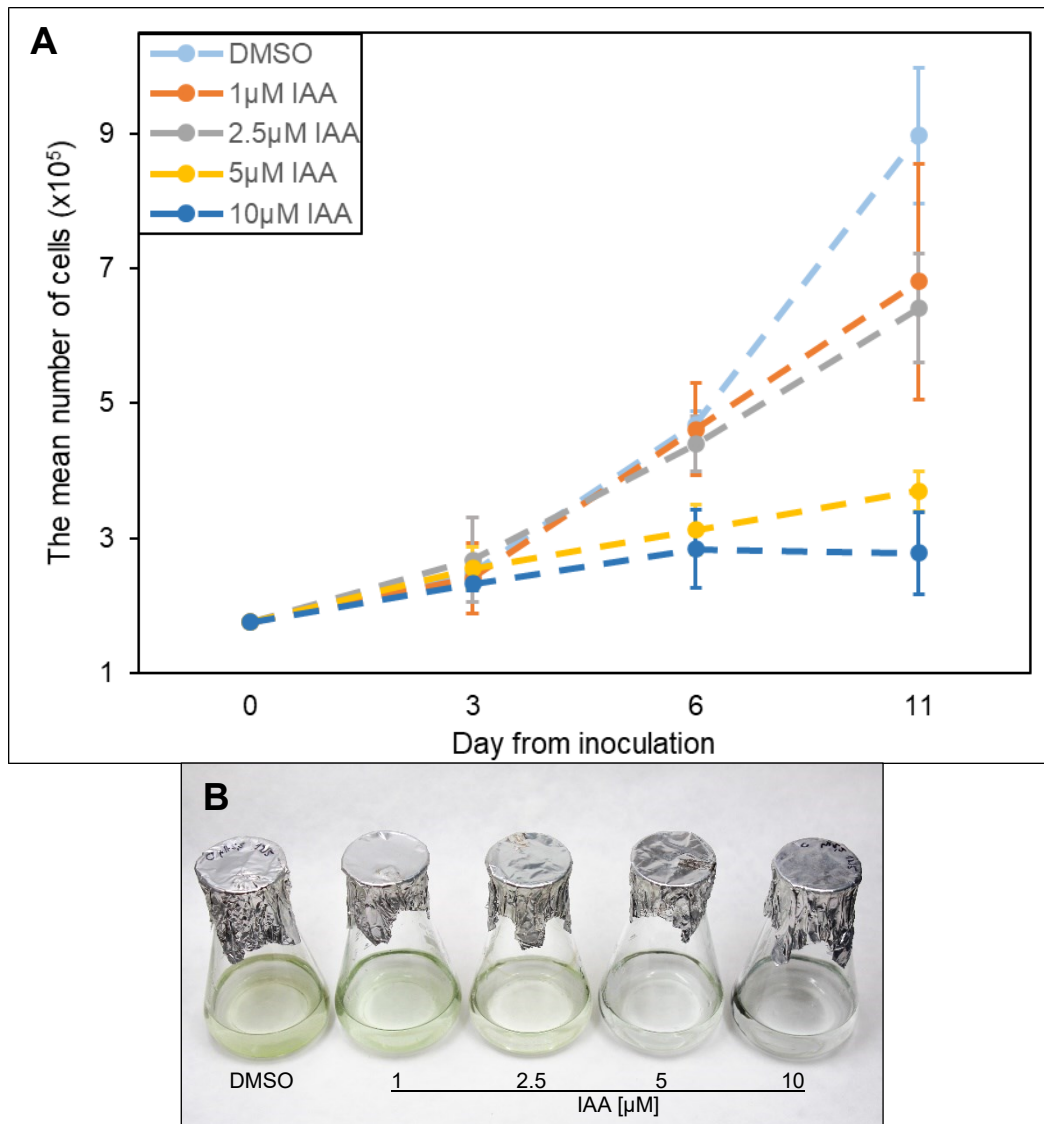


Figure 4.7 | Concentration-dependent effect of IAA on the growth of *Closterium* cultures. A) Growth curves of IAA-treated cultures, day 0 is the day of inoculation (1.75×10^5 cells), error bars represent standard deviation. **B)** Cultures before sampling (day 11).

4.3 Native and heterologous transformation of *Closterium*-derived gene constructs and optimization of biolistic transformation method for the alga *Closterium*

Particle bombardment (or biolistic method) is a technique developed for plant and fungal cell transformation, where foreign nucleic acid molecules coated onto golden, or tungsten particles (microcarriers) are delivered to the nucleus or plastid. Microcarriers are accelerated to a high speed to penetrate the cell wall. Once the DNA is located and expressed in the nucleus, the cell is considered transiently transformed. Delivered DNA can also be designed to incorporate into the genome, in which case, cells can be transformed stably (Sanford *et al.*, 1993).

This optimization followed up on methodical approaches applied by Abe *et al.* (2008, 2011) and Regensdorff *et al.* (2018) in the transformation of *Closterium* and *Mougeotia*, respectively. *Chlamydomonas*-adapted green fluorescent protein (cGFP) and mScarlet-H red fluorescent protein were used as reporters of transformation, expressed under the native promoter (and terminator) of chlorophyll a/b-binding protein1 (*CpCAB1*). Golden microcarriers with 0.6 μm in diameter were used for all biolistic experiments. Within the scope of optimization, the appropriate setup of several parameters was determined for the highest yield of transformed cells per one plate.

4.3.1 Optimization - setup of the gene gun device

BioRad PDS 1000/He system is a static device with a chamber, where the plate with target cells is inserted. The chamber is designed to adjust the microcarrier flight distance (gun-to-target distance, i.e. the distance between the stopping screen and target cells) by placing the target shelf in four defined positions (Figure 4.8A). Target shelf positioning affects how much the microcarriers disperse before hitting the target cells. This system uses a high-pressure burst of helium to accelerate microcarriers to high velocity, which can be adjusted by rupture disks designed to snap under specific pressure (Figure 4.8B). Using 6cm Petri dishes with solid medium (1.5% agar) coated with target cells, only positions 2 and 3 were selected for determining the optimal distance. Rupture disks for 650 psi, 1100 psi, and 1350 psi of helium were tested for the effect of different microcarrier velocities. To find the optimal combination of the distance and velocity, the effect of the two latter parameters was tested simultaneously. The highest number of transformed cells was observed in variants at the 6cm distance (position 2) and the pressure of 1350 psi, whereas position 3 with all pressure values exhibited a near-zero number of transformed cells (Figure 4.9). Thus, the microcarrier flight distance has a much stronger effect than the velocity.

4.3.2 Optimization - the effect of the microcarrier amount

For the transformation of higher plant material, 0.5 mg of golden microcarriers is typically used per single bombardment (BioRad, 2013). Using this microcarrier amount resulted in the observation of a small amount (units) of fluorescent *Closterium* cells per plate (Figure 4.10A), however, on the 4th day after transformation, a lethal effect was apparent in the middle of the plate, where the microcarrier density is the highest (Figure 4.10B). *Closterium* cells are elongated and narrow with a nucleus in the isthmus, between semi-cells. This shape perhaps makes the cell susceptible to be killed by multiple penetrations while using a high amount of microcarriers (Figure 4.10B and C). Therefore, the effects of 5x, 10x, and 20x lower

microcarrier amounts were tested (i.e. 0.1 mg, 0.05 mg, and 0.025 mg). The other parameters were set as per the highest transformation efficiency observed previously (see subchapter 4.3.1), i.e. placing the target cells in position 2 and setting the pressure to 1350 psi. The highest numbers of transformed cells per plate were observed in the 0.05mg variants (Figure 4.10A).

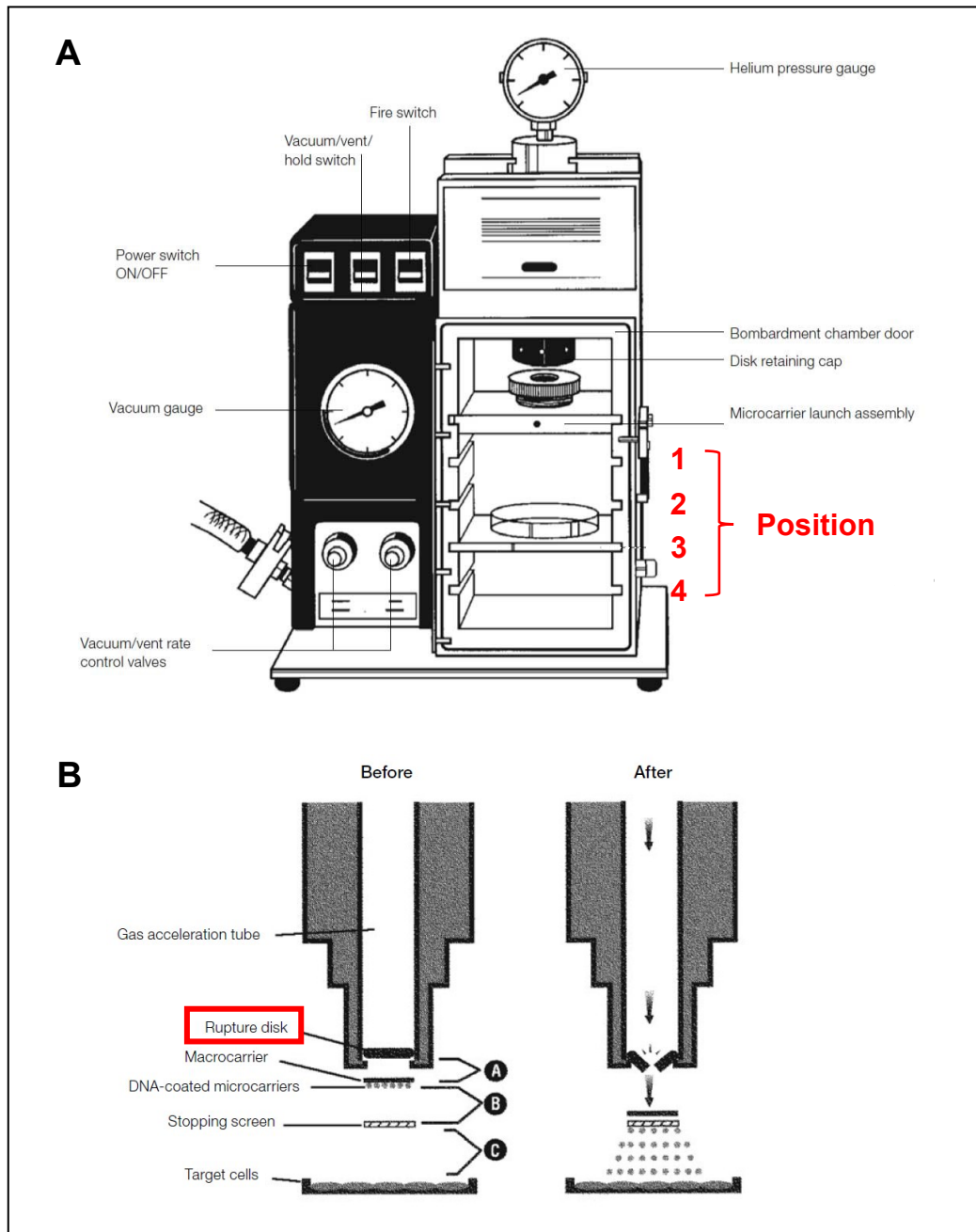


Figure 4.8 | Scheme of the BioRad PDS 1000/He™ system. A) Front view on the main unit of the device with described parts. Four optional positions of the target shelf are highlighted in red. **B)** Simplified scheme of particle delivery to target cells. Particle acceleration is controlled by the thickness of the rupture disk (red box), which is designed to snap under the specific pressure of helium. Adapted and modified from the device manual (BioRad, 2013)

These observations were consistent in both biological replications, even though the overall efficiency varied (Figure 4.10A). Also, the lethal effect on cells in the plates' centre was suppressed by lowering the microcarrier amount (Figure 4.10B).

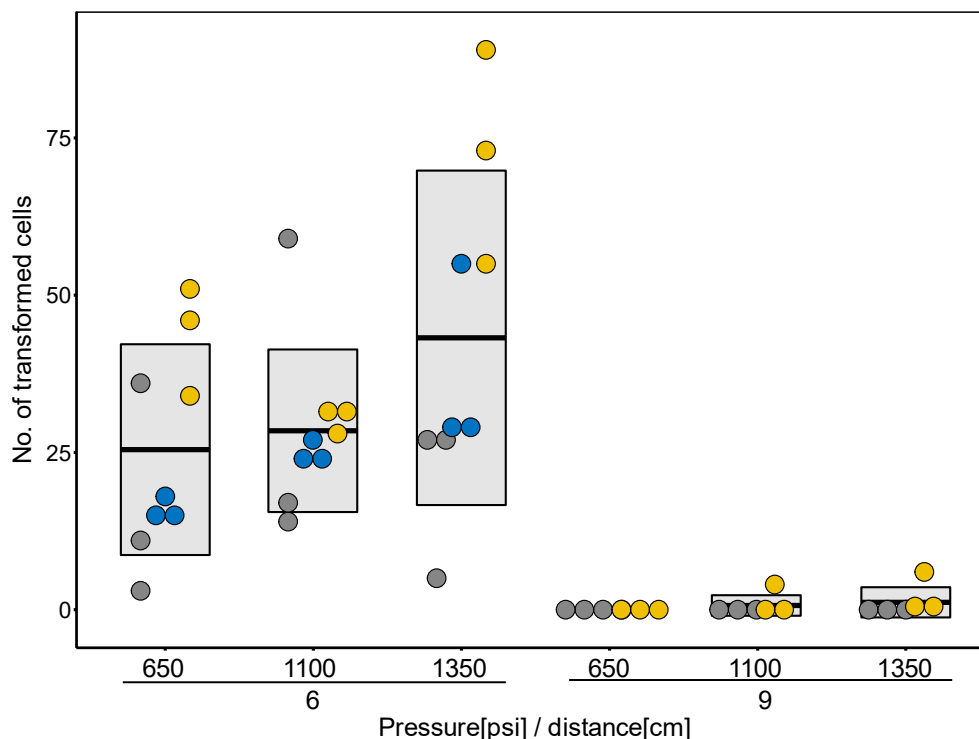


Figure 4.9 | The effect of pressure and position. The effectivity of biolistic transformation expressed as the number of fluorescent cells on one plate, with combinations of the pressure of particle acceleration and position of the target shelf. Different colors denote independent experiments, each with $n = 3$. The box with a horizontal bar represents the mean with quartiles.

4.3.3 The effect of DNA concentration

According to the protocol for the BioRad PDS 1000/He system (BioRad, 2013), microcarriers should be coated with the DNA concentrated to $1 \mu\text{g}/\mu\text{l}$ (i.e. $0.24 \mu\text{g}$ per one bombardment). To use the DNA in this concentration, an additional step of DNA precipitation (by sodium acetate) was required when using plasmid DNA isolated by a miniprep kit. The alternative way of obtaining concentrated plasmid DNA would be a midiprep isolation. Because the usual concentration of miniprep-isolated pSA106 vector was approximately 10-fold lower than suggested in the BioRad manual (BioRad, 2013), the effectivity of $0.1 \mu\text{g}/\mu\text{l}$ and $1 \mu\text{g}/\mu\text{l}$ DNA concentrations were compared to test, whether a DNA dose comparable to the concentrations obtainable by miniprep would be feasible. Target cells were placed in position 2 and the pressure was set to 1350 psi. After two biological replications, the mean number of transformed cells on one plate was found to be identical (49) for both tested concentrations (Figure 4.11).

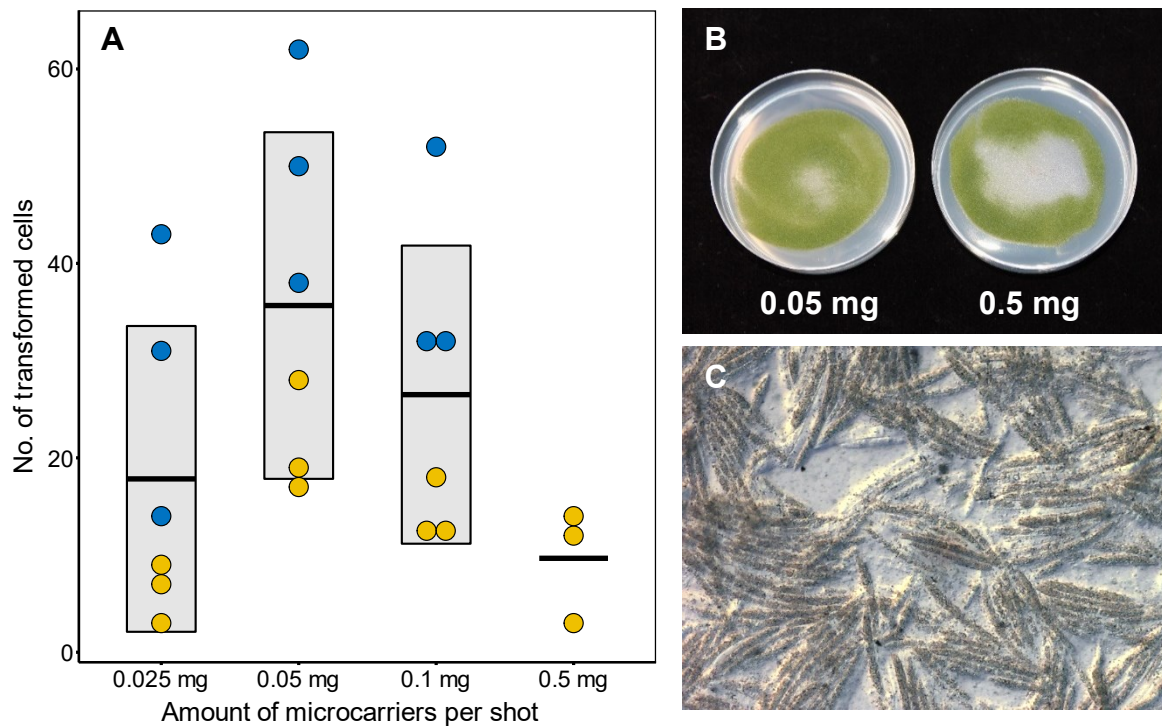


Figure 4.10 | Optimization of the microcarrier amount. **A)** The effectivity of biolistic transformation expressed as the number of fluorescent cells on one plate, with different amounts of golden microcarriers used per one shot. Different colors denote independent experiments, each with $n = 3$ (individual plates). The box with a horizontal bar represents the mean with quartiles. **B, C)** The lethal effect of 0.5 mg of gold particles (0.6 μm) observed on the 4th day after transformation. **C)** Detail of dead cells in the center of the plate, particles are very abundant and visible in the background.

4.3.4 The comparison of two fluorophores

In *Closterium*, Abe *et al.* (2008) managed to express and visualize a modified green fluorescent protein, which was optimized for the codon usage of *Chlamydomonas reinhardtii* (*Chlamydomonas*-adapted green fluorescent protein, cGFP; Fuhrmann *et al.*, 1999). In our setup, cGFP was tested together with a red fluorescent protein mScarlet-H (Bindels *et al.*, 2016), not similarly codon-optimized. Target cells were placed in position 2 and the pressure was set to 1350 psi. On average, mScarlet-H showed a slightly higher number of transformed cells (Figure 4.12). However, each of the three biological replications of both fluorophore variants exhibited a high variability of transformed cell number.

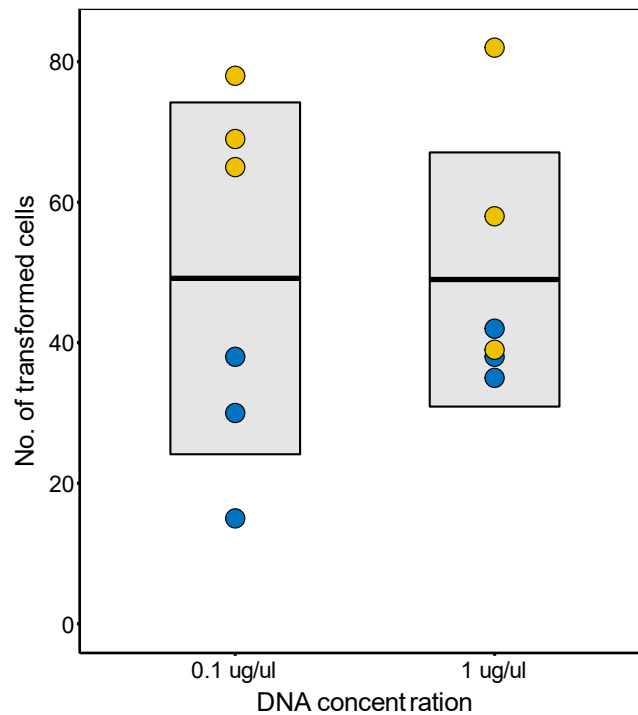


Figure 4.11 | The effect of DNA concentration. The effectivity of biolistic transformation expressed as the number of fluorescent cells on one plate, with two concentrations of DNA used for microcarrier coating. Different colors denote independent experiments, each with $n = 3$ (individual plates). The box with a horizontal bar represents the mean with quartiles.

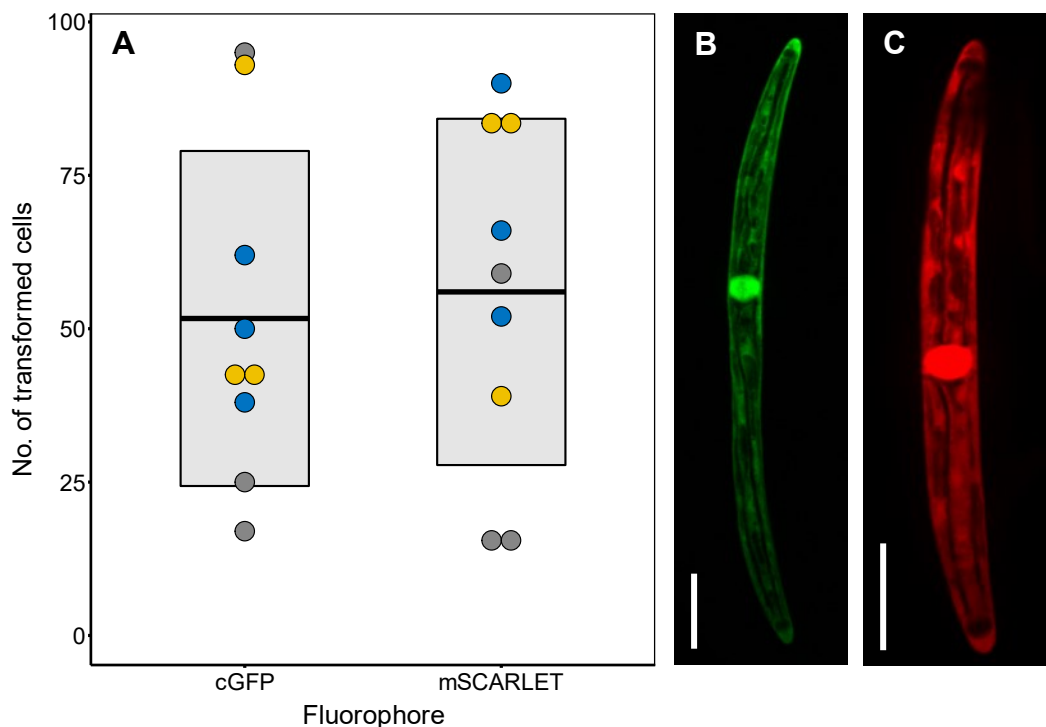


Figure 4.12 | cGFP and mScarlet-H as two tested fluorophores. A) The effectivity of biolistic transformation, expressed as the number of fluorescent cells on one plate expressing two different fluorophores: *CpCAB1::cGFP* (B) and *CpCAB1::mScarlet-H* (C). Different colors denote independent experiments, each with $n = 3$ (individual plates). The box with a horizontal bar represents the mean with quartiles. Images of transformed *Closterium* cells are converted from “Z-stack” to maximum intensity projection; scale = 20 μm .

4.3.5 Native expression of *CpPIN* was not successful

Optimized parameters of the biolistic transformation method were used for the delivery of *CpPIN:mScarlet-H*, i.e. pressure of 1350 psi, 6cm gun-to-target distance, 0.05 mg of microcarriers per bombardment, and DNA in 1µg/µl concentration. Despite the efforts of optimizing the biolistic method for *Closterium*, no fluorescent cells were observed after four transformation attempts.

4.3.6 Heterologous expression of *CpPIN* in BY-2 cells

As a complementary approach to *Closterium* transformation, *CpPIN* was introduced by particle bombardment to the BY-2 heterologous system, where it probably localized to the PM and endomembrane compartments (Figure 4.13A).

In addition, the stable transformation of *CpPIN:mScarlet-H* (under estradiol-inducible system) into BY-2 via *Agrobacterium tumefaciens* was performed by Mgr. Zuzana Vondráková, as part of the larger project undertaken in our laboratory. Receiving these transformed lines from her, my contribution consisted of analysing the lines by confocal microscopy. The *CpPIN* localization pattern therein resembled the localization observed in BY-2 cells transformed via particle bombardment (Figure 4.13). The PM localization was corroborated by a short-term staining with the FM1-43, marking the PM and its derivatives. A pronounced endocytosis of the PM-derived marked vesicles was prevented by a short-term staining (5 min) on ice.

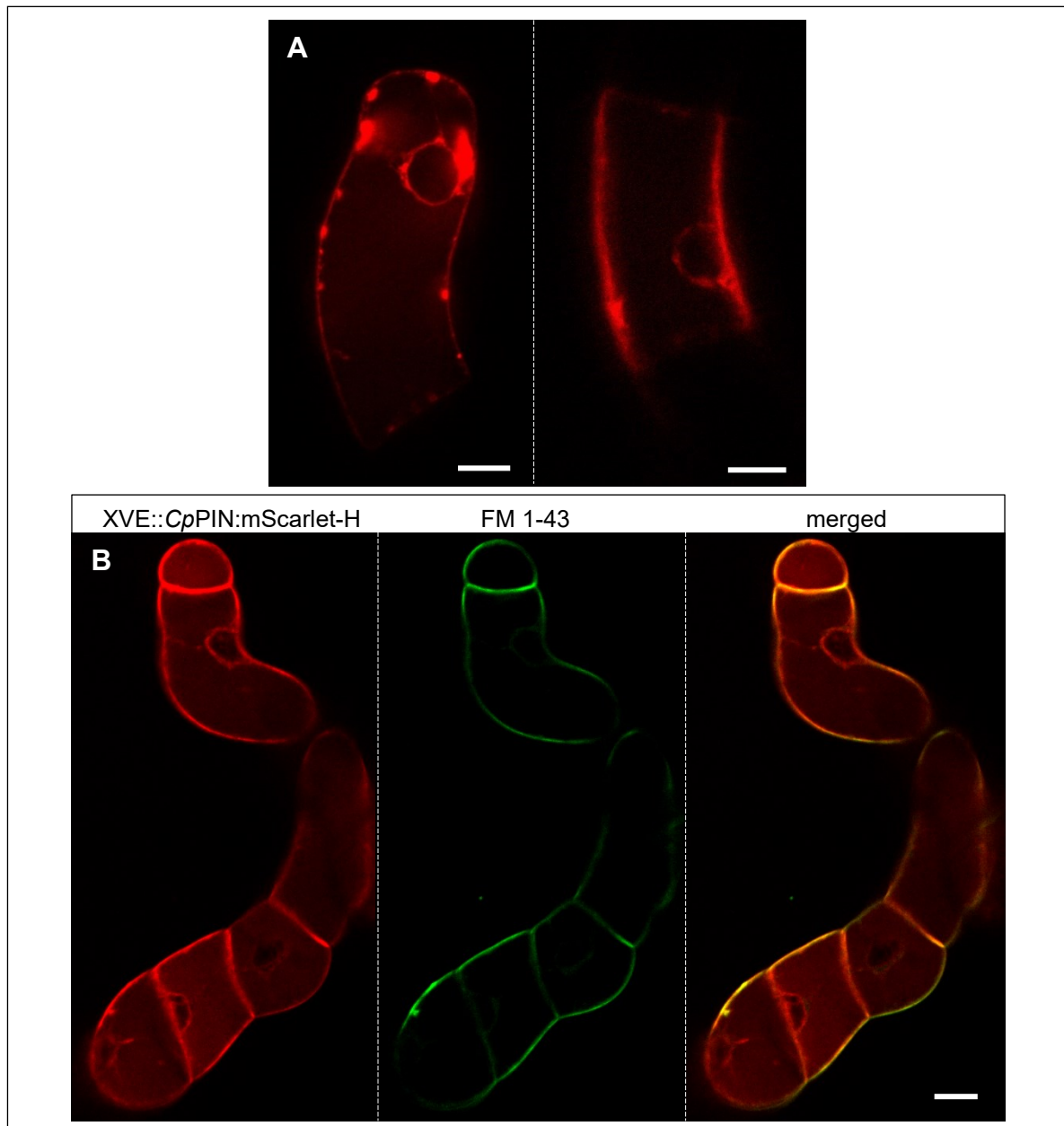


Figure 4.13 | Localization of *CpPIN:mScarlet-H* in BY-2 cells. A) Transiently transformed BY-2 cells (G10-90::*CpPIN:mScarlet-H*, introduced via particle bombardment). **B)** Stable transformed BY-2 cell line (red channel, XVE::*CpPIN:mScarlet-H*, via *A. tumefaciens* transformation) stained by FM 1-43 plasma membrane marker (green channel; stained by 5-minute incubation on ice, $1:10^4$). Scale = 20 μm .

5 Discussion

5.1 Endogenous levels of auxins in charophytes

As described in the introduction, genomic-based studies indicate that green algae do not have orthologs for the pathway of IAA biosynthesis via IPyA, which is major in land plants. Instead, orthologs of IAM pathway have been identified in all six charophyte lineages. Also, orthologs of genes involved in land plant-like IAA metabolism were not identified in algae. To date, these findings are not supported by any hormonal analysis in streptophyte algae. It was this work's aim to analyse and compare the levels of IAA and relative compounds across charophytes.

5.1.1 Endogenous auxin levels are variable among algae

IAA, as the focal point of this work, was detected in all sampled species. The results of this work thus complemented the IAA presence detected in a wide range of chlorophytes (Stirk *et al.*, 2013; Žižková *et al.*, 2017). Endogenous IAA concentration ranged from units of pmol to dozens of pmol per g FW. In comparison, dozens of pmol/g FW were also detected in *Physcomitrium patens* tissues (Ludwig-Müller *et al.*, 2009) and dozens of pmol to units of nmol/g FW in angiosperms (Ding *et al.*, 2012; Raspor *et al.*, 2020). IAA levels in charophytes were somewhat mutually dissimilar, even between similar morphotypes (e.g., *Mougeotia* and *Spirogyra*). There was also no correlation between higher amounts of IAA or its metabolites and the morphological complexity of studied algae. It was also shown that auxin levels in biomass often increased with the age of some algal cultures or were maintained in others. Analysis of culture media revealed several species to have released IAA therein. Interestingly, this phenomenon was observed in all tested species naturally growing in subaerial habitats. IAA release in liquid cultures was rather ambiguous, while the older culture of *Mougeotia* released a relatively massive amount of IAA into its culture medium, the culture media of *Closterium* and *Coleochaete* exhibited IAA levels similar to blank at both young and old culture stages. If auxin serves as a hypothetical signal between algae and surrounding microorganisms, the intentional IAA efflux would be more reasonable in a biofilm-type niches of subaerial algae, where the diffusion rate is lower than in a water environment. This issue remains to be addressed in future research.

Significant presence of IAM as IAA precursor in all sampled species, coupled with the presence of AMI1 hydrolases orthologs across the green lineage, are highly suggestive of a possible IAM biosynthetic pathway in green algae, as proposed by de Smet *et al.* (2011), Di *et*

al., (2015), and Bowman *et al.* (2021). IAM was detected also in a wide range of chlorophytes (Stirk *et al.*, 2013). AMI1 facilitates the conversion of IAM to IAA, but the mechanism of IAM synthesis is still unknown in plants (Morffy & Strader, 2020).

Levels of IAA conjugates and catabolites in land plants are substantially higher than free IAA levels, which shows the importance of complex IAA homeostasis therein (Ludwig-Müller *et al.*, 2009; Kramer & Ackelsberg, 2015). Quite an opposite situation was observed in the majority of sampled algae, where levels of IAA metabolites were minor compared to IAA. While we could detect the presence of the oxidized form of IAA in our tested algae, no orthologs of DAO oxygenases were not detected in charophytes (Bowman *et al.*, 2021), which perhaps suggests the presence of an unknown IAA oxidative pathway. The same discrepancy between our measurements and the available sequence information was observed in the case of the oxIAA-Asp conjugate. It appears that IAA in charophytes is either catabolized, or exported to the surroundings. This is consistent with the previously proposed strategies of regulating IAA levels in algae, i.e. biosynthesis/degradation or efflux (Sztein *et al.*, 2000; Vosolsobě *et al.*, 2020). But whether these strategies are employed in algae is still an open question, as the nature of IAA as a signalling compound vs. a (by)product of cellular metabolism is still not resolved in non-land plant Viridiplantae.

PAA is derived from the amino acid phenylalanine, which would explain its widespread presence not only in the green lineage (Cook, 2019). It has been recognized as a weak auxin, based on interactions with the TIR1 signaling pathway (Shimizu-Mitao & Kakimoto, 2014; Sugawara *et al.*, 2015). In land plants, PAA is substantially more abundant, than IAA (Sugawara *et al.*, 2015; Aoi *et al.*, 2020). A similar situation was observed in the majority of charophytes. Our data for strains cultivated on solid media are equivocal due to the natural occurrence of PAA in blank media. With greater confidence, it can be stated that PAA was produced by all species cultivated in liquid media, from which *Closterium* and *Mougeotia* exhibited significant release into the culture media. Interestingly, in *Mesotaenium* PAA level decreased substantially with culture age indicating its metabolic conversion or efflux. It is unknown whether PAA serves any signaling function in algae, but it is known to mediate various interactions between land plants and microbes (reviewed by Cook, 2019), so an existence of a similar role in common algal-microbe niches is also possible.

5.1.2 Obstacles in data interpretation

Analyses of endogenous auxin levels in algae are a crucial part of studying the evolution of its action. However, up-to now studies measuring phytohormones in algae did not address the

effects of media (Sztein *et al.*, 2000; Stirk *et al.*, 2013; Žižková *et al.*, 2017). In this work, it was shown that auxins are present in some blank media, especially in those containing organic compounds. PAA was abundant in media solidified with agar, IAA was likely present in soil extract, and some IAA metabolites may have originated from peptone. On one hand, this complicates the interpretation of data measured in biomass and culture media because it cannot be distinguished whether auxins are produced by an organism or taken up from the surroundings. On the other hand, it points out (for the first time, to our knowledge) the possibility of a very significant influence of the culture medium on the compounds analysed in the algal biomass, an option typically not considered in similar studies. Indeed, rigorous controls are apparently necessary to properly evaluate the native biosynthesis of known phytohormones and their metabolites in algae. Moreover, concentrations of IAA measured in culture media over time are influenced by spontaneous IAA decay (Dunlap *et al.*, 1986). This was also shown by the data from blank media. Lastly, the detected concentrations might have also been influenced by bacterial contamination (Spaepen & Vanderleyden, 2011), which was present substantially in *Mesostigma*, *Chlorokybus*, and *Coleochaete* cultures, and slightly in *Mougeotia*, and *Spirogyra* cultures.

5.2 The reaction of *Closterium* to exogenous auxin is pleiotropic

Closterium morphology was affected by the exposure to exogenous IAA. But all tested concentrations caused a high variability of measured parameters. After the IAA treatment, the majority of cells tended to be less elongated, wider, and therefore more circular, but on the other hand, a smaller population of cells was extremely elongated in contrast to control. Thus, the auxin effect on morphology seems to be rather pleiotropic. Assuming, that the inoculum consisted of a mixture of cells in different stages of their physiological status, cells might have responded to IAA differently and thus exhibited various phenotypes. For instance, auxin could have had an inhibitory effect on cell elongation, as reported in *Klebsormidium* using a substantially higher concentration (Ohtaka *et al.*, 2017). In other cells, the treatment could have impaired the process of cytokinesis, in which case the daughter cells remain connected and thus recognized as one extremely elongated cell. But the aspect of disrupted cell division was beyond the resolving power of image analysis applied in this work. The highest amount of aberrant phenotypes was shown in cultures treated with 2.5 μ M IAA, in higher concentrations these phenotypes were less frequent. That correlated with the dose-dependent inhibitory effect

of IAA on *Closterium* culture growth suggesting, that the auxin effect on cell morphology manifested more in lower concentrations, where the culture still proliferated. Then, higher concentrations would particularly inhibit cell division, with the effect on cell elongation negligible in near non-dividing cultures. In the previous objective, we showed that the native concentration of IAA in *Closterium* is much lower than the doses applied into the culture medium in this experiment. IAA treatments with concentrations in lower orders of magnitude could possibly have had a different effect on culture growth. In an unrelated alga *Chlorella vulgaris*, Piotrowska-Niczyporuk & Bajguz (2014) observed both stimulating and inhibitory effects of lower and higher IAA concentrations, respectively.

Speculatively, auxin might somehow affect the cytoskeleton or cell wall biosynthesis in growing cells. Thus, it is important to broaden the knowledge also in other aspects of cell biology and the life cycles of algae to better interpret these auxin responses. To further investigate the background of IAA-induced malformed phenotypes of *Closterium*, our future effort will focus on the synchronization of cell division cycle in an entire culture, before proceeding to auxin treatments. As described in Domozych *et al.* (2007), antibodies against specific components of the cell wall will be applied to visualize the possible differences in cell wall morphogenesis during auxin treatments. In search for other possible responses to auxin in charophytes, treatments with exogenous auxins will be performed also with different species in our culture established within this work.

5.3 Native and heterologous transformation of *Closterium*-derived gene constructs and optimization of biolistic transformation method for the alga *Closterium*

Mastering of genetic manipulation methods in algae is a crucial step for in-depth studies of these organisms. Currently, the only successful transformation method published for *Closterium* is the particle bombardment allowing both transient and stable transformation (Abe *et al.*, 2008, 2011). By using the standard protocol for the BioRad PDS 1000/He system (BioRad, 2013), we were only able to transform up to ten cells per one bombardment, compared to hundreds of cells reported in Abe *et al.* (2008) using a different biolistic delivery system.

The optimization of several parameters increased the efficiency of the transformation to higher dozens of fluorescent cells. As we found out, the most important step toward a more efficient transformation lay in the tenfold lowering of the total microcarrier amount per

bombardment (0.05 mg, down from 0.5 mg). Additionally, the 6cm gun-to-target distance was substantially more effective than 9cm distance. However, the optimal parameters differed from Abe *et al.* (2008), where the microcarrier amount was not lowered, and the gun-to-target distance was set to 12 cm. Also, the optimal particle size was different (0.25 μm), but in this optimization only 0.6 μm particles were used, as was recommended for algae (BioRad, 2013), and because smaller-sized particles were not available at that time. To further disclose the differences between optimal parameters used in this work vs. the approach of Abe *et al.* (2008), a possible future experiment could test the gun-to-target distance together with the microcarrier amount to determine the relationship between the microcarrier density and dispersion.

The so far discussed findings concerned mostly mechanistic aspects. In addition, we also tested the parameters pertaining to DNA solution used for the coating of microcarrier particles. The results showed that concentrating the DNA solution as high as 1 $\mu\text{g}/\mu\text{l}$, as described in BioRad protocol (BioRad, 2013), is not necessary for *Closterium* transformation. Hence, the plasmid DNA isolated via a simple miniprep procedure can be used directly for coating, which reduces the amount of auxiliary work significantly. Similarly lowered DNA concentrations were reported to be usable for BY-2 transformation (Barbez *et al.*, 2013).

Abe *et al.* (2008) reported that a GFP version used in transformation of land plant material is not feasible for expression in *Closterium* and also showed that this alga has a similar codon usage bias as *Chlamydomonas reinhardtii*, where a codon-optimized GFP was prepared previously (Fuhrmann *et al.*, 1999). Therefore, as in Abe *et al.* (2008), a correspondingly adapted form of GFP (cGFP) was used as a reporter of successful *Closterium* transformation. Despite not being similarly optimized, the red fluorophore mScarlet-H exhibited similarly good expression in *Closterium* as cGFP, in terms of number of cells transformed per plate. Apparently, codon optimization of coding sequences used in *Closterium* transformation is not necessary in all cases and varies in individual sequences.

There is still a series of parameters, which have not been addressed in this optimization. For instance, the acceleration of microcarriers is dependent not only on the helium burst intensity but also on the degree of underpressure. Also, the density of cells on a plate may have a substantial effect. Next to the hitherto mentioned parameters, there is the microcarrier coating process itself, which is one of the main sources of variation in results (Sanford *et al.*, 1993). Despite the extensive initial sonication (before DNA coating) and continuous vortexing of the gold particles, an aggregation and fast sedimentation was observed in every coating process in all biolistic experiments. This phenomenon may have affected the uniform transfer of the gold particle suspension onto macrocarriers and thus could have been the cause of a high variability

within biological replications. Still, the methodological optimization undertaken in this work set the starting point for introducing sequences of interest into *Closterium*, using a generally widely available delivery system, and can be also utilized for the future transformation of other algae.

Besides free fluorophores, our laboratory was also successful with transient expression of fluorescently-tagged actin marker in *Closterium* (LifeAct:cGFP; Skokan 2021). However, the primary purpose of the optimization part was the *in vivo* visualisation of a fluorescently-tagged *Closterium* PIN ortholog (*CpPIN:mScarlet-H*). However, this effort was not yet successful. The fluorescence could have been either weak and undetectable, or the construct was silenced by the alga. To investigate the former possibility, we are currently preparing “dual-marker” vectors including both fluorescently tagged *CpPIN* and a free fluorophore of different excitation spectrum and a putatively different subcellular localization compared to *CpPIN*. The free fluorophore will mark the transformed cells in which to search for the potentially weak signal of the tagged *CpPIN*. Our laboratory is also currently attempting to visualise *CpPIN* in *Closterium* cells via the immunofluorescence approach, using specifically synthesized antibodies against *CpPIN*. Both transient and stable heterologous expression of *CpPIN:mScarlet-H* in BY-2 system showed fluorescence at the PM and endomembrane compartments. The *CpPIN:mScarlet-H* localization pattern observed in BY-2 resembled the one observed for another PIN ortholog from *Klebsormidium* (*KfPIN*), which was previously expressed in the same material (Skokan *et al.*, 2019). As *KfPIN* was capable of cellular auxin efflux in BY-2 (Skokan *et al.*, 2019), it is possible that the experiments planned in the very near future will show similar or identical results in BY-2 lines stably expressing the *CpPIN* gene constructs..

6 Conclusions

The first objective of this work was to select and cultivate representative species of charophytes for subsequent analysis of auxins levels. Ten strains were introduced to our cultivation, including one outgroup strain of chlorophytes. LC-MS analysis showed that IAA is present in all tested algae in distinct concentrations and is exported to the media predominantly by terrestrial algae. The existence of putative oxidative pathways in all charophyte lineages and the outgroup was indicated by the detection of oxIAA and oxIAA-Asp, but their levels were mostly lower than of IAA. A more in-depth interpretation of the measured data was limited by the natural occurrence of auxins in some types of control media.

As the second objective, the effect of exogenous auxin on the morphology of *Closterium* cells was investigated. This effect was shown as pleiotropic and manifested more in lower auxin concentrations, while in higher doses it rather inhibited culture growth. The observed phenotype variability implicated the need to better understand the cell biology and life cycle of the studied algae, in order to better interpret growth responses to exogenously applied phytohormones.

The third objective aimed at the optimization of biolistic transformation of *Closterium* using free fluorophores, to pave the way for a subsequent transformation with *CpPIN:mScarlet-H*. Pressure set to 1350 psi, tenfold dilution of microcarriers, and 6cm microcarrier particle flight distance provided the best transformation results. Additionally, the relatively high doses of DNA officially recommended for microcarrier coating were proven unnecessary in our optimization effort, significantly reducing the overall laboriousness of the transformation procedure.

While the biolistic method was successfully optimized for *Closterium* in our work conditions, the transformation with the *CpPIN:mScarlet-H* fusion gene construct was not successful. However, the heterologous expression of the same gene construct in tobacco BY-2 cell culture suggested *CpPIN* subcellular localization at the plasma membrane as well as in endomembrane compartments.

The results of this work prepared the ground a follow-up research of evolutionary aspects of auxin action in green algae within my future doctoral studies.

7 References

- Abe, J. *et al.* (2008) 'Expression of exogenous genes under the control of endogenous HSP70 and CAB promoters in the *Closterium peracerosum-strigosum-littorale* complex', *Plant and Cell Physiology*, 49(4), pp. 625–632. doi: 10.1093/pcp/pcn039.
- Abe, J. *et al.* (2011) 'Stable nuclear transformation of the *closterium peracerosum-strigosum-littorale* complex', *Plant and Cell Physiology*, 52(9), pp. 1676–1685. doi: 10.1093/pcp/pcr103.
- Adamowski, M. and Friml, J. (2015) 'PIN-dependent auxin transport: Action, regulation, and evolution', *Plant Cell*, 27(1), pp. 20–32. doi: 10.1105/tpc.114.134874.
- Aoi, Y. *et al.* (2020) 'GH3 Auxin-Amido Synthetases Alter the Ratio of Indole-3-Acetic Acid and Phenylacetic Acid in *Arabidopsis*', *Plant and Cell Physiology*. Oxford University Press, 61(3), pp. 596–605. doi: 10.1093/pcp/pcz223.
- Archibald, J. M. (2015) 'Endosymbiosis and eukaryotic cell evolution', *Current Biology*. Elsevier, pp. R911–R921. doi: 10.1016/j.cub.2015.07.055.
- Arriola, M. B. *et al.* (2017) 'Genome sequences of *Chlorella sorokiniana* UTEX 1602 and *Micractinium conductrix* SAG 241.80: implications to maltose excretion by a green alga', *The Plant Journal*. Blackwell Publishing Ltd, 93(3), pp. 566–586. doi: 10.1111/tpj.13789.
- Barbez, E. *et al.* (2013) 'Single-cell-based system to monitor carrier driven cellular auxin homeostasis', *BMC Plant Biology*, 13(1). doi: 10.1186/1471-2229-13-20.
- Bartel, B. & Fink, G. (1995) 'ILR1, an amidohydrolase that releases active indole-3-acetic acid from conjugates', *Science*, 268(5218), pp. 1745–1748. doi: 10.1126/science.7792599.
- Basu, S. *et al.* (2002) 'Early Embryo Development in *Fucus distichus* Is Auxin Sensitive', *Plant Physiology*. Oxford University Press, 130(1), p. 292. doi: 10.1104/PP.004747.
- Bates, D. *et al.* (2015) 'Fitting linear mixed-effects models using lme4', *Journal of Statistical Software*, 67(1). doi: 10.18637/jss.v067.i01.
- Becker, B. (2013) 'Snow ball earth and the split of Streptophyta and Chlorophyta', *Trends in Plant Science*. Elsevier Ltd, 18(4), pp. 180–183. doi: 10.1016/j.tplants.2012.09.010.
- Bennett, T. A. *et al.* (2014) 'Plasma Membrane-Targeted PIN Proteins Drive Shoot Development in a Moss', *Current Biology*. Cell Press, 24(23), pp. 2776–2785. doi: 10.1016/J.CUB.2014.09.054.
- Bindels, D. S. *et al.* (2016) 'MScarlet: A bright monomeric red fluorescent protein for cellular imaging', *Nature Methods*, 14(1), pp. 53–56. doi: 10.1038/nmeth.4074.
- BioRad, (2013) 'PDS-1000 | He™ and Hepta™ Systems', <https://www.bio-rad.com/en-cz/product/pds-1000-he-hepta-systems?ID=1730e08d-f43a-46ea-b7f3-7b35c04c36eb>
- Bischoff, H. W. & Bold, H. C. (1963). 'Phycological Studies IV. Some Soil Algae from Enchanted Rock and Related Algal Species' University of Texas Publication No. 6318, Austin, Texas.

- Boer, D. R. *et al.* (2014) ‘Structural basis for DNA binding specificity by the auxin-dependent ARF transcription factors’, *Cell*. Cell Press, 156(3), pp. 577–589. doi: 10.1016/j.cell.2013.12.027.
- Boot, K. J. M. *et al.* (2012) ‘Polar auxin transport: An early invention’, *Journal of Experimental Botany*, 63(11), pp. 4213–4218. doi: 10.1093/jxb/ers106.
- Bowman, J. L. (2013) ‘Walkabout on the long branches of plant evolution’, *Current Opinion in Plant Biology*. Elsevier Ltd, 16(1), pp. 70–77. doi: 10.1016/j.pbi.2012.10.001.
- Bowman, J. L. *et al.* (2017) ‘Insights into Land Plant Evolution Garnered from the *Marchantia polymorpha* Genome’, *Cell*, 171(2), pp. 287–304.e15. doi: 10.1016/j.cell.2017.09.030.
- Bowman, J. L. *et al.* (2019) ‘Something ancient and something neofunctionalized—evolution of land plant hormone signaling pathways’, *Current Opinion in Plant Biology*. Elsevier Ltd, pp. 64–72. doi: 10.1016/j.pbi.2018.09.009.
- Bowman, J. L., Sandoval, E. F. and Kato, H. (2021) ‘On the evolutionary origins of land plant auxin biology’, *Cold Spring Harbor Perspectives in Biology*, 13(6). doi: 10.1101/cshperspect.a040048.
- Brumos, J. *et al.* (2018) ‘Local Auxin Biosynthesis Is a Key Regulator of Plant Development’, *Developmental Cell*. Cell Press, 47(3), pp. 306–318.e5. doi: 10.1016/j.devcel.2018.09.022.
- Buschmann, H. (2020) ‘Into another dimension: How streptophyte algae gained morphological complexity’, *Journal of Experimental Botany*. Oxford University Press, pp. 3279–3286. doi: 10.1093/jxb/eraa181.
- Casanova-Sáez, R. & Voß, U. (2019) ‘Auxin Metabolism Controls Developmental Decisions in Land Plants’, *Trends in Plant Science*, pp. 741–754. doi: 10.1016/j.tplants.2019.05.006.
- Cheng, S. *et al.* (2019) ‘Genomes of Subaerial Zygnematophyceae Provide Insights into Land Plant Evolution’, *Cell*, 179(5), pp. 1057–1067.e14. doi: 10.1016/j.cell.2019.10.019.
- Cho, M. & Cho, H. T. (2013) ‘The function of ABCB transporters in auxin transport’, *Plant Signaling and Behavior*, 8(2), p. e22990. doi: 10.4161/psb.22990.
- Cook, S. D. (2019) ‘An Historical Review of Phenylacetic Acid’, *Plant and Cell Physiology*. Oxford University Press, 60(2), pp. 243–254. doi: 10.1093/pcp/pcz004.
- Damodaran, S. & Strader, L. C. (2019) ‘Indole 3-Butyric Acid Metabolism and Transport in *Arabidopsis thaliana*’, *Frontiers in Plant Science*. Frontiers Media S.A., 10, p. 851. doi: 10.3389/fpls.2019.00851.
- Delaux, P. M. *et al.* (2015) ‘Algal ancestor of land plants was preadapted for symbiosis’, *Proceedings of the National Academy of Sciences of the United States of America*, 112(43), pp. 13390–13395. doi: 10.1073/pnas.1515426112.
- Delwiche, C. F. (2016) *The Genomes of Charophyte Green Algae*, *Advances in Botanical Research*. Elsevier Ltd. doi: 10.1016/bs.abr.2016.02.002.
- Dharmasiri, N. *et al.* (2005) ‘Plant development is regulated by a family of auxin receptor F box proteins’, *Developmental Cell*, pp. 109–119. doi: 10.1016/j.devcel.2005.05.014.

- Di, D.-W. *et al.* (2015) ‘The biosynthesis of auxin: how many paths truly lead to IAA?’, *Plant Growth Regulation*, 78(3), pp. 275–285. doi: 10.1007/s10725-015-0103-5.
- Ding, Z. *et al.* (2012) ‘ER-localized auxin transporter PIN8 regulates auxin homeostasis and male gametophyte development in Arabidopsis’, *Nature Communications*. Nature Publishing Group, 3. doi: 10.1038/ncomms1941.
- Domozych, D. S. *et al.* (2007) ‘The structure and biochemistry of charophycean cell walls: I. Pectins of *Penium margaritaceum*’, *Protoplasma*, 230(1–2), pp. 99–115. doi: 10.1007/s00709-006-0197-8.
- Dubey, S. M. *et al.* (2021) ‘No Time for Transcription—Rapid Auxin Responses in Plants’, *Cold Spring Harbor Perspectives in Biology*, p. a039891. doi: 10.1101/cshperspect.a039891.
- Dunlap, J. R., Kresovich, S. & McGee, R. E. (1986) ‘The Effect of Salt Concentration on Auxin Stability in Culture Media’, *Plant Physiology*, 81(3), pp. 934–936. doi: 10.1104/pp.81.3.934.
- Eklund, D. M. *et al.* (2015) ‘Auxin Produced by the Indole-3-Pyruvic Acid Pathway Regulates Development and Gemmae Dormancy in the Liverwort *Marchantia polymorpha*’, *The Plant Cell*. Oxford University Press, 27(6), p. 1650. doi: 10.1105/TPC.15.00065.
- Enders, T. A. & Strader, L. C. (2015) ‘Auxin activity: Past, present, and future’, *American Journal of Botany*. Botanical Society of America Inc., 102(2), pp. 180–196. doi: 10.3732/ajb.1400285.
- Fawley, M. W. & Lee, C. M. (1990) ‘Pigment composition of the scaly green flagellate *Mesostigma viride* (Micromonadophyceae) is similar to that of the siphonous green alga *Bryopsis plumosa* (Ulvophyceae)’, *Journal of Phycology*, 26(4), pp. 666–670. doi: 10.1111/j.0022-3646.1990.00666.x.
- Fendrych, M. *et al.* (2018) ‘Rapid and reversible root growth inhibition by TIR1 auxin signalling’, *Nature Plants*. Springer US, 4(7), pp. 453–459. doi: 10.1038/s41477-018-0190-1.
- Feraru, E. *et al.* (2012) ‘Evolution and structural diversification of PILS putative auxin carriers in plants’, *Frontiers in Plant Science*, 3(OCT), pp. 1–13. doi: 10.3389/fpls.2012.00227.
- Flores-Sandoval, E. *et al.* (2018) ‘Class C ARFs evolved before the origin of land plants and antagonize differentiation and developmental transitions in *Marchantia polymorpha*’, *New Phytologist*, 218, pp. 1612–1630. doi: 10.1111/nph.15090.
- Fuhrmann, M., Oertel, W. and Hegemann, P. (1999) ‘A synthetic gene coding for the green fluorescent protein (GFP) is a versatile reporter in *Chlamydomonas reinhardtii*’, *Plant Journal*, 19(3), pp. 353–361. doi: 10.1046/j.1365-313X.1999.00526.x.
- Gao, Y. *et al.* (2015) ‘Auxin binding protein 1 (ABP1) is not required for either auxin signaling or Arabidopsis development’, *Proceedings of the National Academy of Sciences of the United States of America*, 112(7), pp. 2275–2280. doi: 10.1073/pnas.1500365112.
- Geisler, M. *et al.* (2017) ‘A critical view on ABC transporters and their interacting partners in auxin transport’, *Plant and Cell Physiology*. Oxford University Press, 58(10), pp. 1601–1604. doi: 10.1093/pcp/pcx104.

- Gelová, Z. *et al.* (2021) ‘Developmental roles of Auxin Binding Protein 1 in *Arabidopsis thaliana*’, *Plant Science*. Elsevier Ireland Ltd, 303. doi: 10.1016/j.plantsci.2020.110750.
- Gitzendanner, M. A. *et al.* (2018) ‘Plastid phylogenomic analysis of green plants: A billion years of evolutionary history’, *American Journal of Botany*, 105(3), pp. 291–301. doi: 10.1002/ajb2.1048.
- Gray, W. M. *et al.* (2001) ‘Auxin regulates SCFTIR1-dependent degradation of AUX/IAA proteins’, *Nature*, 414(6861), pp. 271–276. doi: 10.1038/35104500.
- Hagen, G. & Guilfoyle, T. (2002) ‘Auxin-responsive gene expression: Genes, promoters and regulatory factors’, *Plant Molecular Biology*, 49(3–4), pp. 373–385. doi: 10.1023/A:1015207114117.
- Hamann, T. *et al.* (2002) ‘The *Arabidopsis* BODENLOS gene encodes an auxin response protein inhibiting MONOPTEROS-mediated embryo patterning’, *Genes and Development*, 16(13), pp. 1610–1615. doi: 10.1101/gad.229402.
- Harholt, J., Moestrup, Ø. & Ulvskov, P. (2016) ‘Why Plants Were Terrestrial from the Beginning’, *Trends in Plant Science*. Elsevier Ltd, 21(2), pp. 96–101. doi: 10.1016/j.tplants.2015.11.010.
- Heckman, D. S. *et al.* (2001) ‘Molecular evidence for the early colonization of land by fungi and plants’, *Science*, 293(5532), pp. 1129–1133. doi: 10.1126/science.1061457.
- Hori, K. *et al.* (2014) ‘*Klebsormidium flaccidum* genome reveals primary factors for plant terrestrial adaptation’, *Nature Communications*. Nature Publishing Group, 5(May), pp. 2–6. doi: 10.1038/ncomms4978.
- Ichimura T (1971) ‘Sexual cell division and conjugation-papilla formation in sexual reproduction of *Closterium strigosum*’ Proc Seventh Int Seaweed Symp, Univ Tokyo Press Tokyo, p. 208–214.
- Ichimura, T. & Itoh, T. (1977) 17. Preservation methods of microalgae (I). In *Preservation methods of microorganisms [Biseibutsu Hozonhô]*, Ed. by Nei, T., University of Tokyo Press, Tokyo, p. 355-373.
- Ishige, F. *et al.* (1999) ‘A G-box motif (GCCACGTGCC) tetramer confers high-level constitutive expression in dicot and monocot plants’, *The Plant Journal*, 18(4), pp. 443–448. doi: 10.1046/j.1365-313X.1999.00456.x.
- Ivanov Dobrev, P. & Kamínek, M. (2002) ‘Fast and efficient separation of cytokinins from auxin and abscisic acid and their purification using mixed-mode solid-phase extraction’, *Journal of Chromatography A*, 950(1–2), pp. 21–29. doi: 10.1016/S0021-9673(02)00024-9.
- Jiao, C. *et al.* (2020) ‘The *Penium margaritaceum* Genome: Hallmarks of the Origins of Land Plants’, *Cell*. Elsevier, 181(5), pp. 1097-1111.e12. doi: 10.1016/j.cell.2020.04.019.
- Kanda, N. *et al.* (2017) ‘CRISPR/Cas9-based knockouts reveal that CpRLP1 is a negative regulator of the sex pheromone PR-IP in the *Closterium peracerosum-strigosum-littorale* complex’, *Scientific Reports*, 7(1), p. 17873. doi: 10.1038/s41598-017-18251-8.

- Kato, H. *et al.* (2015) ‘Auxin-Mediated Transcriptional System with a Minimal Set of Components Is Critical for Morphogenesis through the Life Cycle in *Marchantia polymorpha*’, *PLoS Genetics*. Public Library of Science, 11(5). doi: 10.1371/JOURNAL.PGEN.1005084.
- Korasick, D. A., Enders, T. A. & Strader, L. C. (2013) ‘Auxin biosynthesis and storage forms’, *Journal of Experimental Botany*, pp. 2541–2555. doi: 10.1093/jxb/ert080.
- Kramer, E. M. & Ackelsberg, E. M. (2015) ‘Auxin metabolism rates and implications for plant development’, *Frontiers in Plant Science*, 6(MAR). doi: 10.3389/fpls.2015.00150.
- Lam, H. K. *et al.* (2015) ‘Evidence That Chlorinated Auxin Is Restricted to the Fabaceae But Not to the Fabeae’, *Plant Physiology*. American Society of Plant Biologists, 168(3), pp. 798–803. doi: 10.1104/pp.15.00410.
- Lavy, M. *et al.* (2016) ‘Constitutive auxin response in *Physcomitrella* reveals complex interactions between Aux/IAA and ARF proteins’, *eLife*. eLife Sciences Publications Ltd, 5(JUN2016). doi: 10.7554/ELIFE.13325.
- Leebens-Mack, J. H. *et al.* (2019) ‘One thousand plant transcriptomes and the phylogenomics of green plants’, *Nature*, 574(7780), pp. 679–685. doi: 10.1038/s41586-019-1693-2.
- Leliaert, F. *et al.* (2012) ‘Phylogeny and Molecular Evolution of the Green Algae’, *Critical Reviews in Plant Sciences*, 31(1), pp. 1–46. doi: 10.1080/07352689.2011.615705.
- Leliaert, F., Verbruggen, H. & Zechman, F. W. (2011) ‘Into the deep: New discoveries at the base of the green plant phylogeny’, *BioEssays*. Bioessays, pp. 683–692. doi: 10.1002/bies.201100035.
- Lewis, L. A. & McCourt, R. M. (2004) ‘Green algae and the origin of land plants’, *American Journal of Botany*, 91(10), pp. 1535–1556. doi: 10.3732/ajb.91.10.1535.
- Leyser, O. (2018) ‘Auxin signaling’, *Plant Physiology*. American Society of Plant Biologists, pp. 465–479. doi: 10.1104/pp.17.00765.
- Li, L. *et al.* (2020) ‘The genome of *Prasinoderma coloniale* unveils the existence of a third phylum within green plants’, *Nature Ecology and Evolution*. Nature Research. doi: 10.1038/s41559-020-1221-7.
- Libertín, M. *et al.* (2018) ‘Sporophytes of polysporangiate land plants from the early Silurian period may have been photosynthetically autonomous’, *Nature Plants*. Springer US, 4(5), pp. 269–271. doi: 10.1038/s41477-018-0140-y.
- Liscum, E. & Reed, J. W. (2002) ‘Genetics of Aux/IAA and ARF action in plant growth and development’, *Plant Molecular Biology*, 49(3–4), pp. 387–400. doi: 10.1023/A:1015255030047.
- Ljung, K. (2013) ‘Auxin metabolism and homeostasis during plant development’, *Development (Cambridge)*, 140(5), pp. 943–950. doi: 10.1242/dev.086363.
- Ljung, K., Bhalerao, R. P. & Sandberg, G. (2001) ‘Sites and homeostatic control of auxin biosynthesis in *Arabidopsis* during vegetative growth’, *Plant Journal*, 28(4), pp. 465–474. doi: 10.1046/j.1365-313X.2001.01173.x.

- Löbner, M. & Klämbt, D. (1985) 'Auxin-binding protein from coleoptile membranes of corn (*Zea mays* L.). I. Purification by immunological methods and characterization.', *Journal of Biological Chemistry*, 260(17), pp. 9848–9853. doi: 10.1016/s0021-9258(17)39314-6.
- Ludwig-Müller, J. *et al.* (2009) 'Moss (*Physcomitrella patens*) GH3 proteins act in auxin homeostasis', *New Phytologist*, 181(2), pp. 323–338. doi: 10.1111/j.1469-8137.2008.02677.x.
- Ludwig-Müller, J. (2011) 'Auxin conjugates: Their role for plant development and in the evolution of land plants', *Journal of Experimental Botany*, pp. 1757–1773. doi: 10.1093/jxb/erq412.
- Luria, S. E. & Burrous, J. W. (1957) 'HYBRIDIZATION BETWEEN *ESCHERICHIA COLI* AND *SHIGELLA*', *Journal of Bacteriology*, 74(4), pp. 461–476. doi: 10.1128/jb.74.4.461-476.1957.
- Marchant, A. *et al.* (2002) 'AUX1 promotes lateral root formation by facilitating indole-3-acetic acid distribution between sink and source tissues in the *Arabidopsis* seedling', *Plant Cell*. Oxford University Press, 14(3), pp. 589–597. doi: 10.1105/tpc.010354.
- Martin-Arevalillo, R. *et al.* (2019) 'Evolution of the Auxin response factors from charophyte ancestors', *PLoS Genetics*. Public Library of Science, 15(9). doi: 10.1371/journal.pgen.1008400.
- Merchant, S. S. *et al.* (2007) 'The *Chlamydomonas* genome reveals the evolution of key animal and plant functions', *Science*. American Association for the Advancement of Science, 318(5848), pp. 245–251. doi: 10.1126/science.1143609.
- Metzker, M. L. (2010) 'Sequencing technologies — the next generation', *Nature Reviews Genetics*. Nature Publishing Group, 11(1), pp. 31–46. doi: 10.1038/nrg2626.
- Mikhailyuk, T. *et al.* (2014) 'Morphology and ultrastructure of Interfilum and Klebsormidium (Klebsormidiales, Streptophyta) with special reference to cell division and thallus formation', *European Journal of Phycology*, 49(4), pp. 395–412. doi: 10.1080/09670262.2014.949308.
- Mikhailyuk, T. *et al.* (2018) 'New Taxa of Streptophyte Algae (Streptophyta) from Terrestrial Habitats Revealed Using an Integrative Approach Europe PMC Funders Group', *Protist*, 169(3), pp. 406–431. doi: 10.1016/j.protis.2018.03.002.
- Morffy, N. & Strader, L. C. (2020) 'Old Town Roads: routes of auxin biosynthesis across kingdoms', *Current Opinion in Plant Biology*. Elsevier Ltd, pp. 21–27. doi: 10.1016/j.pbi.2020.02.002.
- Morris, J. L. *et al.* (2018) 'The timescale of early land plant evolution', *Proceedings of the National Academy of Sciences of the United States of America*. National Academy of Sciences, 115(10), pp. E2274–E2283. doi: 10.1073/pnas.1719588115.
- Mutte, S. K. *et al.* (2018) 'Origin and evolution of the nuclear auxin response system', *eLife*. eLife Sciences Publications Ltd, 7. doi: 10.7554/eLife.33399.
- Nagata, T., Nemoto, Y. & Hasezawa, S. (1992) 'Tobacco BY-2 Cell Line as the "HeLa" Cell in the Cell Biology of Higher Plants', in *Change*, pp. 1–30. doi: 10.1016/S0074-7696(08)62452-3.

- Nishiyama, T. *et al.* (2018) 'The Chara Genome: Secondary Complexity and Implications for Plant Terrestrialization', *Cell*, 174(2), pp. 448-464.e24. doi: 10.1016/j.cell.2018.06.033.
- Nonhebel, H. M. (2015) 'Tryptophan-independent indole-3-acetic acid synthesis: Critical evaluation of the evidence', *Plant Physiology*. American Society of Plant Biologists, pp. 1001–1005. doi: 10.1104/pp.15.01091.
- Normanly, J., Cohent, J. D. & Fink, G. R. (1993) 'Arabidopsis thaliana auxotrophs reveal a tryptophan-independent biosynthetic pathway for indole-3-acetic acid (auxin/gas chromatography-selected ion monitoring-mass spectrometry)', *Proc. Natl. Acad. Sci. USA.*, p. 10355-10359, doi: 10.1073/pnas.90.21.10355
- Ohtaka, K. *et al.* (2017) 'Primitive auxin response without TIR1 and Aux/IAA in the charophyte alga Klebsormidium nitens', *Plant Physiology*. American Society of Plant Biologists, 174(3), pp. 1621–1632. doi: 10.1104/pp.17.00274.
- Ouyang, J., Shao, X. & Li, J. (2000) 'Indole-3-glycerol phosphate, a branchpoint of indole-3-acetic acid biosynthesis from the tryptophan biosynthetic pathway in Arabidopsis thaliana', *Plant Journal*, 24(3), pp. 327–334. doi: 10.1046/j.1365-313X.2000.00883.x.
- Parfrey, L. W. *et al.* (2011) 'Estimating the timing of early eukaryotic diversification with multigene molecular clocks', *Proceedings of the National Academy of Sciences of the United States of America*, 108(33), pp. 13624–13629. doi: 10.1073/pnas.1110633108.
- Petrášek, J. *et al.* (2003) 'Do phytohormones inhibit auxin efflux by impairing vesicle traffic?', *Plant Physiology*, 131(1), pp. 254–263. doi: 10.1104/pp.012740.
- Petrášek, J. & Friml, J. (2009) 'Auxin transport routes in plant development', *Development*, 136(16), pp. 2675–2688. doi: 10.1242/dev.030353.
- Petrášek, J., Laňková, M. & Zažímalová, E. (2014) 'Determination of auxin transport parameters on the cellular level', *Methods in Molecular Biology*, 1056, pp. 241–253. doi: 10.1007/978-1-62703-592-7_22.
- Piotrowska-Niczyporuk, A. & Bajguz, A. (2014) 'The effect of natural and synthetic auxins on the growth, metabolite content and antioxidant response of green alga Chlorella vulgaris (Trebouxioophyceae)', *Plant Growth Regulation*, 73(1), pp. 57–66. doi: 10.1007/s10725-013-9867-7.
- Porco, S. *et al.* (2016) 'Dioxygenase-encoding AtDAO1 gene controls IAA oxidation and homeostasis in Arabidopsis', *Proceedings of the National Academy of Sciences of the United States of America*. National Academy of Sciences, 113(39), pp. 11016–11021. doi: 10.1073/pnas.1604375113.
- Přerostová, S. *et al.* (2021) 'Light Quality and Intensity Modulate Cold Acclimation in Arabidopsis', *International Journal of Molecular Sciences*. Multidisciplinary Digital Publishing Institute, 22(5), p. 2736. doi: 10.3390/ijms22052736.
- Prigge, M. J. *et al.* (2020) 'Genetic analysis of the Arabidopsis TIR1/AFB auxin receptors reveals both overlapping and specialized functions', *eLife*, 9, pp. 1–28. doi: 10.7554/eLife.54740.
- Raspor, M. *et al.* (2020) 'Endogenous levels of cytokinins, indole-3-acetic acid and abscisic acid in in vitro grown potato: A contribution to potato hormonomics', *Scientific Reports*, 10(1), p. 3437. doi: 10.1038/s41598-020-60412-9.

- Regensdorff, M. *et al.* (2018) ‘Transient genetic transformation of *Mougeotia scalaris* (Zygnematophyceae) mediated by the endogenous α -tubulin1 promoter’, *Journal of Phycology*. Edited by S. Lin. Blackwell Publishing Inc., 54(6), pp. 840–849. doi: 10.1111/jpy.12781.
- Reineke, G. *et al.* (2008) ‘Indole-3-acetic acid (IAA) biosynthesis in the smut fungus *Ustilago maydis* and its relevance for increased IAA levels in infected tissue and host tumour formation’, *Molecular Plant Pathology*. Wiley-Blackwell, 9(3), pp. 339–355. doi: 10.1111/j.1364-3703.2008.00470.x.
- Rensing, S. A. *et al.* (2008) ‘The *Physcomitrella* genome reveals evolutionary insights into the conquest of land by plants’, *Science*, 319(5859), pp. 64–69. doi: 10.1126/science.1150646.
- Rensing, S. A. (2018) ‘Great moments in evolution: the conquest of land by plants.’, *Current opinion in plant biology*. Elsevier Ltd, 42(Figure 1), pp. 49–54. doi: 10.1016/j.pbi.2018.02.006.
- Rensing, S. A. (2020) ‘How Plants Conquered Land’, *Cell*. Elsevier, 181(5), pp. 964–966. doi: 10.1016/j.cell.2020.05.011.
- Rogers, C. E., Mattox, K. R. & Stewart, K. D. (1980) ‘The Zoospore of *Chlorokybus Atmophyticus*, a Charophyte with Sarcinoid Growth Habit’, *American Journal of Botany*, 67(5), p. 774. doi: 10.2307/2442669.
- Romani, F. (2017) ‘Origin of TAA Genes in Charophytes: New Insights into the Controversy over the Origin of Auxin Biosynthesis’, *Frontiers in Plant Science*, 8(September), pp. 2016–2018. doi: 10.3389/fpls.2017.01616.
- RStudio Team (2020). ‘RStudio: Integrated Development for R. RStudio’, PBC, Boston, MA, <http://www.rstudio.com/>.
- Rubery, P. H. & Sheldrake, A. R. (1974) ‘Carrier-mediated auxin transport’, *Planta*, 118(2), pp. 101–121. doi: 10.1007/BF00388387.
- SAG Culture Collection, (2007) ‘Basal Medium (= ES "Erddekot+Salze)’, http://sagdb.uni-goettingen.de/culture_media/01%20Basal%20Medium.pdf
- Sanford, J. C., Smith, F. D. & Russell, J. A. (1993) ‘Optimizing The Biolistic Process for Different Biological Applications’, *Methods in Enzymology*, 217(C), pp. 483–509. doi: 10.1016/0076-6879(93)17086-K.
- Sarrion-Perdigones, A. *et al.* (2013) ‘GoldenBraid 2.0: A Comprehensive DNA Assembly Framework for Plant Synthetic Biology’, *Plant Physiology*. Oxford Academic, 162(3), pp. 1618–1631. doi: 10.1104/PP.113.217661.
- Schönbrodt, F. (2012) ‘Visually weighted/ Watercolor Plots, new variants: Please vote!’, <https://www.nicebread.de/visually-weighted-watercolor-plots-new-variants-please-vote/>
- Sekimoto, H. & Fujii, T. (1992) ‘Analysis of the gametic protoplast release in the *Closterium peracerosum-strigosum-littorale* complex (Chlorophyta)’, *Journal of Phycology*, 28(5), pp. 615–619. doi: 10.1111/j.0022-3646.1992.00615.x.

- Shimizu-Mitao, Y. & Kakimoto, T. (2014) 'Auxin sensitivities of all arabidopsis aux/IAAs for degradation in the presence of every TIR1/AFB', *Plant and Cell Physiology*. Oxford University Press, 55(8), pp. 1450–1459. doi: 10.1093/pcp/pcu077.
- Simon, S. & Petrášek, J. (2011) 'Why plants need more than one type of auxin', *Plant Science*, 180(3), pp. 454–460. doi: 10.1016/j.plantsci.2010.12.007.
- Skokan, R. *et al.* (2019) 'PIN-driven auxin transport emerged early in streptophyte evolution', *Nature Plants*. Palgrave Macmillan Ltd., 5(11), pp. 1114–1119. doi: 10.1038/s41477-019-0542-5.
- Skokan, R. (2021) 'The evolution of auxin homeostasis mechanisms', Ph.D. thesis, Charles University, RNDr. Jan Petrášek, Ph.D. [cit. 2021-07-20, unpublished]
- de Smet, I. *et al.* (2011) 'Unraveling the evolution of auxin signaling', *Plant Physiology*, 155(1), pp. 209–221. doi: 10.1104/pp.110.168161.
- Sørensen, I. *et al.* (2011) 'The charophycean green algae provide insights into the early origins of plant cell walls', *Plant Journal*, 68(2), pp. 201–211. doi: 10.1111/j.1365-313X.2011.04686.x.
- Sørensen, I. *et al.* (2014) 'Stable transformation and reverse genetic analysis of *Penium margaritaceum*: A platform for studies of charophyte green algae, the immediate ancestors of land plants', *Plant Journal*, 77(3), pp. 339–351. doi: 10.1111/tpj.12375.
- Sousa, F. *et al.* (2018) 'Nuclear protein phylogenies support the monophyly of the three bryophyte groups (Bryophyta Schimp.)', *New Phytologist*. Blackwell Publishing Ltd, 222(1), pp. 565–575. doi: 10.1111/nph.15587.
- Spaepen, S. & Vanderleyden, J. (2011) 'Auxin and Plant-Microbe Interactions', *Cold Spring Harbor Perspectives in Biology*. Cold Spring Harbor Laboratory Press, 3(4), p. a001438. doi: 10.1101/CSHPERSPECT.A001438.
- Stepanova, A. N. & Alonso, J. M. (2016) 'Auxin catabolism unplugged: Role of IAA oxidation in auxin homeostasis', *Proceedings of the National Academy of Sciences of the United States of America*. National Academy of Sciences, pp. 10742–10744. doi: 10.1073/pnas.1613506113.
- Stirk, W. A. *et al.* (2013) 'Auxin and cytokinin relationships in 24 microalgal strains', *Journal of Phycology*. Edited by R. Bassi, 49(3), pp. 459–467. doi: 10.1111/jpy.12061.
- Sugawara, S. *et al.* (2015) 'Distinct Characteristics of Indole-3-Acetic Acid and Phenylacetic Acid, Two Common Auxins in Plants', *Plant and Cell Physiology*. Oxford Academic, 56(8), pp. 1641–1654. doi: 10.1093/PCP/PCV088.
- Swarup, R. *et al.* (2001) 'Localization of the auxin permease AUX1 suggests two functionally distinct hormone transport pathways operate in the Arabidopsis root apex', *Genes and Development*. Cold Spring Harbor Laboratory Press, 15(20), pp. 2648–2653. doi: 10.1101/gad.210501.
- Swarup, R. & Bhosale, R. (2019) 'Developmental Roles of AUX1/LAX Auxin Influx Carriers in Plants', *Frontiers in Plant Science*. Frontiers Media S.A. doi: 10.3389/fpls.2019.01306.

- Sztein, A. E., Cohen, J. D. & Cooke, T. J. (2000) 'Evolutionary Patterns in the Auxin Metabolism of Green Plants', *International Journal of Plant Sciences*, 161(6), pp. 849–859. doi: 10.1086/317566.
- Tan, X. *et al.* (2007) 'Mechanism of auxin perception by the TIR1 ubiquitin ligase', *Nature*, 446(7136), pp. 640–645. doi: 10.1038/nature05731.
- Timme, R. E., Bachvaroff, T. R. & Delwiche, C. F. (2012) 'Broad phylogenomic sampling and the sister lineage of land plants', *PLoS ONE*, 7(1). doi: 10.1371/journal.pone.0029696.
- Tromas, A., Paponov, I. & Perrot-Rechenmann, C. (2010) 'Auxin binding protein 1: Functional and evolutionary aspects', *Trends in Plant Science*. Elsevier Ltd, 15(8), pp. 436–446. doi: 10.1016/j.tplants.2010.05.001.
- Tsuchikane, Y. & Sekimoto, H. (2019) 'The genus *Closterium*, a new model organism to study sexual reproduction in streptophytes', *New Phytologist*, 221(1), pp. 99–104. doi: 10.1111/nph.15334.
- Turmel, M. & Lemieux, C. (2018) 'Evolution of the Plastid Genome in Green Algae', *Advances in Botanical Research*. Academic Press Inc., 85, pp. 157–193. doi: 10.1016/BS.ABR.2017.11.010.
- Ulmasov, T. *et al.* (1995) 'Composite structure of auxin response elements', *Plant Cell*, 7(10), pp. 1611–1623. doi: 10.1105/tpc.7.10.1611.
- Ulmasov, T., Hagen, G. & Guilfoyle, T. J. (1999) 'Dimerization and DNA binding of auxin response factors', *Plant Journal*. Blackwell Publishing Ltd., 19(3), pp. 309–319. doi: 10.1046/j.1365-313X.1999.00538.x.
- Vanneste, S. & Friml, J. (2009) 'Auxin: A Trigger for Change in Plant Development', *Cell*, 136(6), pp. 1005–1016. doi: 10.1016/j.cell.2009.03.001.
- Viaene, T. *et al.* (2014) 'Directional Auxin Transport Mechanisms in Early Diverging Land Plants', *Current Biology*. Cell Press, 24(23), pp. 2786–2791. doi: 10.1016/j.cub.2014.09.056.
- Vosolsobě, S., Skokan, R. & Petrášek, J. (2020) 'The evolutionary origins of auxin transport: what we know and what we need to know', *Journal of Experimental Botany*. Edited by A. Holzinger. Oxford University Press, 71(11), pp. 3287–3295. doi: 10.1093/jxb/eraa169.
- De Vries, J. *et al.* (2018) 'Embryophyte stress signaling evolved in the algal progenitors of land plants', *Proceedings of the National Academy of Sciences of the United States of America*. National Academy of Sciences, 115(15), pp. E3471–E3480. doi: 10.1073/pnas.1719230115.
- Wang, B. *et al.* (2015) 'Tryptophan-independent auxin biosynthesis contributes to early embryogenesis in *Arabidopsis*', *Proceedings of the National Academy of Sciences of the United States of America*, 112(15), pp. 4821–4826. doi: 10.1073/pnas.1503998112.
- Wang, S. *et al.* (2020) 'Genomes of early-diverging streptophyte algae shed light on plant terrestrialization', *Nature Plants*. Nature Research, 6(2), pp. 95–106. doi: 10.1038/s41477-019-0560-3.

- Weijers, D. & Wagner, D. (2016) 'Transcriptional Responses to the Auxin Hormone', *Annual Review of Plant Biology*, pp. 539–574. doi: 10.1146/annurev-arplant-043015-112122.
- Wickett, N. J. *et al.* (2014) 'Phylotranscriptomic analysis of the origin and early diversification of land plants', *Proceedings of the National Academy of Sciences of the United States of America*, 111(45), pp. E4859–E4868. doi: 10.1073/pnas.1323926111.
- Wickham H. (2016). 'ggplot2: *Elegant Graphics for Data Analysis*', Springer-Verlag New York. ISBN 978-3-319-24277-4, <https://ggplot2.tidyverse.org>.
- Wodniok, S. *et al.* (2011) 'Origin of land plants: Do conjugating green algae hold the key?', *BMC Evolutionary Biology*. BioMed Central Ltd, 11(1), p. 104. doi: 10.1186/1471-2148-11-104.
- Xiong, J. *et al.* (2015) 'Tracing the structural evolution of eukaryotic ATP binding cassette transporter superfamily', *Scientific Reports*. Sci Rep, 5. doi: 10.1038/srep16724.
- Xu, Y. X. *et al.* (2014) 'The B subfamily of plant ATP binding cassette transporters and their roles in auxin transport', *Biologia Plantarum*. Kluwer Academic Publishers, pp. 401–410. doi: 10.1007/s10535-014-0423-8.
- Yoon, H. S. *et al.* (2004) 'A Molecular Timeline for the Origin of Photosynthetic Eukaryotes', *Molecular Biology and Evolution*. Oxford Academic, 21(5), pp. 809–818. doi: 10.1093/molbev/msh075.
- Yue, J., Hu, X. & Huang, J. (2014) 'Origin of plant auxin biosynthesis', *Trends in Plant Science*. Elsevier Ltd, 19(12), pp. 764–770. doi: 10.1016/j.tplants.2014.07.004.
- Žabka, A. *et al.* (2016) 'PIN2-like proteins may contribute to the regulation of morphogenetic processes during spermatogenesis in *Chara vulgaris*', *Plant Cell Reports*, 35(8), pp. 1655–1669. doi: 10.1007/s00299-016-1979-x.
- Zažímalová, E. *et al.* (2010) 'Auxin transporters--why so many?', *Cold Spring Harbor perspectives in biology*, pp. a001552–a001552. doi: 10.1101/cshperspect.a001552.
- Zhang, J. & Peer, W. A. (2017) 'Auxin homeostasis: the DAO of catabolism', *Journal of Experimental Botany*, 68(12), pp. 3145–3154. doi: 10.1093/jxb/erx221.
- Zhang, Y. *et al.* (2020) 'Functional innovations of PIN auxin transporters mark crucial evolutionary transitions during rise of flowering plants', *Science Advances*, 6(50), pp. 1–15. doi: 10.1126/sciadv.abc8895.
- Zhao, Y. (2014) 'Auxin Biosynthesis', *The Arabidopsis Book*. BioOne, 12(12), p. e0173. doi: 10.1199/tab.0173.
- Zhou, H., Von Schwartzberg, K. & Buschmann, H. (2020) 'Zygnematophyceae: From living algae collections to the establishment of future models', *Journal of Experimental Botany*. Oxford University Press, pp. 3296–3304. doi: 10.1093/jxb/eraa091.
- Žižková, E. *et al.* (2017) 'Control of cytokinin and auxin homeostasis in cyanobacteria and algae', *Annals of Botany*, 119(1), pp. 151–166. doi: 10.1093/aob/mcw194.